New Jersey Water Resources Research Institute
Annual Technical Report
FY 2014

Introduction

The New Jersey Water Resources Research Institute (NJWRRI) supports a diverse program of research projects and information transfer activities. With oversight from the Advisory Council, which sets the Institute's Research Priorities, the available funds are divided between supporting faculty with 'seed' projects or new research initiatives and funding graduate students to develop their thesis research. The funding is intended to initiate novel and important research efforts by both faculty and students, thus emphasizing new research ideas that do not have other sources of funding. We hope to support the acquisition of data that will enable further grant submission efforts and in the case of students, lead to research careers focused on cutting-edge research topics in water sciences.

Research Program Introduction

The New Jersey Water Resources Research Institute (NJWRRI) has a policy, yearly reaffirmed by the NJWRRI Advisory Council, of using research dollars to promote novel directions of water resources research. To this end, two faculty initiated projects were awarded and seven grants-in-aid were awarded in FY2014 to graduate students who are beginning their research. We expect that the research is exploratory and is not supported by other grants. The intent is that these projects will lead to successful proposals to other agencies for further support. The larger goal of the research component of the Institute's program is to promote the development of scientists who are focused on water resources issues of importance to the state.

Modeling hydrologic and stream temperature response to land-use and climate change in developed and developing watersheds: a comprehensive analysis

Basic Information

Title:	Modeling hydrologic and stream temperature response to land-use and climate change in developed and developing watersheds: a comprehensive analysis
Project Number:	2014NJ350B
Start Date:	3/1/2014
End Date:	2/29/2016
Funding Source:	104B
Congressional District:	NJ-001
Research Category:	Not Applicable
Focus Category:	Models, Water Supply, Management and Planning
Descriptors:	None
Principal Investigators:	Joseph A Daraio

Publications

1. Bechtold, A., M. McCarthy, C. Spurgin, J. Tucci (undergraduate students) and J.A. Daraio, 2015, Climate Change Impacts on Stream Flow in Two New Jersey Watersheds,17th Annual Rowan University Science, Technology, Engineering, & Mathematics (STEM) Student Research Symposium, April 24, 2015, Glassboro, NJ (Poster)
2. Daraio, J.A., 2014, A Comparative Analysis of Hydrologic Response to Climate Change in Developed and Undeveloped Watersheds on the New Jersey Coastal Plain, AGU Fall Meeting, December 15 19, 2014, San Francisco, CA (Poster)

Modeling hydrologic and stream temperature response to climate change in developed and developing watersheds: a comparative analysis.

Progress Report

PI Information

Investigator: Dr. Joseph A Daraio

Institutional Address: Department of Civil and Environmental Engineering

Rowan University

201 Mullica Hill Road

Glassboro, NJ 08028

Telephone Number: (856) 256-5308

Fax Number: (856) 256-5242

Email Address: daraio@rowan.edu

Number of students supported:

Undergraduates: 6

Master's students: 2

Ph.D students: 0

Postdoctoral: 0

Project Summary

Problem and Research Objectives

While the processes controlling runoff response to land-use change and urbanization are relatively well understood and have been much documented (WEF and ASCE, 2012), each watershed is unique. The basic runoff generating processes may be the same or similar, however the interactions between rainfall, infiltration, overland flow, subsurface flow, groundwater flow, and stream flow are likely to differ between watersheds and even within sub-basins of a watershed, e.g. within urbanized sub-basins of a larger watershed. Climate change can affect basin hydrologic response through changes in precipitation that affect runoff timing, volume, and intensity, but few generalizations can be made. Including the effects of climate change adds complexity and uncertainty to our understanding and prediction of hydrologic response, but it must be included in any such analysis.

There is a need for place-based research that can illuminate both general hydrologic understanding and provide insight to the response of local watersheds and potential economic and infrastructure impacts. The main aspect this work is to develop rainfall-runoff models in two watersheds in New Jersey in order to assess and understand through a comparative approach how each watershed responds. These models will be used for issues that are particularly important for New Jersey. For example, rising sea level due to climate change could impact coastal infrastructure for over 6 million people in New Jersey (Williamson et al, 2008), and there is little known about how hydrologic impacts may interact with seal level rise, e.g. to affect both coastal and inland flooding. The impacts of Hurricane Sandy highlight the vulnerability of New Jerseys coastal infrastructure. Additionally, it is not known if and how sea level rise may impact freshwater ecosystems further inland.

Climate change can affect stream temperatures directly due to increases in air temperature, and indirectly by altering meteorological inputs, e.g. including changes in precipitation and changes in cloud cover. Land use change, loss of riparian shading, changes in channel morphology, changes in groundwater exchange, and release of water from impoundments can locally impact

heat flux processes as well (Hester and Doyle, 2011). For example, LeBlanc et al. (1997) reported increases up to 4° C due to land-use change. As with stream flow, heat flux processes in streams are influenced by a complex array of interacting climate, land-use, and instream parameters (Webb, 1996; Webb et al., 2008), and there is a need to understand and parse out the relative importance of these heat flux processes. At present, there are little or no data available on stream temperature in New Jersey watersheds, and it is vital to have a network of instruments to collect stream temperature data from the field in order to better understand stream temperature response to land-use and climate change.

The work proposed here is to develop hydrologic models for two watersheds in New Jersey and set up a small network of temperature sensors in these watersheds in order to address some of the issues discussed above. Specifically, the work proposed will provide some insight into the potential impacts of climate change on hydrology, help to identify some potentially important issues in New Jersey watersheds, and contribute to our general knowledge of potential impacts of climate change on water resources. The objectives of the proposed project are

1. to develop, calibrate, and validate rainfall-runoff models for two watersheds in New Jersey with urban, developing, and undeveloped areas,

2. to use these models to assess the potential impacts of climate change through 2100 on hydrologic response in these basins under current land-use conditions, and

3. to put in place a network of stream temperature sensors in these watersheds for collection of field data to be used for analysis and the development of stream temperature models.

Methodology

Rainfall-runoff models will be developed for 2 watersheds in New Jersey where sufficient stream flow data are available for model calibration. The Maurice River has several USGS gages with enough stream flow data to calibrate and validate a rainfall-runoff model. The Maurice River watershed includes a mixture of urbanized (Vineland is the largest urban area) and agricultural

land-use and is an area where population growth rates are expected to be relatively high. The Batsto River watershed has a USGS stream flow gage with data available for model calibration and validation. This is in the Pinelands region, which is mostly forested and where development is occurring and is expected to continue in the future.

The USGS Precipitation-Runoff Modeling System (PRMS) (Leavesly et al, 2006), a distributed rainfall-runoff model with a one day time step, was used for hydrologic simulations. Meteorological data available from the United States Geological Survey (USGS) Geo Data Portal were used to drive PRMS simulations. These data included both observed and projected gridded climate data. Observed 12 km gridded data from (Maurer et al., 2002) was used for PRMS calibration and validation in each of the watershes models.

The calibrated and validated PRMS model simulations driven by downscaled climate projections through 2100 were used to assess potential changes in stream flow due to climate change. PRMS requires daily precipitation, maximum temperature, and minimum temperature data for simulations. These data were downloaded through the USGS Geo Data Portal both for historical collected data between 1970-2000 and for future climate projections between 2006-2100. Data from 16 General Circulation Models (GCM) were used. GCM simulations from 1970–2000 were used for baseline to estimate potential changes in stream flow and precipitation due to climate change. Air temperature, stream flow, and precipitation anomalies were calculated from these baseline simulations.

Bias corrected downscaled climate projections from the World Climate Research Programmes Coupled Model Inter-comparison Project phase 5 (CMIP5) were used in these analyses. The purpose of these data is for climate and hydrologic projections at spatial scales that are relevant to the watershed and basin-scale decisions that water resources managers and planners face. There are several types of analyses that are permitted with access to the archive including assessment of potential climate change impacts, assessment of climate projection uncertainty, and risk exploration of policy responses that are outlined by potential climate changes. The CMIP5 projections originally launched on the archive during May 2013, and the CMIP5 projections continued to expand

until June 2014.

Although downscaled climate projections were bias-corrected, PRMS simulations using GCM derived data for the historical period 1970–2000 were compared with PRMS simulations driven by observed data from 1970-2000 in order to test for bias in stream flow simulations. This will help in determining uncertainty and validity of projections of changes in stream flow due to climate change.

Stream temperature loggers were placed at selected sites within each watershed, and stream temperature data has been logged since October 2014. These data will be made publically available upon download.

Principal Findings and Significance

Work is ongoing and will be completed February 2016. To date, PRMS models have been calibrated and validated for both the Batsto River watershed and the Maurice River watershed. In the Maurice River, observed data from USGS stream gage 01411500 at Norma NJ (Latitude $39°29'44''$, Longitude $75°04'37''$) were used for model calibration and validation. In the Batsto River, observed data from USGS stream gage 01409500 at Batsto NJ (Latitude $39°38'30''$, Longitude $74°39'01''$) were used for model calibration and validation. Model calibration was done using observed data from water years 1989–1996 (Figures 1 and 2), and model validation was done using observed data from water years 1997–2003 (Figures 3 and 4) for both the Maurice and Batsto PRMS models. Model fit was tested with the R package hydroGOF (Zambrano-Bigiarini, 2014).

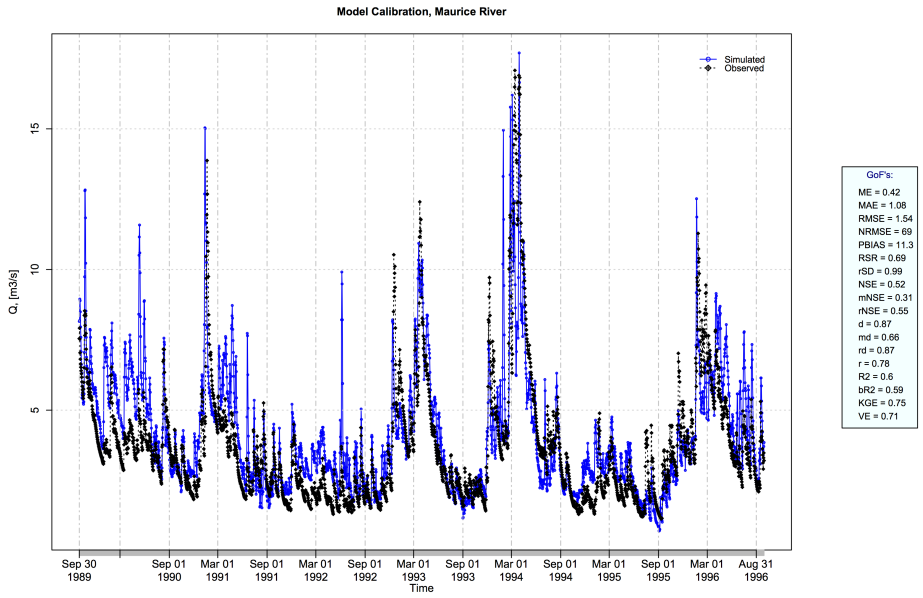

Figure 1: Results of calibration for the PRMS model representing the Maurice River. See text for description of goodness-of-fit (GOF) measures.

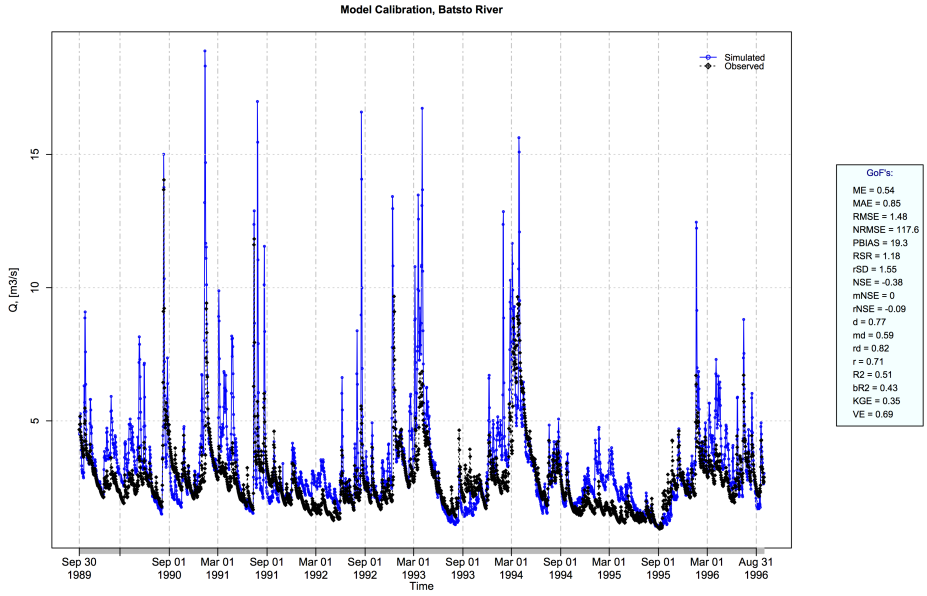

Figure 2: Results of calibration for the PRMS model representing the Batsto River. See text for description of goodness-of-fit (GOF) measures.

Model calibration showed a good fit for both models using a variety of goodness-of-fit (GOF) measures (Table 1). Both models showed some systematic errors that included over estimation of

peak flows and underestimation of low flows. However these errors can be accounted for in our analyses, and model validation indicates that both models are acceptable for our purposes here.

Table 1: Goodness-of-fit (GOF) measures reported by hydroGOF package (Zambrano-Bigiarini, 2014)

Variable	Description
ME	Mean Error
MAE	Mean Absolute Error
RMSE	Root Mean Square Error
NRMSE	Normalized Root Mean Square Error
PBIAS	Percent Bias
RSR	Ratio of RMSE to the Standard Deviation of the Observations, RSR = rms /sd(obs). ($0 \leq$ RSR $\leq$ +Inf)
rSD	Ratio of Standard Deviations, rSD = sd(sim) / sd(obs)
NSE	Nash-Sutcliffe Efficiency (-Inf $\leq$ NSE ≤ 1)
mNSE	Modified Nash-Sutcliffe Efficiency
rNSE	Relative Nash-Sutcliffe Efficiency
d	Index of Agreement ($0 \leq$ d ≤ 1)
md	Modified Index of Agreement
rd	Relative Index of Agreement
r	Pearson product-moment correlation coefficient ($-1 \leq$ r ≤ 1)
R2	Coefficient of Determination ($0 \leq$ R2 ≤ 1). Gives the proportion of the variance of one variable that is predictable from the other variable
bR2	R2 multiplied by the coefficient of the regression line between sim and obs ($0 \leq$ bR2 ≤ 1)
KGE	Kling-Gupta efficiency between sim and obs ($0 \leq$ KGE ≤ 1)
VE	Volumetric efficiency between sim and obs (-Inf $\leq$ VE ≤ 1)

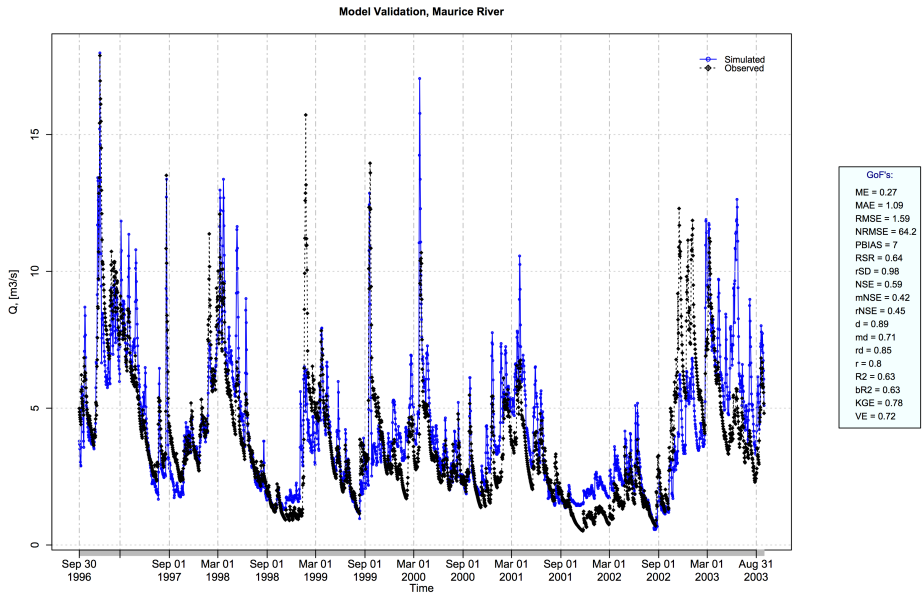

Figure 3: Results of validation for the PRMS model representing the Maurice River. See text for description of goodness-of-fit (GOF) measures.

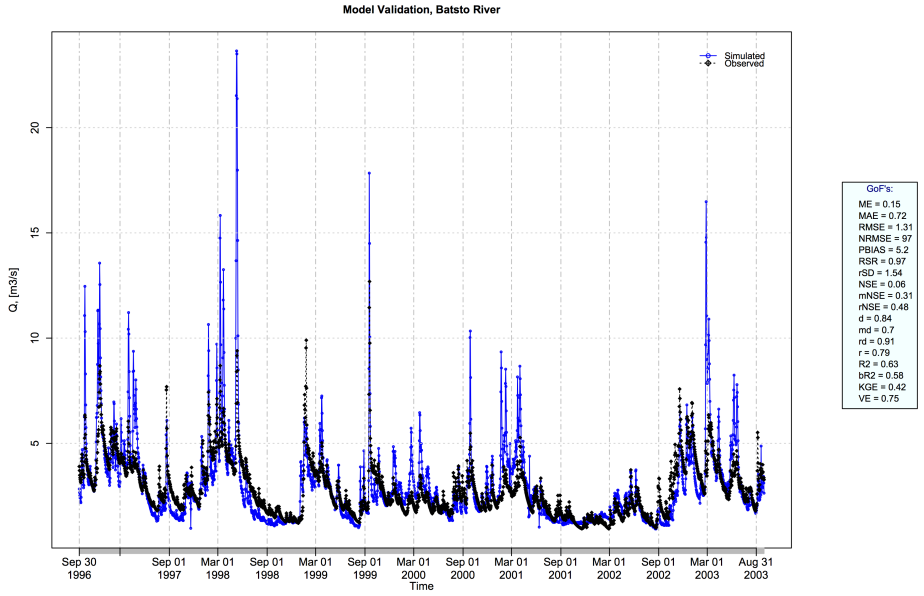

Figure 4: Results of validation for the PRMS model representing the Batsto River. See text for description of goodness-of-fit (GOF) measures.

Several simulations were run using downscaled climate projections through 2065 and through 2099 under Representative Concentration Pathway (RCP) 8.5, which represents the worst case scenerio for greenhouse gas emissions. Preliminary results show that the potential impacts of climate change on stream flow are different in each basin (Figures 5 and 6). Air temperature anomalies and precipitation anomalies showed similar trends in each watershed. However simulations indicated an increase in stream flow in winter and early spring in the Maurice River, and a decrease in stream flows in the winter and spring in the Batsto watershed. Continued analyses as the project moves forward will help elucidate if these changes are consistent with other simulations.

Stream temperature data loggers were set up at 18 sites total, 10 sites in the Maurice River and 8 sites in the Batsto River (Figure 7). Data was collected at all sites in November 2014, and data will be collected at sites in September 2015. Temperature data from the Maurice River at Norma and the Batsto River at Batsto are shown in Figure 8, each location representing the outlet of the watershed.

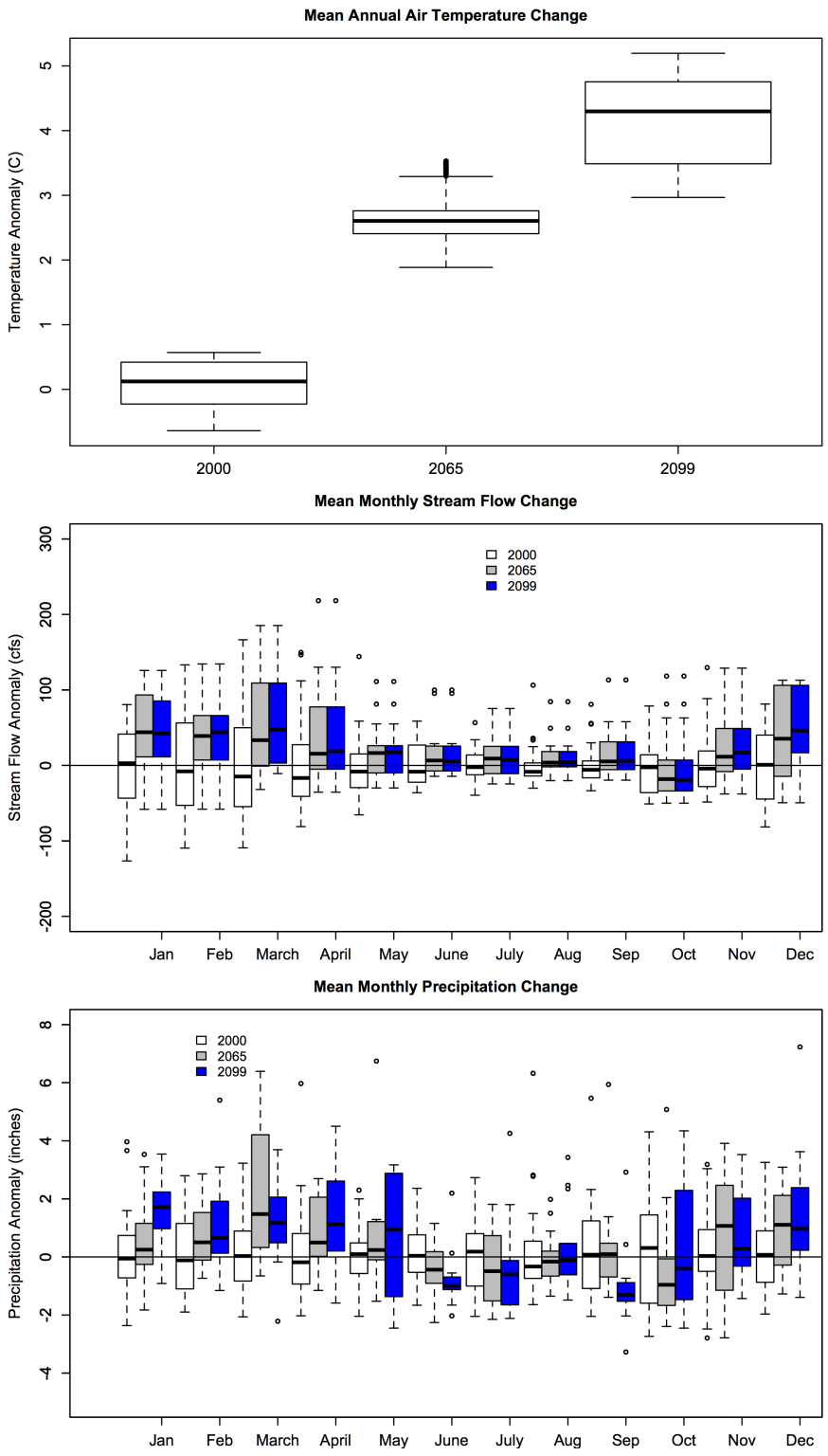

Figure 5: Mean annual air temperature anomalies (°C) for 2050–2065 and 2084-2099 (top), mean monthly stream flow anomalies (cfs) for 2050–2065 and 2084–2099 (middle), and mean monthly total precipitation (in) for 2050–2065 and 2084–2099 (bottom) based on PRMS simulations for the Maurice River.

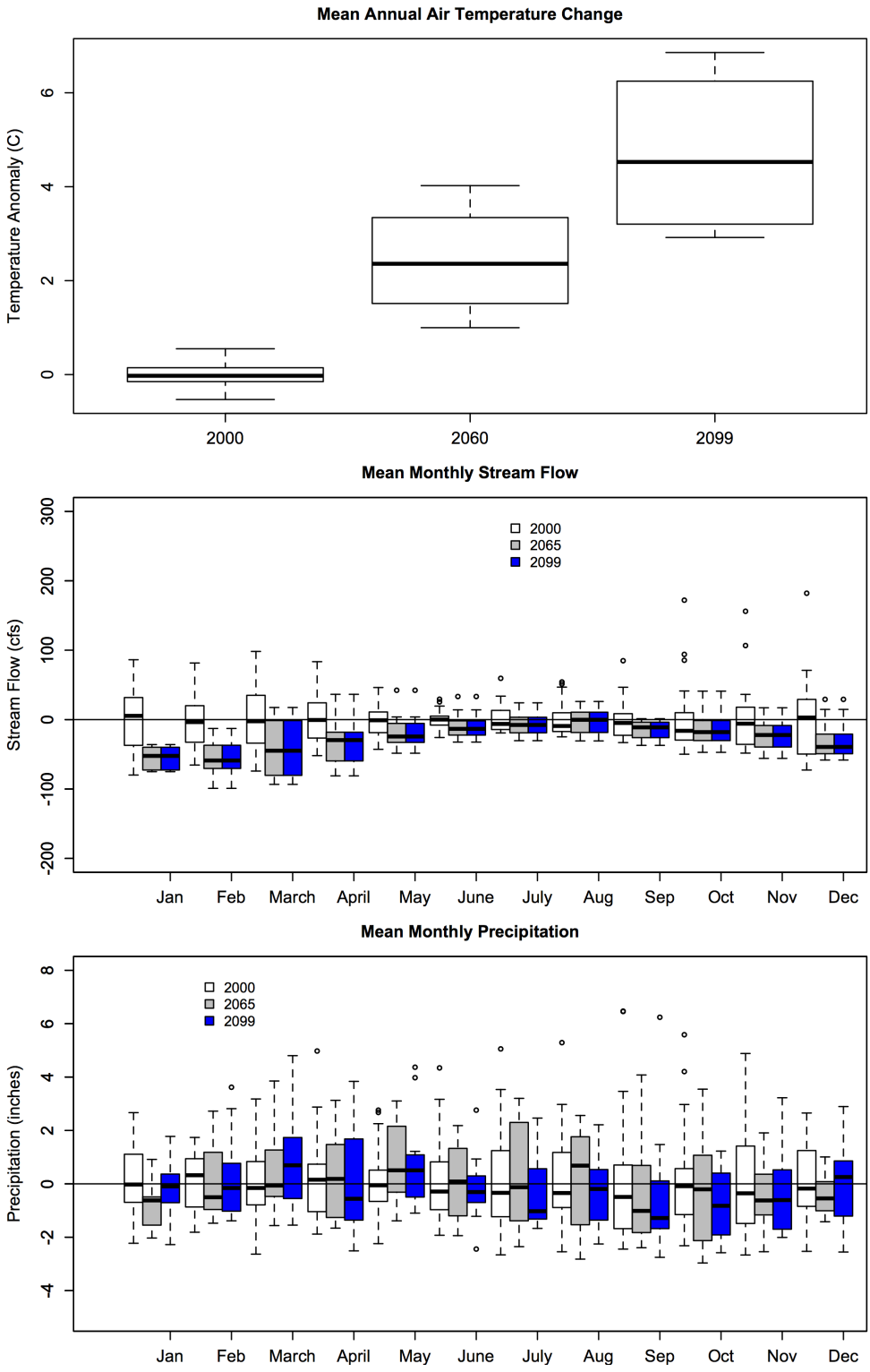

Figure 6: Mean annual air temperature anomalies (°C) for 2050–2065 and 2084-2099 (top), mean monthly stream flow anomalies (cfs) for 2050–2065 and 2084–2099 (middle), and mean monthly total precipitation (in) for 2050–2065 and 2084–2099 (bottom) based on PRMS simulations for the Batsto River.

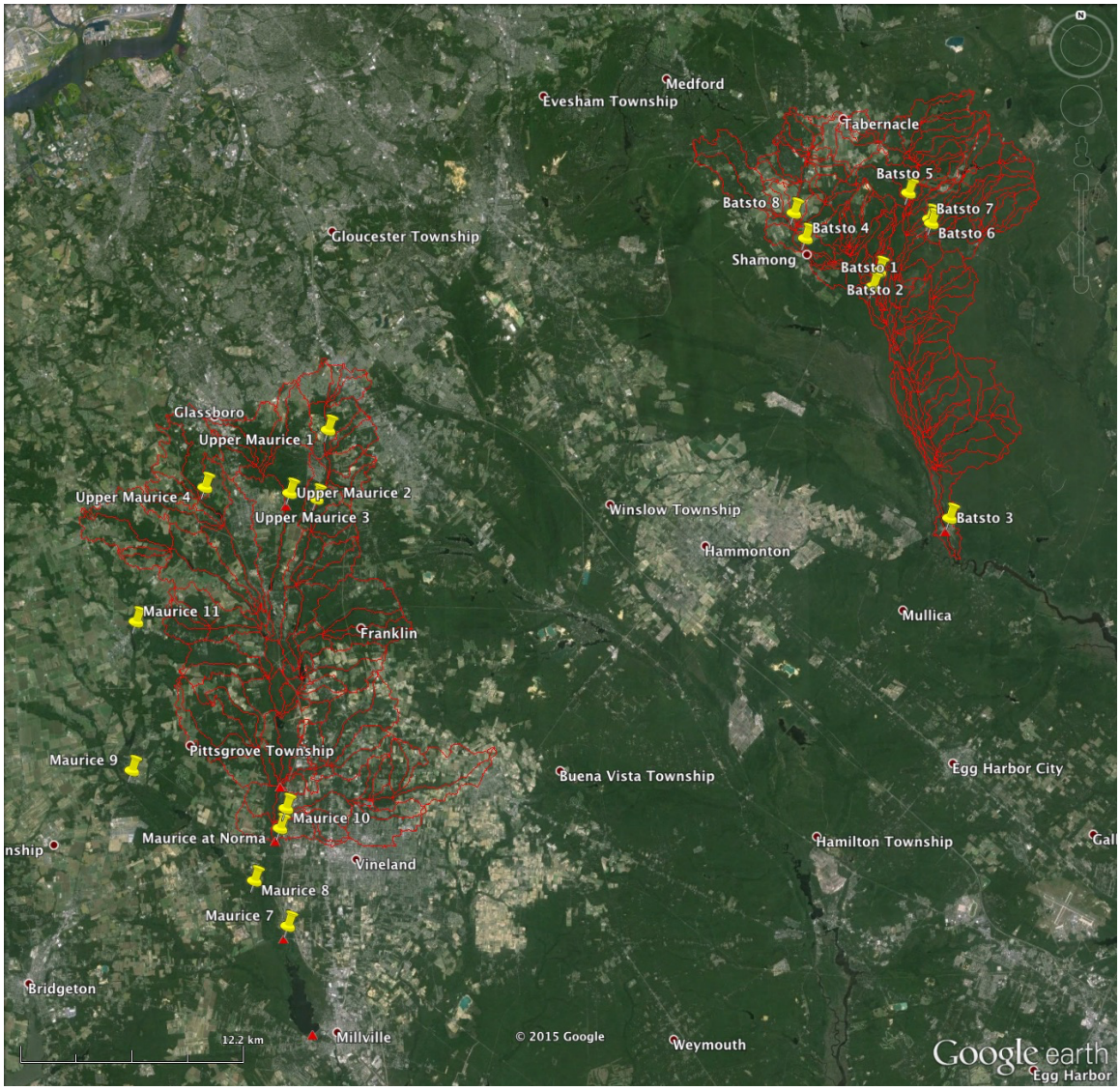

Figure 7: Site location of temperature data loggers in the Maurice and Batsto Rivers (yellow pins). USGS stream gages are shown as red triangles, and polygons show the watershed and hydrologic response units (HRU) in each simulated basin.

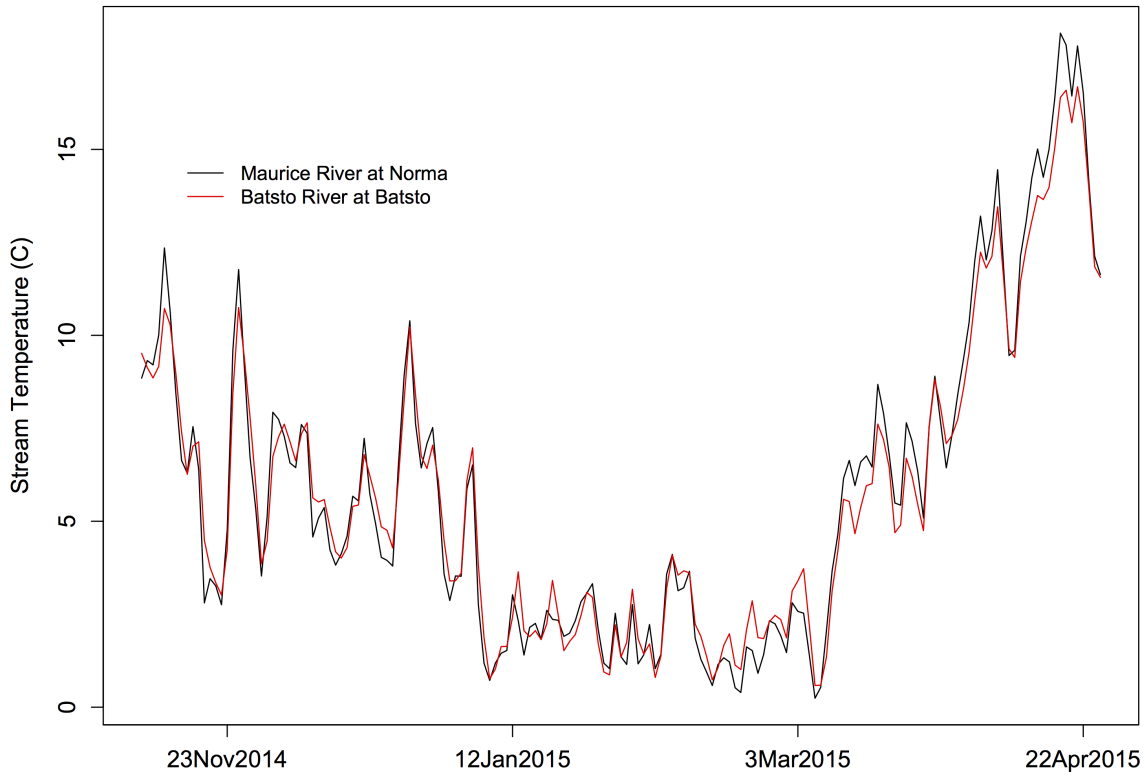

Figure 8: Mean daily stream temperature at sites located at the outlet of each basin.

Publications and Presentations

Posters:

Bechtold, A., M. McCarthy, C. Spurgin, J. Tucci (undergraduate students) and J.A. Daraio. 2015. "Climate Change Impacts on Stream Flow in Two New Jersey Watersheds." 17th Annual Rowan University Science, Technology, Engineering, & Mathematics (STEM) Student Research Symposium, Glassboro, NJ, April 24, 2015

Daraio, J.A. 2014. "A Comparative Analysis of Hydrologic Response to Climate Change in Developed and Undeveloped Watersheds on the New Jersey Coastal Plain." AGU Fall Meeting, San Francisco, CA, December 15–19, 2014.

References

Hester, ET, MW Doyle (2011). Human impacts to river temperature and their effects on biological processes: A quantitative synthesis. *J. Amer. Water Resour. Assoc.* **47**(3): 571–587. DOI: 10.1111/j.1752-1688.2011.00525.x.

LeBlanc, R, RD Brown, JE FitzGibbon (1997). Modeling the Effects of Land Use Change on the Water Temperature in Unregulated Urban Streams. *J. Environ. Manage.* **49**(4): 445–469. DOI: 10.1006/jema.1996.0106.

Maurer, EP, AW Wood, JC Adam, DP Lettenmaier, B Nijssen (2002). A Long-Term Hydrologically-Based Data Set of Land Surface Fluxes and States for the Conterminous United States. *J. Climate* **15**(22): 3237–3251.

Webb, BW (1996). Trends in stream and river temperature. *Hydrol. Process.* **10**(2): 205–226.

Webb, BW, DM Hannah, RD Moore, LE Brown, F Nobilis (2008). Recent advances in stream and river temperature research. *Hydrol. Process.* **22**(7): 902–918. DOI: 10.1002/hyp.

WEF, ASCE (2012). *Design of Urban Stormwater Controls*. MOP 87/WEF FD-23. Water Environment Federation; Environmental and Water Resources Institute of ASCE; McGraw-Hill Professional.

Zambrano-Bigiarini, M (2014). *hydroGOF: Goodness-of-fit functions for comparison of simulated and observed hydrological time series*. R package version 0.3-8.

Assessing Impervious Cover for Application of Green Infrastructure Practices "Undergraduate Student Research Initiative"

Basic Information

Title:	Assessing Impervious Cover for Application of Green Infrastructure Practices "Undergraduate Student Research Initiative"
Project Number:	2014NJ351B
Start Date:	3/1/2014
End Date:	2/28/2015
Funding Source:	104B
Congressional District:	NJ-006
Research Category:	Not Applicable
Focus Category:	Water Quality, Management and Planning, Floods
Descriptors:	None
Principal Investigators:	Christopher Obropta

Publications

1. Obropta, Christopher and S. Mellor, May 2015,Impervious Cover Assessments: A New Tool in Urban Extension to Reduce Flooding and Improve Water Quality in New Jersey, National Urban Extension Conference, Atlanta, GA (Poster)
2. Obropta, Christopher, January 2015, Planning and Designing Green Infrastructure Resiliency in the Raritan River Basin, International Low Impact Development Conference 2015, Houston, TX (Presentation)
3. Del Monaco, Nicole, C. Obropta, D. Swiderski-Soto, May 2015, Impervious Cover Assessments: A New Tool for Promoting Climate Resiliency in New Jersey, New Jersey Water Environment Association, Atlantic City, NJ (Poster)

Project Summary:

The project engaged undergraduate students in research on the impacts of impervious cover and assessing viability of impervious surfaces for management with green infrastructure practices that will help municipalities become more resilient to the changing climate. The project focused on the municipalities within the Raritan River Basins. The Raritan River Basin is approximately 1,100 square miles in size and contains portions of seven counties and 98 municipalities. Based upon a preliminary land cover analysis of the entire basin, the basin contains 140 square miles of impervious cover or 89,482 acres of impervious cover. For the New Jersey Water Quality Design Storm of 1.25 inches of rain over two-hours, approximately three billion gallons of stormwater runs off these impervious surfaces. Assuming an annual rainfall of 44 inches, approximately 107 billion gallons of stormwater runs off these impervious surfaces per year. As the climate continues to change, New Jersey can expect more intense storms and more annual rainfall, which will result in more flooding and higher risk for residents and businesses within the Raritan River Basin. To help municipalities in the Raritan River Basin become more resilient, stormwater runoff from impervious surfaces has to be better managed. This project developed tools to identify, assess and prioritize impervious surfaces for applications of green infrastructure practices to help successfully reduce flooding, improving water quality, and enhancing resiliency.

Methodology:

The first step to reducing the impacts from impervious surfaces was to conduct an impervious cover assessment. New Jersey Department of Environmental Protection's (NJDEP) land use/land cover geographic information system (GIS) data layer was used to determine the impervious cover for three municipalities within the Raritan River Watershed (Hillsborough Township, Manville Borough, and Montgomery Township). For example, single unit, medium density development has been defined by the NJDEP as residential urban/suburban neighborhoods greater than 1/8-acre and up to and including 1/2-acre lots. These areas generally contain about 30 to 35% impervious surface areas[1]. In the NJDEP land use/land cover GIS data layer each land cover polygon has an associated impervious cover percentage. These percentages were used to determine the acres of impervious cover for each municipality.

In developed landscapes, stormwater runoff from parking lots, driveways, sidewalks, and rooftops flows to drainage pipes that feed the sewer system. The cumulative effect of these impervious surfaces and thousands of connected downspouts reduces the amount of water that can infiltrate into soils and greatly increases the volume and rate of runoff that flows to waterways. Stormwater runoff volumes for the impervious surfaces were calculated for the New Jersey Water Quality Design Storm of 1.25 inches of rain, an annual rainfall of 44 inches, the 2-year design storm (3.3 inches of rain), the 10-year design storm (5.0 inches of rain), and the 100-year design storm (8.3

[1] Anderson, James R., et al. 1976. A Land Use And Land Cover Classification System for Use with Remote Sensor Data: Geological Survey Professional Paper 964. Edited by NJDEP, OIRM, BGIA, 1998, 2000, 2001, 2002, 2005. http://www.state.nj.us/dep/gis/digidownload/metadata/lulc02/anderson2002.html

inches of rain). While these assessments were completed on a municipal basis, they were further divided by watershed within the municipality.

After the completion of the impervious cover assessment for each municipality, a reduction action plan was completed for each municipality. Digital imagery will be used to identify opportunities for implementing impervious cover management strategies. Several factors were considered including property ownership, availability of useable land on site, and proximity to waterways. For each opportunity the appropriate green infrastructure practices was identified. Large scale systems such as constructed wetlands or bioretention system were considered to treat residential or commercial developments. Small scale systems also were considered such as rain gardens will be considered for individual lots (e.g., churches, schools, businesses, homes). The environmental benefits for each recommended practice were provided in the plan including stormwater volume managed, expected pollutant load reductions, and wildlife habitat enhancements.

Principle Findings and Significance:

The two students that completed the impervious cover assessments and reduction action plans presented their work at the New Jersey Water Environmental Association meeting in the poster session. Their poster won first place in the competition. Impervious cover in each municipality was determined and 20 to 40 potential green infrastructure projects were identified in each municipality. Calculations were made to determine the runoff volume reductions that could be achieved by implementing the recommended projects and the pollutant load reduction associated with these projects. Concept plans were developed for several sites and the towns are considering implementing several of the recommended projects.

Developing nano-activated carbon based technology for groundwater remediation

Basic Information

Title:	Developing nano-activated carbon based technology for groundwater remediation
Project Number:	2014NJ352B
Start Date:	3/1/2014
End Date:	2/29/2016
Funding Source:	104B
Congressional District:	NJ-006
Research Category:	Not Applicable
Focus Category:	Groundwater, Treatment, Toxic Substances
Descriptors:	None
Principal Investigators:	Chengyu Chen, Weilin Huang

Publications

There are no publications.

NJWRRI FY2014 Annual Report – Progress Report

Developing carbon nanoparticles (CNPs) based technology for groundwater remediation

Chengyu Chen

(1) PI information:

Dr. Weilin Huang (thesis advisor)

Rutgers, The State University of New Jersey, Department of Environmental Sciences, 14 College Farm Road, New Brunswick, New Jersey 08901; Email: whuang@envsci.rutgers.edu; Telephone: (848) 932-5735; FAX: (732) 932-8644.

(2) Numbers of Students Supported:

1 Ph.D. student: Chengyu Chen

Rutgers, The State University of New Jersey, Graduate School, Department of Environmental Sciences, 14 College Farm Road, New Brunswick, New Jersey 08901; Email: chengyuc@scarletmail.rutgers.edu; Telephone: (732) 789-3077; Amount of funding: $5,000.

(3) Project Summary:

a. Problem and Research Objectives

The proposed research program addresses groundwater pollution and remediation, one of pressing environmental issues in the state of New Jersey. New Jersey has the most superfund sites in the US [1], many of which have volatile organic compound (VOCs), e.g., 4-chlorophenol (4CP) and aniline, as major pollutants in their groundwater systems [2]. Conventional technologies such as pump and treat are not cost effective, and *in situ* remediation technologies such as bioremediation and permeable reactive barriers (PRBs) have disadvantages including the risk of toxic intermediates and adverse impacts on secondary water quality objectives [3]. More recent developments proposed to inject nanoscale zero-valent iron (nZVI) or nano carbon tube (CNT) materials to groundwater for remediation of chlorinated solvents. However, these nanomaterials have limited success due to their poor transport properties. Although nZVI has been reported to have high reactivity [4], it agglomerates rapidly into larger micron-sized particles [5] in water, substantially reducing the efficiency of degradation process [6]. Study demonstrated that nZVI had limited mobility (traveling for a few meters at most from the injection well) and had longevity up to a few months [7]. Similarly, because CNT has lengths up to micrometers [8] and settles quickly in water, it does not have good transport properties for penetrating through aquifer materials or dispersing well in groundwater systems. Meanwhile, CNT does not exhibit high adsorption capacities towards chlorinated solvents [9].

To address these problems, the objectives of this research are to study four novel types of carbon nanoparticles (CNPs), which include nano-sized activated carbons and nano-sized biochars. The CNPs are hypothesized to have stronger adsorption capacities for chlorinated organic compounds in water, and more importantly, have specific properties to remain stable against natural sedimentation and particle aggregation in natural groundwater conditions. Such properties are indicative that the CNPs will remain suspended and dispersed well over extended time period

in natural groundwater conditions, so that they can travel long distance in aquifer to adsorb typical volatile organic compounds.

Systematic experiments have been conducted for characterizing the physicochemical properties of the CNPs, quantifying their adsorption capacities for two model VOCs contaminant in groundwater – 4CP and aniline, and studying the stability properties of CNPs in terms of the sedimentation in quiescent purified water and the CNPs aggregation process in quiescent natural groundwater conditions under different ionic strength and pH conditions. Results so far have shown these CNPs to be very promising for remediating groundwater contaminated with VOCs via an *in situ* injection method.

b. Methodology

i. Sample Characterization

Four types of commercial carbon nanoparticles (CNPs) produced from different raw materials were purchased and named as CNP1, CNP2, CNP3, and CNP4, where CNP1 and CNP2 were nano-sized biochar, and CNP3 and CNP4 were nano-sized activated carbon. A powdered activated carbon (PAC) and a multi-walled carbon nanotube (CNT) material were also used in this study for comparison. All carbonaceous materials were used as received. They were measured for their total N_2-BET specific surface area (SSA), total pore volume, average pore radius, and distribution of the surface area within the pores using a nitrogen gas adsorption technique. Transmission electron microscope (TEM) and Scanning electron microscope (SEM) were employed to examine their sizes and morphologies. Elemental analysis (EA) and X-ray photoelectron spectroscopy (XPS) were conducted to quantify their elemental compositions. Fourier transform infrared spectroscopy (FTIR) spectra were obtained for characterizing the functional groups. Dynamic light scattering (DLS) measurements were performed to determine their size distribution.

ii. Adsorption Experiment

Aqueous adsorption of 4-chlorophenol (4CP) and aniline on the four types of CNPs, PAC, and CNT was investigated in this study. Adsorption isotherms were measured at room temperature (25ºC) and pH 6 using a batch system. Each batch reactor contained 50mL of 4CP or aniline solutions with various initial concentrations. A constant mass of a sorbent was added to achieve around 50% reductions in the initial solute concentration upon equilibrium. Duplicate samples were prepared for each batch system. Reactors were mixed by tumbling top to bottom at 150 rpm. After attainment of adsorption equilibrium, mixtures of solution and sorbent were taken at from the reactors and were filtered through 0.22 μm. The filtrates were analyzed for the aqueous 4CP or aniline concentrations using a high performance liquid chromatography (HPLC) equipped with a diode array UV detector. Control experiment was run to access the loss of solute to reactor components. Both the Freundlich isotherm equation and the Langmuir isotherm equation were employed to fit the adsorption isotherm data obtained from the batch experiments.

Adsorption kinetics experiments were also performed using the batch method. For each type of the sorbents, duplicates of aqueous solution of 4CP or aniline and a fixed mass of sorbent were added to 500mL screw cap flasks. The reactors were mixed completely by tumbling top to bottom at 150rpm and 25ºC. Samples of the solution-sorbent mixtures were taken at different time intervals, and were filtered and analyzed using the same methods as above.

iii. Electrophoretic Mobility Measurements

To investigate the stability of the CNP particles in natural groundwater system against sedimentation and particle aggregation, the electrophoretic mobility (EPM) of the four types of CNPs was measured using electrophoretic light scattering at different solution chemistry. The EPM of the CNPs were converted to zeta potentials (ζ) with the software built-in the instrument. The EPM were measured for CNPs at different solution chemistry resembling natural groundwater conditions, using sodium chloride or calcium chloride at different ionic strength or pH conditions. All measurements were conducted at 20 ºC.

iv. Sedimentation Experiments

Four types of CNPs, PAC, and CNT were prepared in purified water to compare their sedimentation rates. Each sample after sonication was diluted with deionized water to make aqueous solution of the same concentration. 4 mL of stock solution of each sample was introduced into a clean spectrophotometer cuvette. Samples were sealed and stored in dark at room temperature for natural sedimentation. The light intensity, *I*, of the samples were measured periodically over two months by a at 675 nm wavelength. The fraction of particles remained suspending in water over time was measured as the light intensity at time t, *I(t)*, over its initial light intensity, *I(0)*. All experiment and measurements were conducted at pH 6.

v. Determination of CNPs Aggregation Process and Kinetics

To determine the aggregation processes of CNPs in different solution chemistry, time-resolved dynamic light scattering (DLS) measurements were performed for the hydrodynamic sizes of CNPs. The sonicated CNPs aqueous solutions were diluted with deionized water to make the same concentration. For each experiment, 2 mL of CNPs solution was introduced into a clean glass vial. pH of the solution was adjusted before 2 mL of prepared electrolyte solution with predetermined concentration was introduced into the vial containing the NAC suspensions to induce aggregation. The vial was briefly vortexed before being inserted into the DLS instrument and measurement was started immediately. The scattered light was detected by a photo-detector at a scattering angle of 90º. The intensity-weighted hydrodynamic radius, R_h, of the particles measured was determined through cumulant analysis. The aggregation processes of CNP at the starting 20 minutes were recorded by measuring the R_h. The samples were then sealed and left undisturbed in dark for continued aggregation. The hydrodynamic radius and the polydispersity of the CNP samples remained suspending in solution was monitored over two months to observe the stability against aggregation by the electrolytes in solution. All DLS measurements were conducted at 20 ºC.

To estimate the stability of CNPs against aggregation, the aggregation kinetics and the critical coagulation concentration (CCC) of the CNPs at different solution chemistry were determined from the aggregation data obtained above. At the initial stage of nanoparticle aggregation, the hydrodynamic radius measured by DLS, $R_h(t)$, increases linearly with time, *t*. Therefore, the initial aggregation rate constant, *k*, can be determined from the slope of the linear range of the aggregation profiles. The aggregation attachment efficiencies, α (equivalent to the inverse stability ratio, *1/W*), which range from 0 to 1, were calculated to quantify the initial aggregation kinetics of the CNPs at different electrolyte concentrations and pH conditions. The calculation was done by normalizing the slopes obtained under different electrolyte concentrations by the slope obtained under favorable aggregation conditions, which refers to fast or nonrepulsive aggregation conditions. From the determined attachment efficiency profiles, the CCC of the CNPs at different natural groundwater conditions was determined. By extrapolating through the fast and slow aggregation regimes, the

intersections of the extrapolation yield CCC [10], which were indicative of the CNPs stability against aggregation at the specific solution conditions.

c. Principal Findings and Significance

i. Sample Characterization

DLS, TEM, and SEM analysis have shown that all four types of CNPs are mainly spherical particles and some irregularly shaped ones, with diameter around 100 nm; PAC has diameter in micron range; and CNT has diameter in 100 nm while length in microns. N_2-BET SSA analysis showed that the specific surface area of CNP1, CNP2, and CNP3 are around 1000 m^2/g; while CNP4, PAC, and CNT have SSA about 300, 600, and 40 m^2/g, respectively. Such results indicated that CNP1, CNP2, and CNP3 with much higher SSA should have much higher adsorption capacity for VOCs compared to CNP4, PAC, and CNT. BET SSA analysis also showed that for all types of CNPs, more than 80% of pores are within radius of 20 Å, while PAC and CNT have much larger pores. Elemental analysis showed that the oxygen content of CNPs were about 10%, while XPS showed agreed that CNPs have oxygen content of about 6%. The difference in results between EA and XPS is because EA analyzed for the bulk sample while XPS probes the sample surface. Yet the high oxygen content from two analyses both suggested possible negative charges present on the CNP surface. The C-O and C=O stretching vibration from FTIR analysis of CNP samples also demonstrated the presence of oxygen containing functional groups. However, potentiometric titration of CNP samples is still needed to provide further evidence of the origin of CNP charge on the particle surface, which is the key to explaining the stability of CNPs in water against sedimentation and aggregation.

ii. Adsorption Experiments

So far experiments have been performed on the adsorption of 4CP and aniline by the four types of CNPs and PAC. All adsorption data fit better to the Freundlich isotherm equation than the Langmuir isotherm model, where the fitting of the data to the Freundlich isotherm model produced fitting coefficients of determination, R^2, all above 0.98, while Langmuir isotherm had R^2 below 0.98. The difference on the fitting between these two models may be due to the fact that Langmuir isotherm assumes homogeneous sorbent surface and monomolecular layer of adsorbate coverage with no interaction among adsorbed molecules, however, the activated carbon and biochar samples used in the experiments are heterogeneous materials. In general, the adsorption of 4CP was much stronger by CNPs and PAC comparing to the adsorption of aniline. This may be due to the stronger hydrophobic interactions between the carbon materials and 4CP comparing to aniline, where 4CP has a higher $\log(K_{ow})$ value of 2.39 compared to 0.90 for aniline [11]. The lower water solubility of 4CP (26 g/L) compared to aniline (34 g/L) is also consistent with such results [12]. For adsorption of both 4CP and aniline, CNP1, CNP2, and CNP3 showed only slightly higher adsorption capacity compared to PAC, but exhibited much higher adsorption capacity compared to CNP4. This correlated well with the SSA data from sample characterization.

Adsorption kinetics experiments for 4CP showed that CNP1, CNP2, CNP3, and PAC removed up to 50% of 4CP from the aqueous phase in 3 minutes, given that the adsorbent amounts added to solution were up to 80% removal of adsorbate from aqueous phase upon equilibrium. The fast adsorption rates should be due to the high SSA of these four carbon materials. However, CNP1, CNP2, and CNP3 reached equilibrium in 1 hour, while PAC did not reach equilibrium until 5 days. The higher rates of adsorption from CNP1, CNP2, and CNP3 may be due to their much smaller

average pore radius (17 Å) compared to PAC (35 Å). The smaller pores of CNPs may trap 4CP upon entry, while the larger pores of PAC may release adsorbed 4CP thus taking longer time to reach adsorption equilibrium. Compared to these four carbon materials, CNP4 adsorbed 4CP much more slowly because of its much smaller SSA. The adsorption kinetic experiments for aniline showed similar trends as 4CP as discussed, however, the overall adsorption rates of aniline were faster compared to 4CP, given up to about 70% of aniline adsorbed from aqueous phase in 3 minutes of contact with the carbon materials. This phenomenon may be explained from the size of the adsorbate given other conditions the same. Aniline with a smaller molecular weight (93 g/mol) may enter the carbon pores more quickly than 4CP with molecular weight of 128 g/mol, even though the equilibrium adsorption capacity of aniline was lower than 4CP as discussed previously.

The major findings in adsorption experiments so far have shown that CNP1, CNP2, and CNP3, in comparison with PAC and CNP4, have high adsorption capacity for VOCs such as 4CP and aniline, and can remove these contaminants from water in minutes upon contact. Such promising carbonaceous materials can be applied in groundwater remediation of VOCs or act as emergent treatment agents for organic chemical spills.

iii. Stability of CNPs against Sedimentation and Aggregation in Water

The measured EPM values were converted to Zeta Potential (ζ) for the CNPs in purified water. CNP1, CNP2, and CNP3 had Zeta Potential of about -50 mV, while CNP4 had -30 mV. Such negative values indicate that the surface of the CNPs is very negatively charged, which agree with the high oxygen content from EA and XPS analysis. With the negatively charged surface, CNPs should be very stable against sedimentation and aggregation in water because of the strong repulsive electrostatic force existing between each carbon nanoparticle.

We have compared the natural sedimentation rates among the CNPs to PAC, CNT, ZVI, and fullerene nanoparticles (C_{60}) in quiescent purified water. Results showed that CNT and ZVI settled almost completely from water after one hour; PAC and C_{60} settled after 4 days and 20 days, respectively; however, all four types of CNPs had about half of the particles remained suspending in water after 2 months. The hydrodynamic radius, R_h, of CNPs samples after 2 months measured by DLS remained about 50 nm as the original size, indicating no significant aggregation occurred. Therefore, CNPs are very stable in quiescent purified water against settling and aggregation compared to other commonly particles used for groundwater remediation.

The stability of CNPs against aggregation was further examined from the carbon nanoparticles aggregation under different sodium chloride or calcium chloride concentrations. The concentrations of NaCl used in the experiments to induce CNP aggregation ranged from 0 to 600 mM, and $CaCl_2$ ranged from 0 to 200mM at pH 6. For all CNPs, the Zeta Potentials became less negative as electrolyte concentrations increased. As discussed before, the carbon nanoparticles with high negatively charged surface experience strong repulsive electrostatic forces at low electrolyte concentration. However, as salt concentration increases, the negative charges on the CNP surface are screened out and attractive van der Waals forces dominate between the nanoparticles [10]. Therefore, Zeta Potential became less negative and particle aggregation started. Such effects of $CaCl_2$ were much more significant than NaCl, due to the fact that divalent ions are much more effective coagulants than monovalent ions.

The aggregation processes can be observed from the aggregation profiles of CNPs measuring particle R_h with time. Consistent with the change in Zeta Potentials, higher electrolyte concentrations induced faster aggregation rates. However, as electrolyte concentrations increased to certain value, the aggregation rates stopped increasing. By converting the slopes of the

aggregation profiles at different electrolyte concentrations, the attachment efficiencies, α, between 0 and 1 were calculated. By extrapolating through the fast and slow aggregation regimes, the intersections of the extrapolation yield critical coagulation concentrations (CCC) of each CNP at the presence of NaCl and $CaCl_2$. For CNP1, CNP2, and CNP3, the CCC of NaCl were 120 mM, and of $CaCl_2$ were 5 mM. For CNP4, the CCC of NaCl was 70 mM, and of $CaCl_2$ was 3 mM, which is in agreement with the Schultz-Hardy Rule [13]. Because typical natural groundwater has sodium concentrations less than 9 mM, and calcium concentrations less than 2.5 mM [14], CNPs should remain stable against aggregation in groundwater conditions.

Continued observation on the R_h and polydispersity of the aggregated CNPs in previous electrolyte solutions over 1 month has further proven the stability of CNPs against aggregation in natural groundwater conditions. Results showed that in the presence of NaCl concentration less than 15 mM, R_h of CNPs remained within 100 nm over 1 month; and in the presence of $CaCl_2$ concentration less than 1 mM, R_h of CNPs remained within 200 nm over 1 month. The polydispersity index increased with time of aggregation. It suggested that the aggregation process increased the size distribution of CNPs, creating carbon particles with more widely distributed sizes as aggregation proceeded.

The pH effect on the Zeta Potential and aggregation of CNPs was also examined. For all CNPs, their Zeta Potentials become increasingly negative at higher pH conditions. This may be due to the fact that the surface functional groups on the CNPs become deprotonated as pH increases. The aggregation profiles of CNPs in NaCl and $CaCl_2$ at different pH conditions reviewed consistent results with the change of Zeta Potentials. Lower pH enhanced CNPs aggregation rates, while higher pH created more negatively charged surface thus suppressed the aggregation process. Nevertheless, because natural groundwater typically has pH within 6.5 to 8.5, CNPs should remain stable against aggregation as the results obtained at pH 6.

In conclusion, in quiescent or slowly flowing natural groundwater system where the ionic strength and pH are under typical conditions, the novel CNPs may remain relatively stably suspended as nanoparticles without aggregation over months. This may be very different from other agents or nanoparticles such as CNT and ZVI which are commonly used for groundwater remediation. This high resistance to aggregation properties may enable CNPs to remain as nanoparticles when they travel long distance in groundwater systems to reach the contaminated zone. In addition, the CNPs used this study have high adsorption capacity and fast adsorption rate for organic pollutants such as 4CP and aniline. With these two unique properties, it is likely that the carbon nanoparticles examined in this study could be used as strong and reactive particles for effectively remediating groundwater systems polluted with organic chemicals.

Literature Cited

1. EPA *Final National Priorities List (NPL) Sites - by State*; October 23, 2013.
2. GoodGuide, Scorecard, the Pollution Information Site. In *Rank Superfund Sites*, 2011.
3. Interstate Technology & Regulatory Council *Technical and Regulatory Guidance for In Situ Chemical Oxidation of Contaminated Soil and Groundwater*; The Interstate Technology & Regulatory Council: 2005.
4. Gillham, R. W.; O'Hannesin, S. F., Enhanced Degradation of Halogenated Aliphatics by Zero-Valent Iron. *Ground Water* **1994,** *32*, 958-967.
5. Phenrat, T.; Saleh, N.; Tilton, R. D.; Lowry, G. V., Aggregation and Sedimentation of Aqueous Nanoscale Zerovalent Iron Dispersions. *Environmental science & technology* **2007,** *41*, 284-290.
6. Tratnyek, P. G.; Johnson, R. L., Nanotechnologies for environmental cleanup. *Nano Today* **2006,** *1*, 44-48.
7. Mueller, N., Application of nanoscale zero valent iron (NZVI) for groundwater remediation in Europe. *Environmental Science and Pollution Research* **2012,** *19*, 550-558.
8. Gupta, V. K.; Agarwal, S.; Saleh, T. A., Chromium removal by combining the magnetic properties ofiron oxide with adsorption properties of carbon nanotubes. *Water research* **2011,** *45*, 2207-2212.
9. Naghizadeh, A.; Nasseri, S.; Nazmara, S., Removal of Trichloroethylene from water by adsorption on to Multiwall Carbon Nanotubes. *Iran. J. Environ. Health. Sci. Eng.* **2011,** *8*, (4), 317-324.
10. Chen, K. l.; Elimelech, M., Relating Colloidal Stability of Fullerene (C_{60}) Nanoparticles to Nanoparticle Charge and Electrokinetic Properties. *Environ. Sci. Technol.* **2009,** *43*, 7270-7276.
11. Hansch. C., A. L. a. D. H., *Exploring QSAR. Hydrophobic, Electronic, and Steric Constants.* . American Chemical Society.: Washington, DC, 1995.
12. Yang, K.; Wu, W.; Jing, Q.; Zhu, L., Aqueous Adsorption of Aniline, Phenol, and their Substitutes by Multi-Walled Carbon Nanotubes. *Environmental science & technology* **2008,** *42*, 7931-7936.
13. Hunter, R. J., *Foundations of Colloid Science*. Second ed.; Oxford University Press: Oxford, New York, 2001.
14. UNESCO; WHO; UNEP, *Water Quality Assessments - A Guide to Use of Biota, Sediments and Water in Environmental Monitoring.* Second ed.; University Press: Cambridge, Great Britain, 1996.

Microbially mediated dehalogenation of polychlorinated dibenzo-p-dioxins (PCDDs) in New Jersey river sediments

Basic Information

Title:	Microbially mediated dehalogenation of polychlorinated dibenzo-p-dioxins (PCDDs) in New Jersey river sediments
Project Number:	2014NJ353B
Start Date:	3/1/2014
End Date:	2/28/2015
Funding Source:	104B
Congressional District:	NJ-006
Research Category:	Not Applicable
Focus Category:	Water Quality, Sediments, Toxic Substances
Descriptors:	None
Principal Investigators:	Hang Dam, Max M Haggblom

Publications

1. Dam, HT and MM Häggblom,2014, Dehalogenation of Chlorinated Dioxins in Hackensack River Enrichment Cultures, Gordon Research Conference, Environmental Sciences: Water, June 22-27, 2014, Holderness School, Holderness, NH (Poster)
2. Dam, HT and MM Häggblom, 2015, Dehalogenation of Chlorinated Dioxins in Hackensack River Enrichment Cultures, Symposium of Microbiology at Rutgers: Cultivating Traditions, Current Strength and Future Frontiers, January 29-30, 2015, Douglas Campus Center, Rutgers University, New Brunswick, New Jersey (Poster)
3. Dam, HT, W Sun, L McGuinness, L. Kerkhof, and MM Häggblom,2015, Investigation of Active Bacterial Community in Dehalogenating Enrichment Cultures by Using Stable Isotope Probing, Theobald Smith Society Meeting in Miniature, April 30, 2015, Cook Campus Center, Rutgers University, New Brunswick, NJ (Poster)

Microbially Mediated Dehalogenation of Polychlorinated Dibenzo-*p*-dioxins (PCDDs) in New Jersey River Sediments

PIs:

Hang T. Dam, Ph.D. Candidate
Department of Biochemistry and Microbiology
Rutgers University – New Brunswick
76 Lipman Drive, New Brunswick, NJ 08901
Email: hangdam@scarletmail.rutgers.edu
Phone: 84932-5640

Thesis Advisor: Max M. Häggblom, Ph.D.,
Department of Biochemistry and Microbiology
Rutgers University – New Brunswick
76 Lipman Drive, New Brunswick, NJ 08901
Email: haggblom@aesop.rutgers.edu
Phone: 848-932-5646

Awards: January, 2015: Poster Prize, Symposium of Microbiology at Rutgers University: Cultivating Traditions, Current Strength and Future Frontiers

Problem and Research Objectives:

Priority Issues: The New York – New Jersey Harbor Estuary is contaminated with various halogenated compounds including polychlorinated dibenzo-*p*-dioxins (PCDDs). Major point sources have been identified in the area such as Standard Chlorine Chemical Company in Kearny, along the Hackensack River and Diamond Alkali Chemical Company on the west bank of the Passaic River (Bopp *et al*, 1991). New Jersey watersheds have been highly impacted by high concentrations of PCDDs released since the 1950s. The dense population and intense industrial activities in the area also contribute to the release of PCDDs into the environment (e.g. combustion sources). Even though the chemical manufacturing processes that generate PCDDs as by-products no longer exist, a significant amount of dioxins are still released into the environment (Duarte-Davidson *et al*, 1997).

PCDDs belong to a group of chemicals which have two benzene rings linked together by two ether bonds, there are up to 8 chlorine atoms attached to the aromatic rings. PCDDs are highly hydrophobic and have the tendency to absorb onto organic matter and penetrate into deep layers of soils and sediments. River sediments become major reservoir of these compounds. As the reservoir, these sediments can release PCDDs into the water phase and from this, some PCDDs can either volatilize into the atmosphere or enter aquatic biota, or be transferred downstream from the source of contamination. Cleanup plans have been designed to remove contaminated sediments from the contaminated rivers in New Jersey (United States Environmental Protection Agency). However residual PCDDs still can cause health problem because of the bioaccumulation and biomagnification of these compounds. Reductive dehalogenation of PCDDs is a promising approach to bioremediate these contaminated sediments but more understanding of the process should be obtained in order to enhance the efficiency of the approach.

Research objectives: Considering that PCDDs are potential electron acceptors and reductive dehalogenases are key enzymes in anaerobic respiratory dehalogenation, my hypothesis is that long term contamination with PCDDs in the Hackensack River sediment can enrich for dioxin dechlorinating bacteria. The objective of my study is to enrich for dioxin dehalogenating bacteria in order to enhance our understanding of their diversity and physiological activity. Knowledge obtained from the research

can be applied in designing an appropriate approach to bioremediate residual PCDDs in contaminated sites.

Methodology

Culture history: Enrichment cultures were set up in December 2012, using 10 % sediments collected from five locations along the Hackensack River as illustrated in Figure 1. 1,2,3,4-Tetrachlorinated dibenzo-*p*-dioxin (1,2,3,4-TeCDD) was added at 20 µM nominal concentration as the only terminal electron acceptor. A mixture of short chain organic acids (acetate, lactate, and propionate) was used as electron donor and carbon source, each at 150 µM nominal concentrations. Samples were taken every month and kept at -20^{o}C until further analysis.

Figure 1. Sampling locations on the Hackensack River, NJ

Chemical analysis: The last samples were taken after 18 months of incubation. After that, chlorinated dibenzo-*p*-dioxins were extracted into toluene as described (Vargas et al., 2003). The extracts were analyzed by Gas Chromatography/Mass Spectrometry according to Liu et al. (2014). Products of dehalogenation were observed over time to determine dehalogenation pathway.

DNA extraction: Genomic DNA was isolated from 2 or 3 ml of enrichment cultures after 0 and 13 months of incubation by PowerSoil® DNA Isolation Kit (Mobio Laboratories, Inc., Carlsbad, CA, USA) with some modification to obtain higher yields. DNA was kept at -80^{o}C until used.

Putative dehalogenating bacterial community profile: Putative dehalogenating bacteria belonging to the *Chloroflexi* phylum were analyzed via nested – Polymerase Chain Reaction (nested-PCR) and Denaturant Gradient Gel Electrophoresis (DGGE) as described in Park et al. (2011). To identify the phylogenetic affiliation of the DGGE bands, a clone library of bacterial communities in H1 and H5 cultures were established using pGEM®-T Easy Vector Systems (Promega, Inc., Madison, WI, USA) and screened by nested-PCR – DGGE. Desired clones were sequenced via Sanger method (Genewiz Inc., South Plainfield, NJ, USA)

Reductive dehalogenase gene profiles: Reductive dehalogenase homologue A (*rdhA*) genes were amplified using 12 primer pairs which are designed to amplify all *rdhA* genes in two *Dehalococcoides* strains 195 and CBDB1 (Park et al, 2011). Seven microliters of PCR products were run on 1% agarose and visualized on a UV transilluminator. Pictures were taken and band intensity was measured and analyzed using ImageJ software (Rasband, 1997)

Stable Isotope Probing (SIP) coupled to Terminal Restriction Fragment Length Polymorphism (TRFLP) to analyze active communities involved in dehalogenation: SIP cultures were set up in triplicate by transferring 10% from enrichment culture H1 after 18 months of incubation into fresh mineral anaerobic medium. 1,2,3,4-TeCDD at 20 µM was spiked in experimental cultures. ^{13}C acetate was amended as the carbon source at 30 µM or 150 µM. Controls cultures were cultures without terminal electron acceptor amended and ^{12}C acetate amended culture. Genomic DNA from those cultures was isolated after 3

months of incubation when 80% of amended 1,2,3,4-TeCDD in experimental cultures was dehalogenated by PowerSoil® DNA Isolation Kit (Mobio Laboratories, Inc., Carlsbad, CA, USA) as described above. ^{13}C labeled DNA was separated from ^{12}C labeled DNA on a CsCl gradient after centrifuging at 80,000 rpm for 48 hours on a Beckman Optima ultracentrifuge (Palo Alto, CA) using a TLA 120 rotor. ^{13}C labeled Archaeal DNA was added for visualization. 16S rRNA amplification and profiling was done using 2 step PCR followed by Terminal Restriction Fragment Length Polymorphism (TRFLP) as described in Tuorto et al. (2014). Terminal restriction fragment (TRF) identification was done using TRFLP for screening of clones generated from ^{13}C labeled DNA of ^{13}C acetate fed culture. Clones with TRFs of interest were sequenced (Genewiz Inc., South Plainfield, NJ, USA)

Principal Findings

Dechlorination of spiked 1,2,3,4-TeCDD

Dehalogenation occurred in all cultures set up from 5 locations along the Hackensack River to a different extent. Dehalogenation of 1,2,3,4-TeCDD in H1 culture which was set up from fresh water sediment collected from an upstream section of the Hackensack River showed the most rapid dehalogenation. Eighty percent of spiked substrate was dehalogenated into 2-MoCDD, no other chlorinated dibenzo-*p*-dioxin congener was detected. Dehalogenation occurred to a lesser extent in the other cultures (Figure 2). In H5 culture which was set up from estuarine sediment near the New York – New Jersey Harbor, tri- and dichlorinated dibenzo-*p*-dioxins accumulated as the major products after 13 months of incubation. No dehalogenating activity was detected in killed controls, which indicates that abiotic dehalogenation did not occur under experimental conditions. Dechlorination of 1,2,3,4-TeCDD occurred via both para- and laternal dechlorinations (Figure 3)

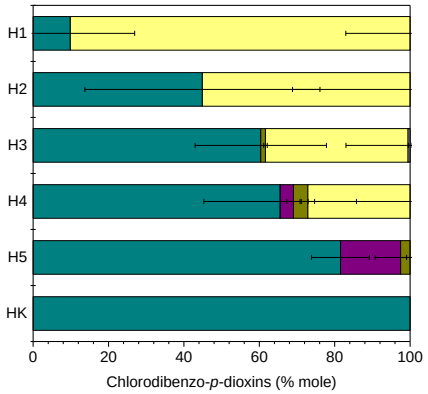

Figure 2. Dehalogenation of spiked 1,2,3,4-TeCDD in Hackensack River enrichment cultures after 13 months of incubation. Control culture (HK) was heat killed.

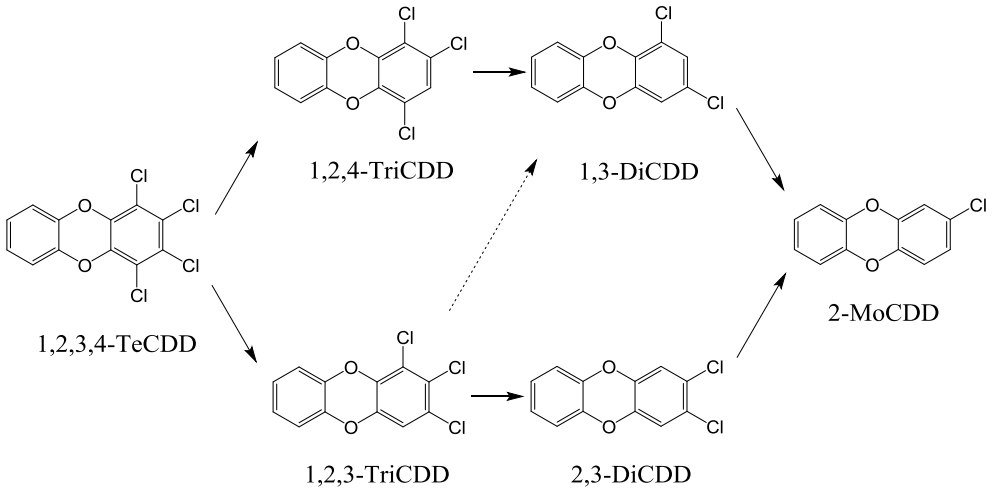

Figure 3. Possible dehalogenation pathways of 1,2,3,4-TeCDD in H1 enrichment cultures. Dashed arrow indicates that the step is likely to happen but further experiments need to be done to confirm.

Putative dehalogenating bacterial Community

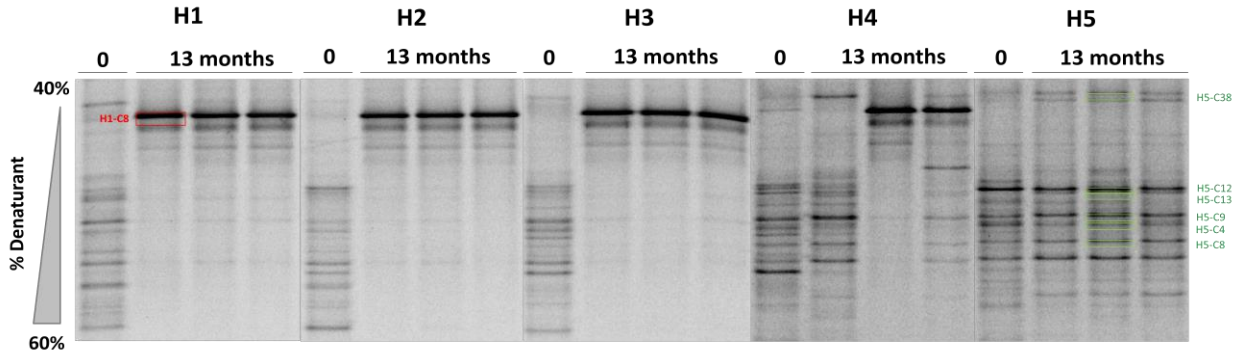

Figure 4. Nested PCR – DGGE analysis of putative dehalogenating *Chloroflexi* community in Hackensack enrichment cultures

Putative dehalogenating bacteria belonging to *Chloroflexi* was determined by nested PCR – DGGE in five enrichment cultures at time 0 and after 13 months of incubation. *Chloroflexi* community was similar in all sediments (time 0) used to set up cultures regardless where they were taken from, although the abundance of each band varied in estuarine sediments (i.e., H4 and H5) compared to fresh water sediments (H1, H2, and H3) (Figure 4). After enrichment, *Chloroflexi* communities in H1, H2, and H3 changed drastically with the enrichment of band H1-C8 which is 100% similar to 16S rRNA gene sequence of *Dehalococcoides* spp. while the other *Chloroflexi* bacteria seemed to be suppressed (Figure 4 & 5). Minor changes in the *Chloroflexi* community were observed in enrichment culture H5 with undetectable band corresponding to *Dehalococcoides* spp. in both sediment and enrichment cultures after 13 months. *Dehalococcoides* spp. was enriched to a different extent in triplicate H4 cultures with H4-2 had the most enriched *Dehalococcoides* population whereas none of the *Dehalococcoides* bands was detected in H4-1 culture. The different in enrichment degrees can be explained by the low abundance of *Dehalococcoides* in the sediment which leads to the uneven distribution of the organism in the inoculum used to set up culture H4. *Dehalococcoides* were found to be present at the abundance as low as 0.1% of the community in natural environments (Hiraishi et al., 2005)

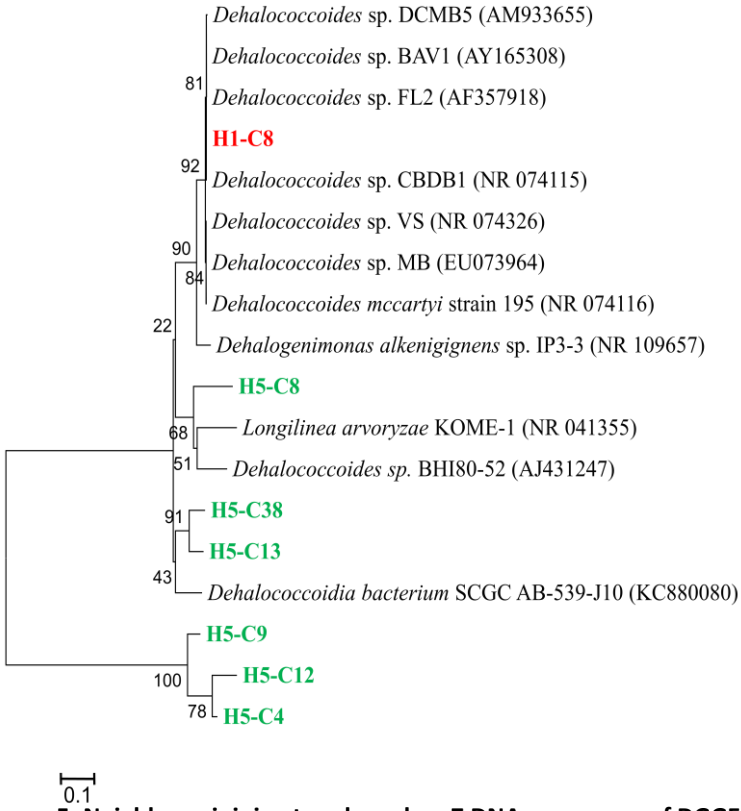

Figure 5. Neighbor – joining tree based on 7 DNA sequences of DGGE bands and published 16S rRNA gene sequences from Genebank. 460 bp of DNA sequences was used for analysis.

Reductive dehalogenase gene profiles

Reductive dehalogenase homologue A (*rdhA*) gene profiles of enrichment cultures set up from 5 locations after 13 months and at time 0 were investigated using PCR with 11 primer pairs as described in Park et al. (2011). The same amount of PCR products were run on agarose gel. Their band intensities were analyzed on ImageJ software. Band intensities of 6 *rdhA* genes (*rdh3, rdh6, rdh7, rdh9, rdh11,* and *rdh12*) differed significantly between H1 and H5 cultures and have a trend to gradually decrease from H1 to H5 cultures. The results of *rdhA* band intensity correlated with the gradual decrease in dehalogenating activities from H1 to H5 cultures. This result implied that these 6 *rdhA* genes may be present in *Dehalococcoides* population which was enriched and was responsible for dehalogenation of 1,2,3,4-TeCDD.

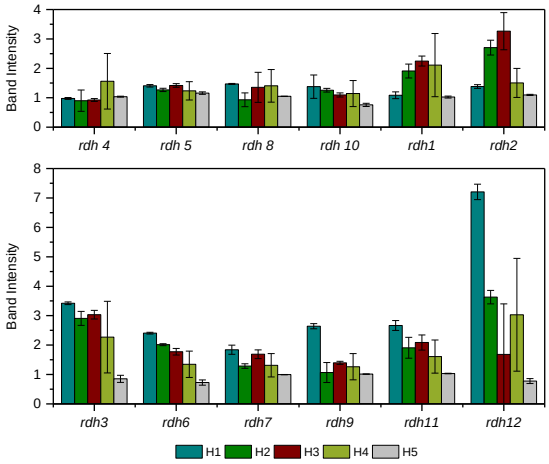

Figure 6. Relative PCR band intensity of 12 putative reductive dehalogenase (*rdh*) genes amplified from Hackensack enrichment cultures after 13 months of incubation.

Band intensity of 4 *rdhA* genes (*rdh4, rdh5, rdh8,* and *rdh10*) showed no significant difference between highly active cultures (i.e., H1, H2, and H3) versus cultures with very low dehalogenating activities (i.e., H5). Band intensity of 2 *rdhA* genes (*rdh1* and *rdh2*) showed difference between samples but their band intensities did not correlate with dehalogenation extent of spiked 1,2,3,4-TeCDD. In all cases, there was a large variation in the band intensity of H4 replicate cultures, indicating differences in the *Dehalococcoides* population.

Active bacterial populations in dehalogenating enrichment cultures

The relative signal of Terminal Restriction Fragment (TRF) of 16S rRNA genes generated from ^{13}C labeled DNA was analyzed and grouped into 6 groups (0 – 0.5%, 0.5 – 1%, 1 – 2.5%, 2.5 – 5%, 5 – 10%, and >10% of total fluorescent signal). Low acetate cultures have less diverse active communities than high acetate cultures. 65 TRFs were detected in cultures amended with 30 µM acetate while 72 TRFs were present in cultures with 150 µM acetate (Figure 7). However, TRF-111 which corresponds to *Dehalococcoides* spp. was present at a substantially higher abundance in both low and high acetate cultures than no electron acceptor controls. Some TRFs depend to a lesser extent on chlorinated dioxins, which was indicated by the drop in fluorescent signal in no terminal electron acceptor controls (TRF-217, TRFs-323, and TRF-419). This result indicated that chlorinated dibenzo-*p*-dioxins are required for incorporation of ^{13}C labeled acetate into some bacterial DNA (Figure 7).

From 4 TRF's sequences identified from clone library of active populations in 30 µM amended culture, TRF-111 was identified to be *Dehalococcoides* and thought to be responsible for reductive dehalogenation of chlorinated dibenzo-*p*-dioxins in the experimental cultures. The other three sequenced TRFs (TRF-166, TRF-237, and TRF-279) are grouped within *Epsilonproteobacteria* and *Betaproteobacteria* (Figure 8).

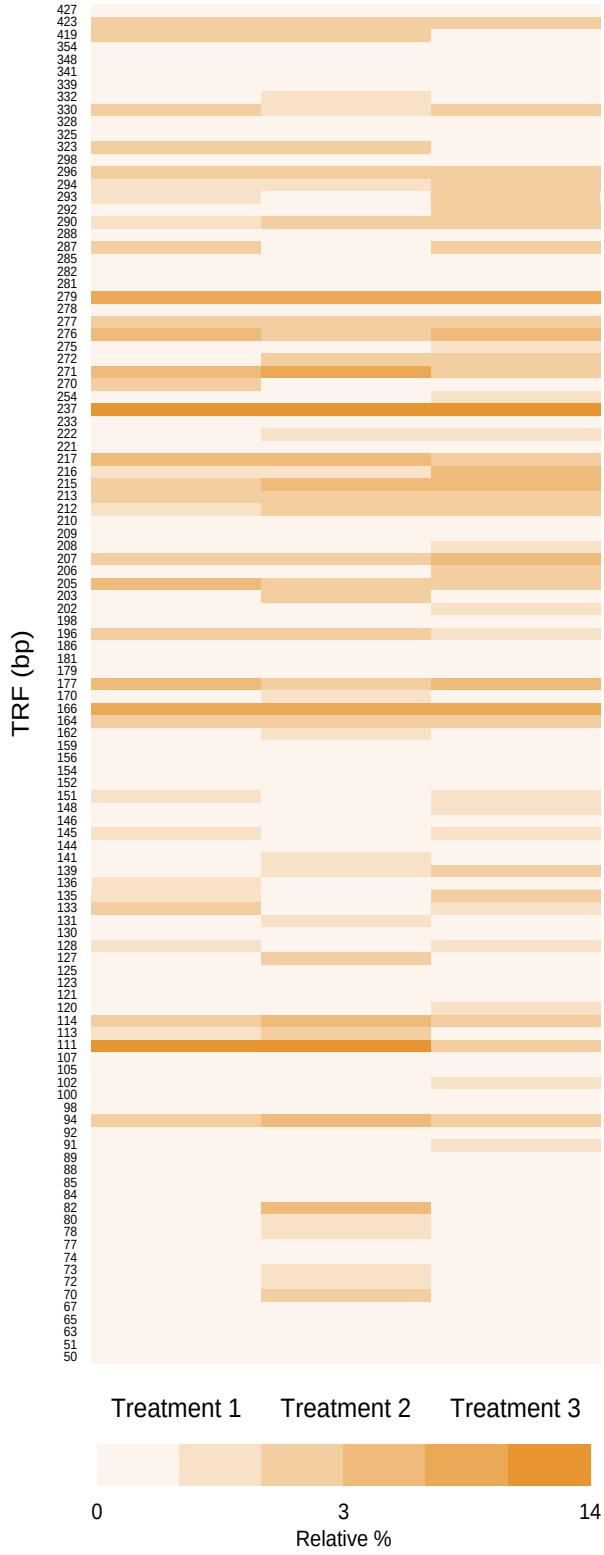

Figure 6. Relative distribution of active bacteria in experimental cultures. Cultures were amended with 1,2,3,4-TeCDD and 30 µM (treatment 1) or 150 µM (treatment 2) ^{13}C acetate. Control culture was amended with only ^{13}C acetate but without 1,2,3,4-TeCDD as terminal electron acceptor (treatment 3)

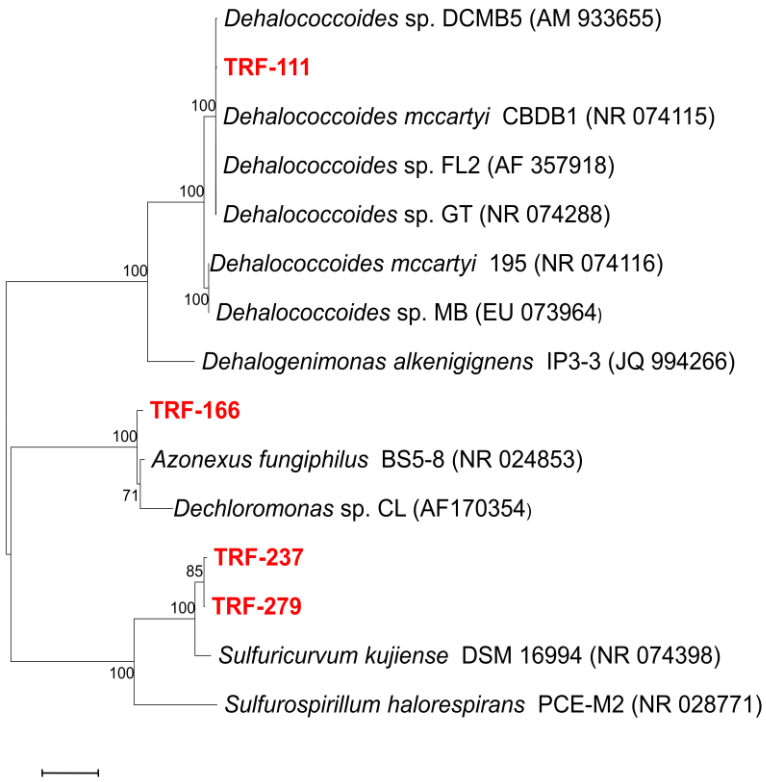

Figure 8. Maximum likelihood phylogenetic tree constructed from ^{13}C labeled 16S rRNA genes of dehalogenating enrichment culture amended with 30 µM ^{13}C-acetate. Approximately 1000 bp of unambiguously aligned positions was used for analysis.

Presentations:

Dam HT & Häggblom MM (2014) Dehalogenation of Chlorinated Dioxins in Hackensack River Enrichment Cultures. Gordon Research Conference, Environmental Sciences: Water (Poster)

Dam HT & Häggblom MM (2015) Dehalogenation of Chlorinated Dioxins in Hackensack River Enrichment Cultures. Symposium of Microbiology at Rutgers: Cultivating Traditions, Current Strength and Future Frontiers (Poster)

Dam HT, Sun W, McGuinness L, Kerkhof L & Häggblom MM (2015) Investigation of Active Bacterial Community in Dehalogenating Enrichment Cultures by Using Stable Isotope Probing. Theobald Smith Society Meeting in Miniature (Poster)

List of conferences attended:

1. Gordon Research Conference – Environmental Sciences: Water "Environmental Sciences in a Human-Impacted World". June 22 – 27, 2014. Holderness School, Holderness, New Hampshire 03264
2. Symposium of Microbiology at Rutgers: Cultivating Traditions, Current Strength and Future Frontiers. January 29 – 30, 2015. Douglas Campus Center, Rutgers University, New Brunswick, New Jersey 08901

3. Theobald Smith Society Meeting in Miniature. April 30, 2015. Cook Campus Center, Rutgers University, New Brunswick, New Jersey 08901

References:

Bopp RF, ML Gross, H Tong, HJ Simpson, SJ Monson, BL Deck, & FC Moser (1991) A major incident of dioxin contamination: sediments of New Jersey Estuary. 25 (5): 951 – 956

Duarte-Davidson R, A Sewart, RE Alcock, IT Cousins, & KC Jones (1997) Exploring the balance between sources, deposition, and the environmental burden of PCDD/Fs in the UK terrestrial environment: An aid to identifying uncertainties and research needs. Environmental Science & Technology 31: 1 – 11

Hiraishi A, N Sakamaki, H Miyakoda, T Maruyama, K Kato, & H Futamara (2005) Estimation of "Dehalococcoides" populations in lake sediments contaminated with low levels of polychlorinated dioxins. Microbes and Environment 20 (4): 216 – 226

Liu H, J-W Park, & MM Häggblom (2014) Enriching for microbial reductive dechlorination of chlorinated dibenzo-p-dioxins and dibenzofurans. Environmental Pollution 184:222-230

Park JW, V Krumins, BV Kjellerup, DE Fennell, LA Rodenburg, KR Sowers, LJ Kerkhof, & MM Häggblom (2011) The effect of co-substrate activation on indigenous and bioaugmented PCB dechlorinating bacterial communities in sediment microcosms. Applied Microbiology and Biotechnology 89: 2005 – 2017

Rasband, W.S., ImageJ, U. S. National Institutes of Health, Bethesda, Maryland, USA, http://imagej.nih.gov/ij/, 1997-2014.

Tuorto SJ, P Darias, LR McGuinness, N Panikov, T Zhang, MM Häggblom, & LJ Kerkhof (2014) Bacterial genome replication at subzero temperatures in permafrost. The ISME Journal 8: 139 – 149

United States Environmental Protection Agency (2013) Dredging begins to remove 20,000 cubic yards of highly contaminated mud from Lyndhurst section of the Passaic river; $20 milliion project to be paid by various companies.

Vargas C, DE Fennell, & MM Häggblom (2001) Anaerobic reductive dechlorination of chlorinated dioxins in estuarine sediments. 57: 786 – 790

Determining the influence of Mn(II)-birnessite interactions on the retention of Zn(II) and implications for other important trace metals in New Jersey

Basic Information

Title:	Determining the influence of Mn(II)-birnessite interactions on the retention of Zn(II) and implications for other important trace metals in New Jersey
Project Number:	2014NJ354B
Start Date:	3/1/2014
End Date:	2/28/2015
Funding Source:	104B
Congressional District:	NJ-010
Research Category:	Not Applicable
Focus Category:	Wetlands, Toxic Substances, Geochemical Processes
Descriptors:	None
Principal Investigators:	Joshua Lefkowitz, Evert Elzinga

Publications

1. Lefkowitz, Joshua P. and Evert J. Elzinga, 2015, Impacts of Aqueous Mn(II) on the Sorption of Zn(II) by Hexagonal Birnessite, Environmental Science & Technology, 49(8), pp 4886-4893
2. Lefkowitz, Joshua P. and Evert J. Elzinga, 2014, Investigation of the synergistic effects of a ternary system containing Zn(II) and Mn(II) interacting with K-birnessite,247th ACS National Meeting and Exposition,March 16-20, 2014, Dallas, Texas (Presentation)

Report for Joshua Lefkowitz, PhD student

(1) **PI information**: List all PIs, addresses, email addresses, phone numbers

Dr. Evert Elzinga
Department of Earth and Environmental Sciences
Rutgers University
101 Warren Street
Newark, NJ 07102

elzinga@andromeda.rutgers.edu
973-353-5238

(2) **Numbers of Students Supported**: list the NUMBER of students in each category that were in any way supported by WRRI funding.
Undergraduates: N/A
Masters' students: N/A
Ph. D. students: 1
Postdoctoral assocs.: N/A

(3) **Any Notable Achievements** (Awards, Recognition, etc.), or direct application of the research by Management Agencies, Nonprofits/NGOs, etc.

Work funded by NJWRRI was presented at the 247th Annual Meeting of the American Chemical Society Dallas TX. The title of the talk was "*Investigation of the synergistic effects of a ternary system containing Zn(II) and Mn(II) interacting with K-birnessite.*" A record of the talk may be found at the following URL:

http://acselb-529643017.us-west-2.elb.amazonaws.com/chem/247nm/program/divisionindex.php?nl=1&act=presentations&val=Advances+in+Understanding+the+Environmental+Geochemistry+of+Manganese+%28Mn%29+Oxides&ses=Advances+in+Understanding+the+Environmental+Geochemistry+of+Manganese+%28Mn%29+Oxides&prog=222956

This work was also published In Environmental Science & Technology. A copy of the article was submitted to NJWRRI. Citation:

Impacts of Aqueous Mn(II) on the Sorption of Zn(II) by Hexagonal Birnessite
Joshua P. Lefkowitz and Evert J. Elzinga
Environ. Sci. Technol., 2015, 49 (8), pp 4886–4893
Publication Date (Web): March 19, 2015 (Article)
DOI: 10.1021/es506019j

An additional article will be submitted this summer to ES&T.

(3) **Project Summary**:
Include the following sections:

Problem and Research Objectives - can be copied from the project proposal; 2-3 paragraphs

Specific objectives and hypotheses: Manganese oxides have long been known to be important players in the geochemical cycling of metals, but the impacts of variable redox condition on the fate of sorbed trace metals is not known. Accordingly, the objective of this project is to assess how reducing conditions impact the retention of sorbed metals by birnessite when transformation of the sorbent is induced. Reducing conditions cause drastic changes in soil chemistry with respect to microbial activity where microbes are forced to switch to alternative electron acceptors for respiration following depletion of O_2. Reductive dissolution of iron- and manganese-(hydr)oxides moderates pH to near-neutral values and leads to the build-up of high aqueous concentration of dissolved Mn(II) and Fe(II). Research over the past few years in the Elzinga lab has revealed that aqueous Mn(II) exerts strong control on solid phase Mn-oxide structure and mineralogy. Elzinga and Lefkowitz et al. demonstrated that interaction of aqueous Mn(II) with birnessite (nominally $Mn(IV)O_2$) causes bulk structural change under anoxic conditions through interfacial electron exchange between Mn(II) and Mn(IV). At pH 7.5, the following reaction occurred:

$$Mn^{2+} + Mn(IV)O_2 + 2H_2O \rightarrow 2Mn(III)OOH + 2H^+ \ (1)$$

Here, birnessite reacts as a sorbent of Mn^{2+}. Sorption of Mn^{2+} onto birnessite causes bulk transformation of the solid substrate to the metastable Mn(III) phasefeitknechtite (β-MnOOH), which is subsequently converted into the more stable Mn(III) phase manganite (γ-MnOOH). The mechanism attributed to the initial transformation is interfacial electron exchange between adsorbed Mn(II) and structural Mn(IV) following coordination of Mn^{2+} to the birnessite surface, producing Mn(III) which is arranged into feitknechtite. Under oxic conditions, surface catalysis provides an additional mechanism by which Mn^{2+}removal is enhanced. In this instance, following adsorption of Mn^{2+} to the solid substrate, molecular oxygen oxidizes the sorbed species to produce additional feitknechtite, described by:

$$4Mn^{2+} + O_2 + 6H_2O \rightarrow 4Mn(III)OOH + 8H^+ \ (2)$$

Lefkowitz et al. evaluated the role of pH on occurring transformation reactions, and discovered that pH has a major influence on the interactions of Mn(II) with birnessite, and exerts strong controlon the final products formed. At pH values below 7, transformation is relatively unfavorable, even at high concentrations of Mn^{2+}. At pH values 8-8.5, an additional transformation pathway was observed, which is described by the following equation:

$$2Mn^{2+} + Mn(IV)O_2 + 2H_2O \rightarrow Mn(II)(III)_2O_4 + 4H^+ \ (3)$$

The end product in this reaction is hausmannite (Mn_3O_4). At pH 8, this binary reaction system is complex, with both reactions (1) and (3) occurring concurrently so long as the Mn^{2+}concentrations are within a low to intermediate range. At high concentrations of Mn^{2+} reaction (3) is favored, and increasing pH also favors formation of hausmannite. Of note is that thermodynamic prediction have limited merit in predicting operational transformation

pathways, which makes it necessary for experimental studies to be conducted to assess the impact of Mn(II)-birnessite interaction on Mn-oxide mineralogy.

The work proposed here aims to examine the effects of Mn(II)-birnessite interactions on the retention of Zn, a common heavy metal pollutant in NJ[1,11,12]. Zn has been previously shown to strongly sorb to birnessite, and its environmental fate is thus likely to be affected strongly by Mn-oxide mineralogical transformation induced by Mn(II) in anoxic and suboxic environments. The applicant will examine the dynamics of Zn uptake and release of a ternary aquatic system, where birnessite, Mn(II) and Zn(II) are reacted under anoxic conditions and at neutral pH, as found in natural riparian systems. To name one specific example, such a scenario is directly applicable to such environments as the Walkill River system, where pH values exceed 7.5 and dissolved concentrations of Zn(II) (9-13 ppm) and Mn(II) (77-97 ppm) are relatively high. In these environments birnessite is expected to be a major sink for Zn. We hypothesize that the reactivity of birnessite and the speciation of Zn are strongly affected by abiotic reactions between Mn(II) and the birnessite substrate. The specific objectives of this study are as follows:

(1) To determine the competitive effects of Zn(II)and Mn(II) interacting with birnessite at pH 7.5.
(2) To determine the macroscopic and microscopic differences that arise between sequential and simultaneous addition of Zn(II) and Mn(II) in a suspension of birnessite at pH 7.5.

Methodology - give a general summary of procedures and methods actually implemented

I used the methodology and experimental design described in my application and described in previous publications. A more extensively detailed explanation of methods and design beyond what is listed here is provided in the Materials and Methods section of the article published by this work (citation above). We used a suite of analytical techniques that provided a comprehensive analytical picture of geochemical and environmental processes from the macro to molecular scale. This comprehensive picture was obtained by a bifurcated analysis of solutions and solids originating from the same sample. Each sample was filtered through a 0.2 micron nitrocellulose membrane. Solutions were analyzed via UV-Vis spectroscopy and (flame) atomic absorption spectroscopy (AAS). Solid samples were analyzed by Fourier-transform infrared spectroscopy (FTIR), scanning electron microscopy (SEM). X-ray diffraction (XRD) and X-ray absorption spectroscopy (XAS).

Principal Findings and Significance - please provide a progress report if the project is to be continued; if a final report, summarize significant findings. All graphics and tables should be included *within* the body of the document.

The principal findings and significance of this work are detailed in the citation listed above. A copy of this article was provided to NJWRRI.

(4) **Publications or Presentations**:
List any publications, presentations, published abstracts reporting the WRRI-supported work. Oral or poster presentations at conferences should be specified as such.

Dallas TX. The title of the talk was "*Investigation of the synergistic effects of a ternary system containing Zn(II) and Mn(II) interacting with K-birnessite."* A record of the talk may be found at the following URL:

http://acselb-529643017.us-west-2.elb.amazonaws.com/chem/247nm/program/divisionindex.php?nl=1&act=presentations&val=Advances+in+Understanding+the+Environmental+Geochemistry+of+Manganese+%28Mn%29+Oxides&ses=Advances+in+Understanding+the+Environmental+Geochemistry+of+Manganese+%28Mn%29+Oxides&prog=222956

This work was also published In Environmental Science & Technology. A copy of the article was submitted to NJWRRI. Citation:

Joshua P. Lefkowitz and Evert J. Elzinga
2015, Impacts of Aqueous Mn(II) on the Sorption of Zn(II) by Hexagonal Birnessite, Environ. Sci. Technol., 49 (8), pp 4886–4893
Publication Date (Web): March 19, 2015 (Article)
DOI: 10.1021/es506019j

Parasite biomass and nutrient stoichiometry in a stream ecosystem

Basic Information

Title:	Parasite biomass and nutrient stoichiometry in a stream ecosystem
Project Number:	2014NJ355B
Start Date:	3/1/2014
End Date:	2/29/2016
Funding Source:	104B
Congressional District:	NJ-006
Research Category:	Not Applicable
Focus Category:	Ecology, Nutrients, Surface Water
Descriptors:	None
Principal Investigators:	Rachel Paseka, Michael V. K. Sukdeo

Publications

1. Paseka, Rachel, 2015, Deviation from homeostasis and elemental imbalance in host-parasite interactions, Theo Murphy International Scientific Meeting - Elements, genomes and ecosystems: cascading nitrogen and phosphorus impacts across levels of biological organisation, Kavli Royal Society International Centre, Buckinghamshire, UK (Poster)
2. Paseka, Rachel, 2015, Deviation from homeostasis and elemental imbalance in host-parasite interactions, Conference on Biological Stoichiometry, Trent University, Peterborough, Ontario, Canada (Poster)
3. Paseka, Rachel, 2015, Elemental imbalance in host-parasite interactions, Rutgers Ecology and Evolution Student Seminar, New Brunswick, NJ (Presentation)
4. Paseka, Rachel and Michael Sukhdeo, 2014, Parasite biomass in streams of the New Jersey Pine Barrens, American Society for Parasitologists, New Orleans, LA (Presentation)

NJWRRI FY2014 Annual Report
Reporting period: March 1, 2014 – February 28, 2015

(1) **PI Information**

Rachel Paseka
PhD Candidate
Ecology & Evolution Graduate Program
Rutgers University
14 College Farm Road
New Brunswick, NJ 08901

rachel.paseka@rutgers.edu

(402) 419-6312

(2) **Numbers of Students Supported**:

Undergraduates: 0
Masters' students: 0
Ph. D. students: 1
Postdoctoral assocs.: 0

(3) **Notable Achievements**

In the past year, I have been awarded the following additional sources of funding to support this research.

2015 Hutcheson Memorial Forest Summer Research Grant ($2,150), Rutgers School of Environmental and Biological Science
2015 Woodstoich Travel Grant to attend Conference on Biological Stoichiometry in Canada ($400)
2014 NSF Junior Scientist Travel Grant to attend Theo Murphy Discussion Meeting in U.K. ($1,500)
2014 National Science Foundation Graduate Research Fellowship ($96,000 stipend and tuition over 3 years)

(4) **Project Summary**:

Elemental imbalance and deviation from homeostasis in host-parasite interactions

Problem and Research Objectives

Consumer-resource interactions are the basic units of community ecology, and the nutritional balance between a consumer and its resources is important to consumer survival, growth, and reproduction. Ecological stoichiometry provides a theoretical framework with which to evaluate the causes and consequences of elemental imbalance in trophic interactions (Sterner and Elser 2002). Elemental imbalance is typically expressed as a differences in C:N, C:P, or N:P, and it occurs when the ratio of elements needed for a consumer's survival, growth, and reproduction differs from the ratio of elements in its resource. Nutritional limitation is common for diverse consumers in both terrestrial and aquatic food webs (Elser et al. 2000), and its consequences may scale up to influence population dynamics (Andersen et al. 2004), community structure (Elser et al. 1988) and nutrient cycling (Elser and Urabe 1999).

Consumers are generally expected to maintain stoichiometric homeostasis by keeping fixed elemental ratios when faced with variable resources, but deviating from homeostasis may be a strategy to reduce the costs of elemental imbalance. Deviation from strict homeostasis has been observed in many taxa (Persson et al. 2010). It is not yet clear what determines an organism's placement along the homeostasis-plasticity gradient, or what tradeoffs are associated with either strategy.

Parasites likely have nutritional requirements that are fundamentally no different than those of free-living consumers. Parasite life history phenomena, such as complex life cycles and low host specificity, may exacerbate the problem of elemental imbalance when parasites within a population must feed on different host species that differ in elemental content. Additionally, parasites are constrained to feeding on specific host tissues, unlike some free-living consumers that select prey to maintain proper dietary ratios (e.g. Behmer 2009).

Previous studies manipulating the quality of host diet have provided some evidence that parasite production is nutrient-limited (Frost et al. 2008a, Bernot 2013). However, the organismal stoichiometry of the parasites themselves has rarely been analyzed (Bernot 2013), so it is unknown whether an elemental imbalance between parasites and their hosts limits parasite production or leads to a deviation from homeostasis.

In this project, I measured the elemental stoichiometry of generalist parasites with complex life cycles in each of their most common hosts. I determined whether parasite-host elemental imbalance differs for each consumer-resource pair, then asked whether these differences in imbalance are related to differences in infection variables. Finally, I considered whether parasites can cope with elemental imbalance by deviating from homeostasis in response to changes in resource quality.

Questions

a) Does parasite-host elemental imbalance suggest that parasites experience limitations in resource quality?
b) For generalist parasites, do different levels of imbalance between host species correspond to differences in rates of parasite survival, growth, or fecundity?
c) Do parasites deviate from strict homeostasis in response to different host resources?

Methodology

I addressed these questions using two parasite species common to streams of the NJ Pine Barrens: the trematode *Phyllodistomum pearsei* and the acanthocephalan *Acanthocephalus tahlequahensis* (Figure 1). All collections for this study took place in Muskingum Brook, where I have recovered these parasites most often from two definitive host species, the pirate perch *Aphredoderus sayanus* and the eastern mudminnow *Umbra pygmaea.* The intermediate host of *P. pearsei* is a fingernail clam in the family Sphaeriidae, and the intermediate host of *A. tahlequahensis* is the isopod *Caecidotea communis.* Both species also feed as larvae in their intermediate hosts. Both parasite species rely on the predation of their intermediate hosts by definitive hosts for life cycle completion. For this reason, individuals of each parasite species will obligately feed in their intermediate hosts, and will live and feed as adults in whichever host species ingests them.

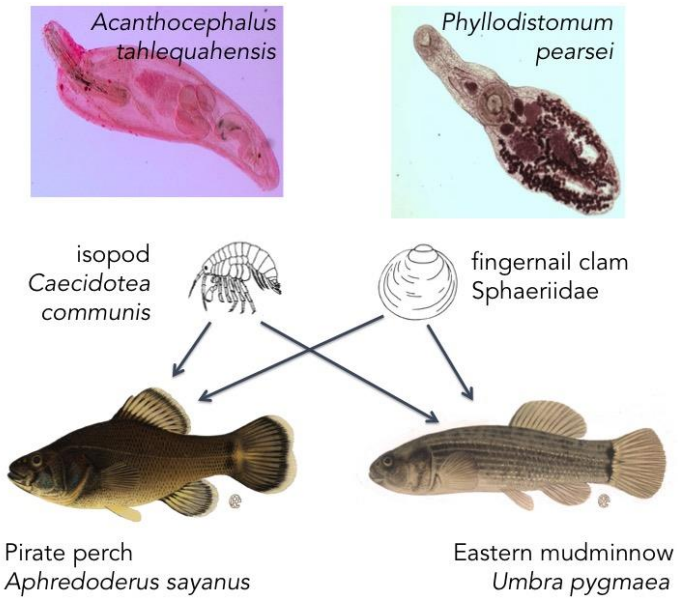

Figure 1: This study system was chosen to take advantage of parasite life history strategies (complex life cycles and host generalism) that lead to variable resource quality for an individual parasite species.

I sampled pirate perch and eastern mudminnow populations at Muskingum Brook monthly from August 2013 to July 2014. I collected fish with a seine net, dissected them to remove parasites using a standardized protocol, and identified all parasites using morphological keys. Because parasite prevalence (percentage of host population parasitized) and infection intensity (number of parasites per infected host) varied seasonally, I calculated the overall prevalence and mean infection intensity for the entire year for comparison with imbalance data.

I collected fish and parasite tissues for elemental analysis from Muskingum Brook in the fall of 2014. I removed parasites from their fish hosts, rinsed them in tap water, and pooled them onto ashed GF/F filters until a sample mass adequate for analysis was reached. For each fish species, I analyzed whole individuals (intestinal contents and parasites removed), urinary bladders (consumed by *P. pearsei*) and dietary material (consumed by *A. tahlequahensis*). All tissues were dried at 60° C and stored in a desiccator until analysis.

Prior to elemental analysis, I ground all fish tissues with a mortar and pestle until visually homogenized. Parasites were analyzed directly on the GF/F filters on which they were collected. I analyzed C and N using a Carlo-Erba NA 1500 CNS analyzer. I analyzed P by ashing and digesting samples in acid, then reading them on a spectrophotometer using a molybdate-blue method.

I calculated the mean elemental imbalance between parasites and the host tissues on which they feed using the mean values of each parasite analyzed from each host (Consumer X:Y) and the mean values of each specific host tissue (Resource X:Y).

Imbalance X:Y = Consumer X:Y – Resource X:Y

Imbalance X:Y = *Phyllodistomum* X:Y – Host bladder X:Y

Imbalance X:Y = *Acanthocephalus* X:Y – Host diet X:Y

Principal Findings and Significance

The parasites in this system differed in infection success depending on the identity of the definitive host (Figure 2). Both parasite prevalence (percentage of host population infected) and mean infection intensity (mean number of parasites per infected host) showed substantial differences between the two fish species considered, with greater parasite success typically occurring in the pirate perch.

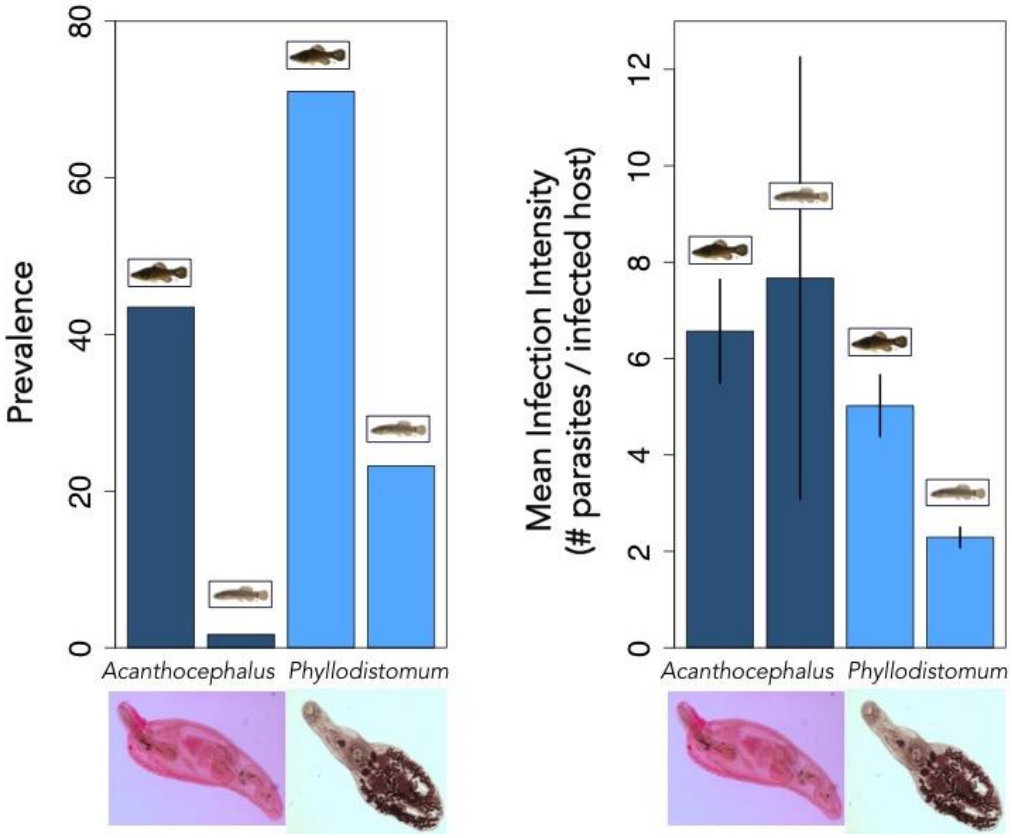

Figure 2. Infection data from Muskingum Brook for two abundant macroparasite species in their most common definitive hosts.

These parasite species are elementally imbalanced from their host resources (Figure 3). In general, positive C:N imbalance values suggest that parasites are limited by C (energy) relative to N. However, negative C:P and N:P imbalance values suggest that these parasites are likely limited by the P content of their host resources.

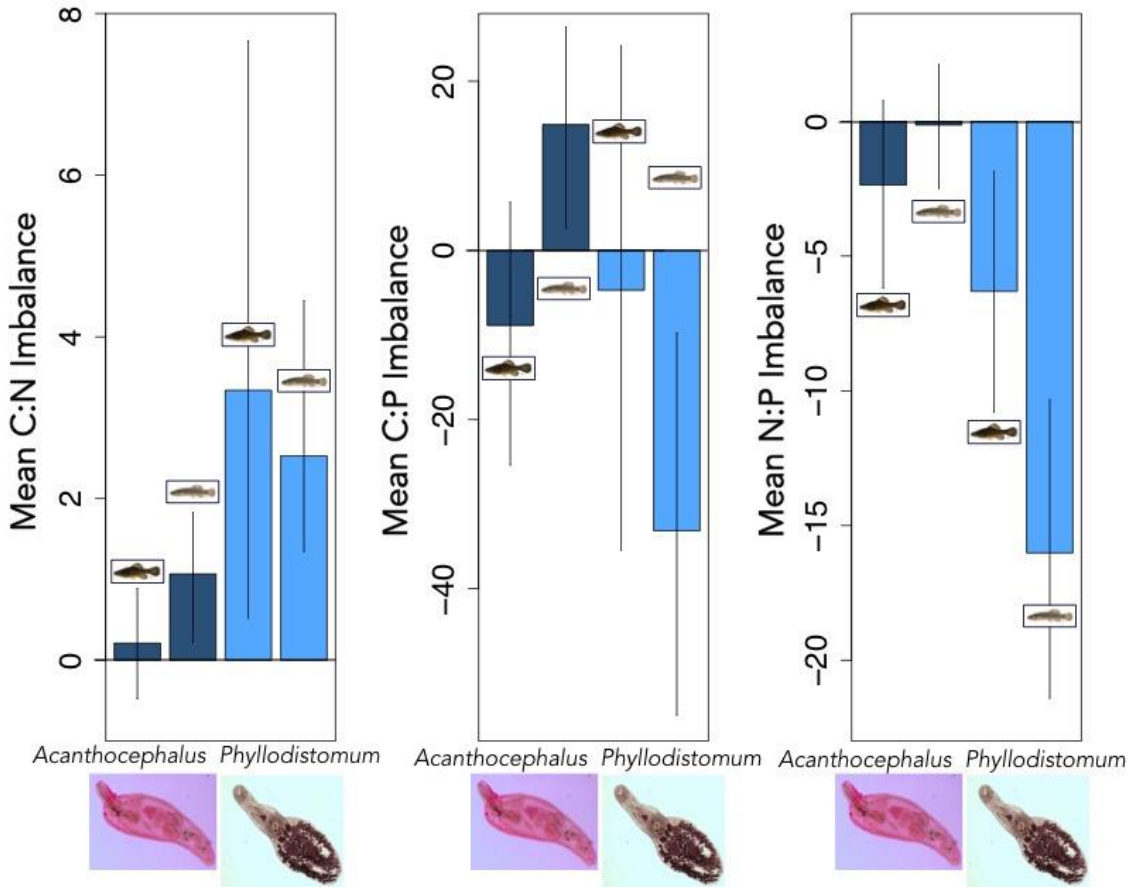

Figure 3. Mean elemental imbalance between parasites and their host resources. Error bars represent bootstrapped 95% confidence intervals.

For each ratio examined, mean infection intensity was highest for host-parasite pairs with the lowest mean elemental imbalance (Figure 4). Infection intensity represents the maximum number of parasites that can survive within an individual host, so it is possible that resource balance is important to the survival of adult parasites. Mean elemental imbalance was not related to differences in prevalence, which may instead be indicative of differences in transmission parameters between host-parasite pairs.

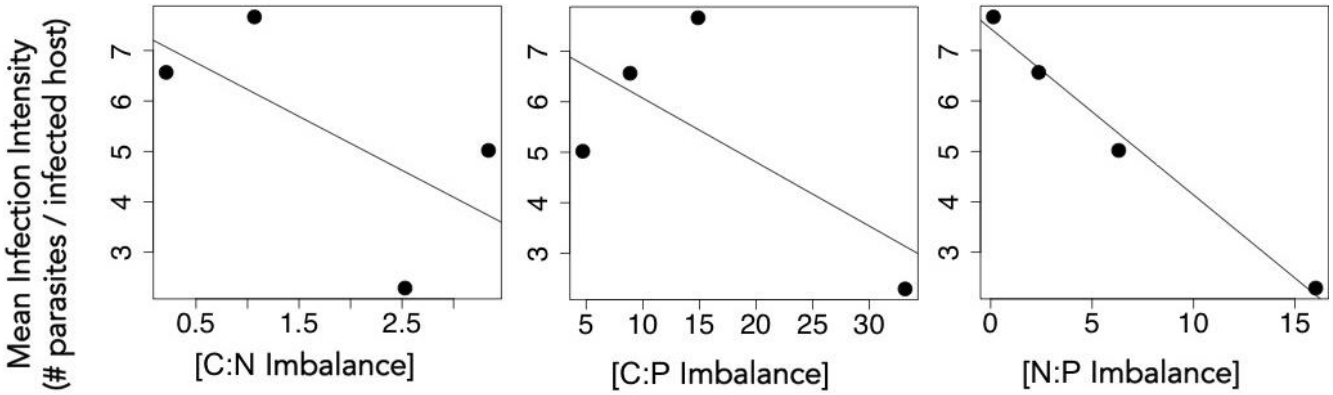

Figure 4. Relationship between mean infection intensity and mean consumer-resource imbalance. Each dot represents one host-parasite pair.

Field collections did not permit reliable measurements of parasite adult body size or fecundity due to variation in infection stage. In the future, I will experimentally establish each of these host-parasite relationships by infecting fish in mesocosms, controlling for time of parasite establishment and infection intensity. By comparing parasite growth rate and fecundity between host species, I will determine whether elemental balance is related to these additional measures of parasite success.

Parasites deviate from strict homeostasis by shifting their elemental makeup between definitive host species (Figure 5). This result was surprising because consumers are generally expected to maintain elemental homeostasis when faced with variable resource quality. This elemental plasticity may provide a mechanism for parasites to utilize multiple resources effectively, as is necessary in the case of complex life cycles and host generalism.

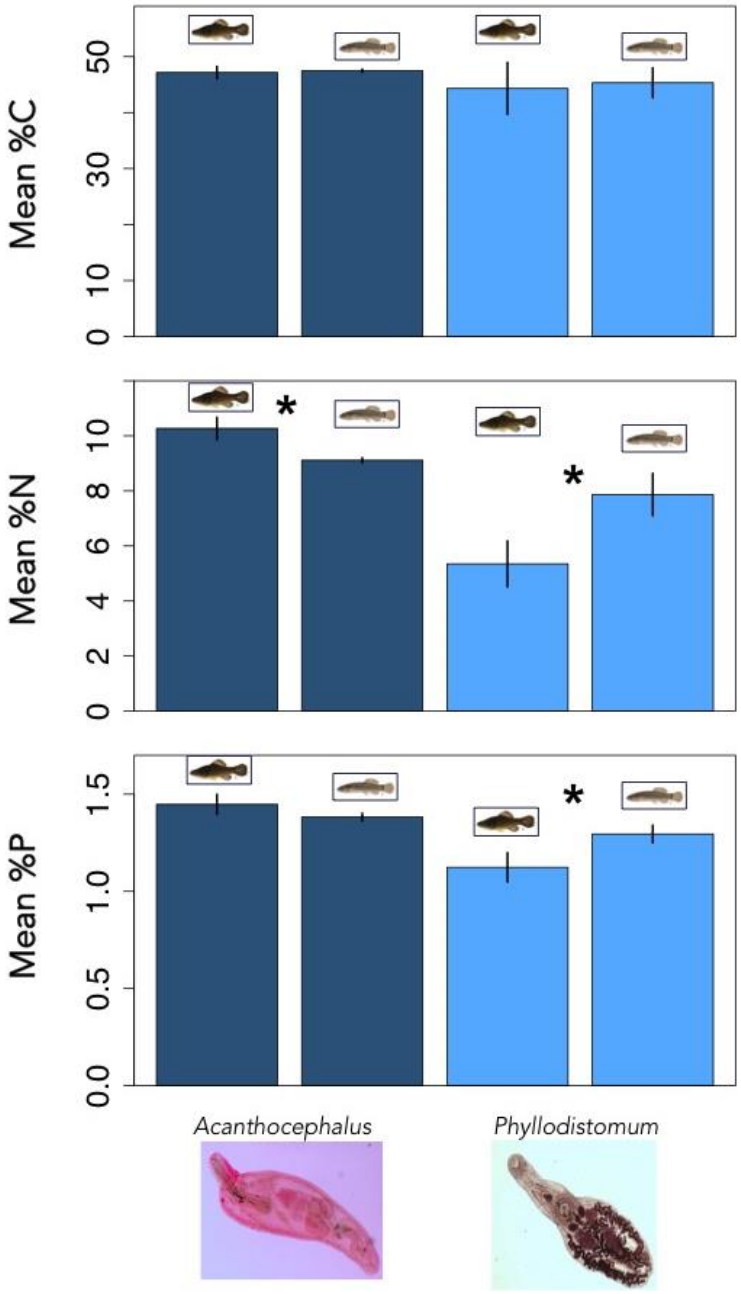

Figure 5. Deviation from strict homeostasis by parasites in response to definitive host identity

Funding from NJWRRI provided much of the sampling equipment, lab supplies, and offset the costs of elemental analysis for the work described above. The items I purchased will also aid in the controlled infection experiments I will conduct to complete this project, as well as two additional chapters of my dissertation.

Works Cited

ANDERSEN, T., J. J. ELSER, AND D. O. HESSEN. 2004. Stoichiometry and population dynamics. Ecology Letters 7:884–900.

BEHMER, S. T. 2009. Insect herbivore nutrient regulation. Annual Review of Entomology 54:165–187.

BERNOT, R. J. 2013. Parasite–host elemental content and the effects of a parasite on host-consumer-driven nutrient recycling. Freshwater Science 32:299–308.

ELSER, J. J., M. M. ELSER, N. A. MACKAY, AND S. R. CARPENTEF. 1988. Zooplankton-mediated transitions between N- and P-limited algal growth. Limnology and Oceanography 33:1–14.

ELSER, J. J., W. F. FAGAN, R. F. DENNO, D. R. DOBBERFUHL, A. FOLARIN, A. HUBERTY, S. INTERLANDI, S. S. KILHAM, E. MCCAULEY, K. L. SCHULZ, E. H. SIEMANN, AND R. W. STERNER. 2000. Nutritional constraints in terrestrial and freshwater food webs. Nature 408:578–80.

ELSER, J. J., AND J. URABE. 1999. The stoichiometry of consumer-driven nutrient recycling: theory, observations, and consequences. Ecology 80:735–751.

FROST, P. C., D. EBERT, AND V. H. SMITH. 2008a. Responses of a Bacterial Pathogen to Phosphorus Limitation of Its Aquatic Invertebrate Host. Ecology 89:313–318.

PERSSON, J., P. FINK, A. GOTO, J. M. HOOD, J. JONAS, AND S. KATO. 2010. To be or not to be what you eat: regulation of stoichiometric homeostasis among autotrophs and heterotrophs. Oikos 119:741–751.

STERNER, R. W., AND J. J. ELSER. 2002. Ecological Stoichiometry: The Biology of Elements from Molecules to the Biosphere. Princeton University Press, Princeton.

(4) **Publications or Presentations**:

Paseka, Rachel (IN PROGRESS)
"Ecological Stoichiometry of Parasitism", Ph.D. Dissertation
Ecology and Evolution Graduate Program
Rutgers University
New Brunswick, NJ

Paseka, Rachel. 2015. "Deviation from homeostasis and elemental imbalance in host-parasite interactions". Theo Murphy International Scientific Meeting-- Elements, genomes and ecosystems: cascading nitrogen and phosphorus impacts across levels of biological organisation, Kavli Royal Society International Centre. Buckinghamshire, UK. (Poster)

Paseka, Rachel. 2015. "Deviation from homeostasis and elemental imbalance in host-parasite interactions". Conference on Biological Stoichiometry. Trent University, Peterborough, Ontario, Canada. (Poster)

Paseka, Rachel. 2015. "Elemental imbalance in host-parasite interactions." Rutgers Ecology and Evolution Student Seminar, New Brunswick, NJ. (Oral)

Paseka, Rachel and Michael Sukhdeo. 2014. "Parasite biomass in streams of the New Jersey Pine Barrens." American Society for Parasitologists, New Orleans, LA. (Oral)

Novel approach to sea and brackish water desalination via membrane distallation

Basic Information

Title:	Novel approach to sea and brackish water desalination via membrane distallation
Project Number:	2014NJ356B
Start Date:	3/1/2014
End Date:	2/28/2015
Funding Source:	104B
Congressional District:	NJ-010
Research Category:	Not Applicable
Focus Category:	Water Supply, Methods, Water Quantity
Descriptors:	None
Principal Investigators:	Smruti Ragunath, Somenath Mitra

Publications

1. Ragunath Smruti, M. Bhadra, S. Roy, S. Mitra, May 2014, Carbon Nanotube Enhanced Membrane Distillation: A New Generation of Membranes for Sea or Brackish Water Desalination, 99th NJWEA Annual Conference, Atlantic City, NJ (Poster)
2. Ragunath Smruti, M. Bhadra, S. Roy, S. Mitra, October 2014, Novel Membranes for Generation of Pure Water from Sea or Brackish Water via Membrane Distillation, Xth Annual Graduate Research Day by Graduate Student Association at NJIT, Newark, NJ (Poster)
3. Ragunath Smruti, S. Roy, S. Mitra, August 2015, Novel Approach to Sea or Brackish Water Desalination via Membrane Distillation at 250th ACS National Meeting to be held at Boston, MA (Presentation)

REPORT SUBMITTED TO NEW JERSEY WATER RESOURCES RESAERCH INSTITUTE IN RESPONSE TO THE REQUEST FOR PROPOSALS FOR THE YEAR 2014

Title: Novel Approach to Sea and Brackish Water Desalination via Membrane Distillation

PI Name: Smruti Ragunath

Address: Department of Chemistry and Environmental Science
New Jersey Institute of Technology
Newark, NJ 07102
Telephone number: 973-642-6456
Fax number: 973-596-3586
Email address: sr262@njit.edu

Any Notable Achievements:

1. Won Graduate Poster Session at 99th Annual New Jersey Water Environment Association Conference at Atlantic City, NJ on May 2014.
2. Won Graduate Poster Session at Xth Annual Graduate Research Day by Graduate Student Association at NJIT, Newark, NJ on October 2014.

Priority Issues:

Recent evidence shows unpredictable rain cycles with fairly extensive dry weather across much of United States. In an article by New Jersey Department of Environmental Protection, 2012 was a year of high water demand due to dry start with late spring rains, depleted ground water levels and stream flows (1). As most parts of the nation continue to suffer from drought, above average heat and dry weather, more attention needs to be paid towards conservation of water resource. The growing demand for water and depleting water reserves forces us to look for engineered water sources by approaches such as water purification and desalination of brackish or sea water.

According to a recent report from Pike Research, there is growing interest in investments on desalination projects due to high demand for generation of pure water. Typically, conventional high-energy processes for generating deionized water include reverse osmosis (RO), Multi Stage Flash (MSF), and Multiple Effect Desalination (MED). While RO requires high pressure and good for low salinity, MSF and MED are energy intensive. These methods have their limitations, and the development of the next generation of water purification technology should provide energy efficiency, smaller and less expensive facilities, and generate soft water for public and industrial consumption.

Membrane Distillation is a typical water removal process used in applications such as desalination, food processing etc. Membrane distillation (MD) is a thermal evaporative process that offers advantages over traditional distillation (2, 3). The principle of separation in MD is based on the difference in volatility with vapor pressure being the driving force. Schematic diagram of a typical membrane distillation experimental setup is shown in Figure.1. Here a hydrophobic porous membrane is employed as a barrier separating heated feed and cold permeate streams. As a heated water solution passes through its lumen, it is partially transformed to water vapor. The hydrophobicity prevents the aqueous solution from entering the pores, however freed from hydrogen bonding, the water vapor passes through, swept by a flow

of air and is condensed on the permeate side of the membrane. MD can be operated at lower temperatures than the boiling point of the feed solutions, requires atmospheric pressure and lower vapor space and is not limited to fouling and has the potential for producing high-purity water. Typically the process requires relatively low operating temperatures in the range of 60 - 90°C unlike the traditional distillation process where the operating temperatures are well above 100°C. Because of their lower energy requirement, membrane distillation is an attractive process for producing pure water.

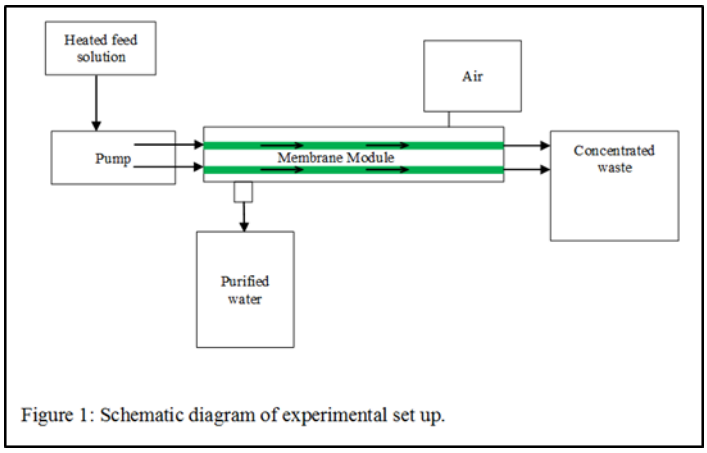

Figure 1: Schematic diagram of experimental set up.

Though membrane distillation is considered as an energy efficient process, the key component in a membrane process is the membrane itself. The separation or purification of the desired contaminants is highly affected by the membrane properties. Hence development of novel membrane architecture is of great importance to enhance the overall performance and efficiency in membrane distillation process. Membrane properties are improved by engineering novel membranes or modification of the surface properties of existing membranes. Taking cost factor into account, recently our group has demonstrated a novel method to modify the surface properties of already existing polymeric membranes. One such approach is to immobilize carbon nanotubes (CNTs) in different types of membranes referred as carbon nanotube immobilized membrane (CNIM) in which the carbon nanotubes served as carrier and provided additional pathways for solute transport. This altered the solute-membrane interactions within the membrane. These have been used in the applications such as pervaporation, solvent-extraction, concentration and removal of volatile organics and pharmaceutical waste products (4-7). We propose to study sea water desalination using a similar approach.

Specific Objectives and Hypotheses:

Based on the above stated issues, this research is geared towards developing a cost-effective process to desalinate brackish and sea water in order to enhance the performance of Membrane Distillation. The specific goal of this project is to utilize carbon nanotubes to create breakthrough membrane properties for generating pure water, thereby developing a high efficiency membrane desalination technique.

Methodology:

The experimental set up for DCMD is illustrated in Figure.2. The set up comprised PTFE membrane cell having an effective membrane area of 14.5 cm^2, Viton O-rings, PTFE tubing, PFA and PTFE connectors, feed and permeate flow pump (Cole Parmer, Vernon Hills, IL), circulating heated temperature bath (GP-200) and circulating chiller (MGW Lauda RM6). The hot aqueous NaCl solution of various concentrations was circulated on one side of the membrane in the DCMD cell. The temperature of the feed brine was maintained by using a temperature regulated hot oil bath. Cold distilled water was circulated on the other side of the membrane. Inlet and outlet temperatures of feed and permeate side was monitored by using a K-type

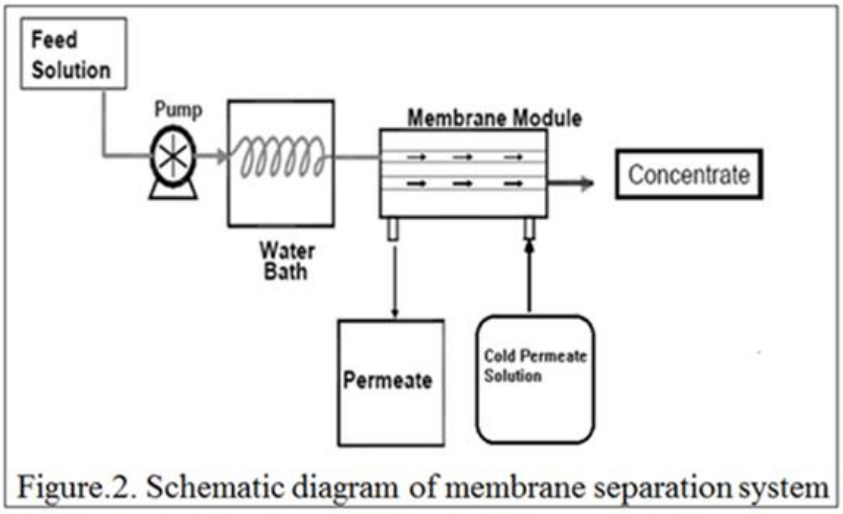

Figure.2. Schematic diagram of membrane separation system

temperature probe (Cole-parmer). Makeup water was added continuously to the feed side to maintain constant concentration throughout the experiment. The concentration of the feed brine and permeate was measured using a conductivity meter (Jenway, 4310). Each experiment was repeated at least three times to ensure reproducibility and relative standard deviation was found less than 1%.

Fabrication of CNT immobilized membrane

Effective dispersal of CNTs and immobilization on the membrane surfaces is considered an essential step in CNIM fabrication. 10 mg of CNTs was dispersed in acetone and sonicated for 3 hr., and 0.2 mg polyvinylidene di fluoride (PVDF) was dissolved in acetone and mixed with CNTs dispersion. The mixture was then sonicated for another 30 min and used to fabricate the CNIM on porous PP. The CNIM–PP membrane was characterized using scanning electron microscopy (SEM) (Leo 1530 VP, Carl Zeiss SMT AG Company, Oberkochen, Germany). The SEM images of both CNIM and unmodified is presented in Figure.3.

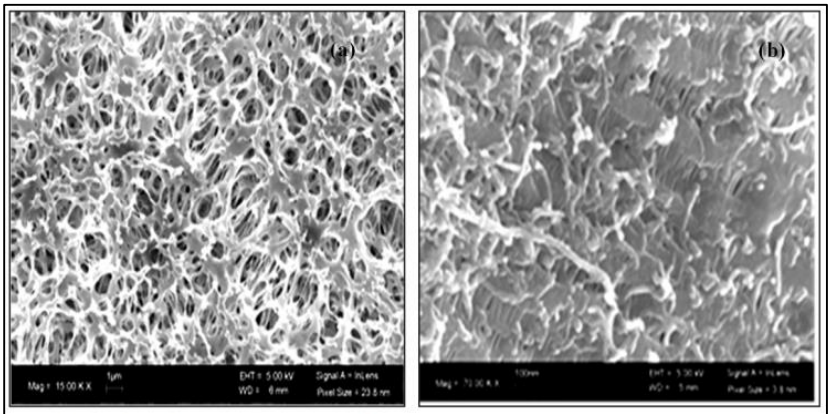

Figure.3. (a) Unmodified Membrane , (b) CNIM

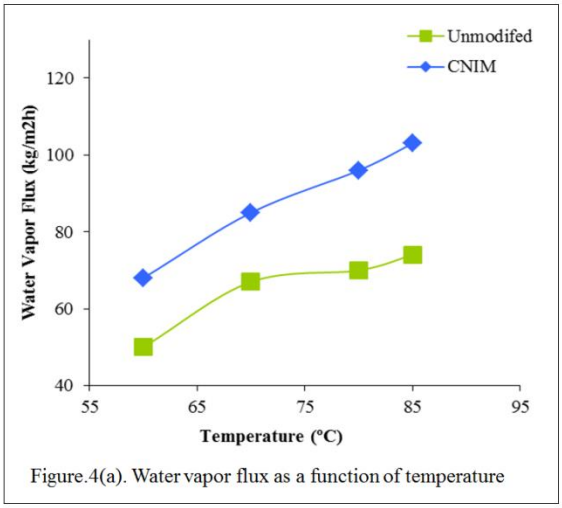

Figure.4(a). Water vapor flux as a function of temperature

Results & Discussion:

The performance of CNIM membrane over unmodified was studied based on the amount of flux attained at varying operating parameters such temperature, flow rate and salt concentration. Figure.4 (a) shows the influence of temperature on water vapor flux of the CNIM membranes compared to the unmodified membrane. It was observed that the permeate fluxes in both the membranes increased with temperature. The temperature increased the vapor pressure

difference between feed and permeate side, hence the driving force for mass transport. As can be seen, the CNIMs exhibited higher water vapor flux compared to the unmodified PP. Flux was as high as 103 kg /m^2 h at 85 ºC for CNIM, which was 39% higher than that of unmodified membrane.

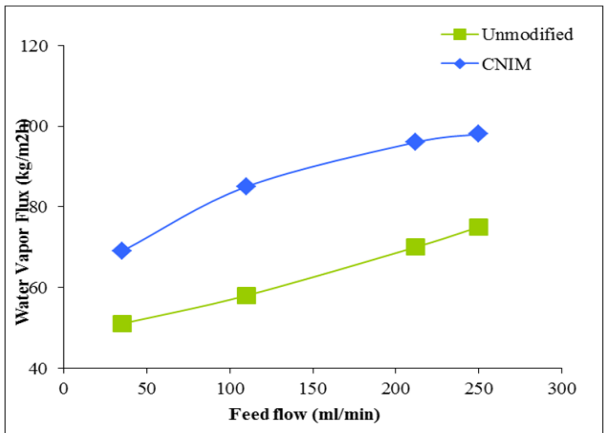

Figure.4(b). Water vapor flux as a function of flowrate

The effect of feed flow rate is shown in Figure. 4 (b). Feed flow rate during the experiment was varied between 35 and 250 mL/min. Permeate flow rate was kept constant around 200 mL/min for all the experiments. The figure clearly demonstrates the increase in water vapor flux with increase in feed velocity. The elevated flow rates increased turbulence and reduced the boundary layer which helped in lowering the temperature polarization and increased the driving force for MD.

Figure.4 (c) demonstrates the performance of CNIM membranes as a function of feed concentration. It is well known that at higher feed concentration, decrease in mass transfer driving force is expected as a significant boundary layer forms due to concentration polarization effect. This results in reduced permeate flux which can be noticed in the unmodified membrane. However it is evident from the figure that CNIM did not have any significant decrease in permeate flux. This could be attributed to the presence of CNTs which contributed to the surface roughness of the membrane and thereby preventing the boundary layer formation.

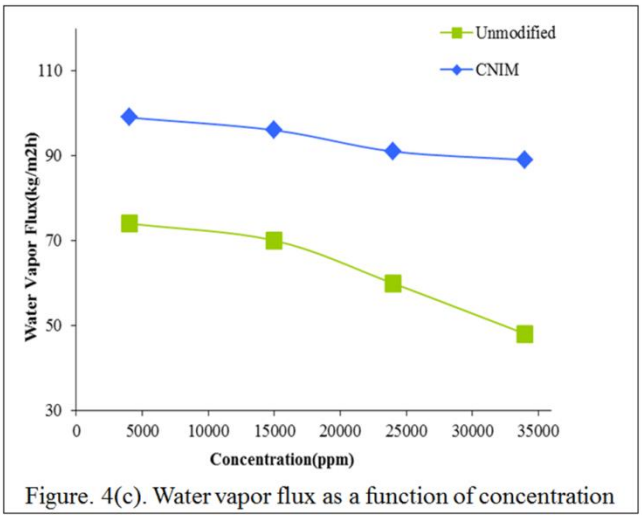

Figure. 4(c). Water vapor flux as a function of concentration

CNIM membranes showed significant enhancement in comparison with conventional membranes. This could be attributed to the fact that CNTs serves as sorption sites for moisture transport while repelling the liquid water. Presence of CNTs increased the effective surface area for generation of water vapors. Furthermore, the hindrance in flow by the presence of CNTs may create more turbulence which decreased the temperature polarization effect, thereby resulting in higher flux.

Conclusion:

Carbon nanotubes immobilized membranes were successfully prepared to enhance the pure water flux in membrane distillation. With the incorporations of CNTs the performance was significantly higher in comparison to conventional membranes. The enhancement attained was as

high as 85%, thus making CNIM as a prospective novel membrane for sea water desalination applications.

Publications/Presentations:

1. Ragunath Smruti, Madhuleena Bhadra, Sagar Roy, Somenath Mitra, May 2014, "Carbon Nanotube Enhanced Membrane Distillation: A New Generation of Membranes for Sea or Brackish Water Desalination" at 99th NJWEA Annual Conference held at Atlantic City, NJ.
2. Ragunath Smruti, Madhuleena Bhadra, Sagar Roy, Somenath Mitra, October 2014, "Novel Membranes for Generation of Pure Water from Sea or Brackish Water via Membrane Distillation" at Xth Annual Graduate Research Day by Graduate Student Association at NJIT held at Newark, NJ.
3. Ragunath Smruti, Sagar Roy, Somenath Mitra, August 2015, "Novel Approach to Sea or Brackish Water Desalination via Membrane Distillation" at 250th ACS National Meeting to be held at Boston, MA.
4. Journal article by Ragunath Smruti, Sagar Roy, Somenath Mitra, titled "Carbon Nanotube Enhanced Membrane Distillation: A New Generation of Membranes for Sea or Brackish Water Desalination" is being prepared for publication.

References:

1. www.njdrought.org
2. Kevin W. Lawson, Douglas R. Lloyd, (1997),"Membrane distillation" *Journal of membrane Science* 124(1), 1-25.
3. Zhigang Lei, Biaohua Chen, Zhongwei Ding, (2005), Membrane distillation. In *Special Distillation Processes*, Elsevier Science: Amsterdam, 241–319.
4. Ornthida Sae-Khow, Somenath Mitra, (2009),"Carbon nanotubes as the sorbent for integrating μ-solid phase extraction within the needle of a syringe" *Journal of Chromatography A*, 1216(12), 2270-2274.
5. Ornthida Sae-Khow, Somenath Mitra, (2009),"Fabrication and characterization of carbon nanotubes immobilized in porous polymeric membranes" *Journal of Material Chemistry*, 19(22), 3713-3718.
6. Ornthida Sae-Khow, Somenath Mitra, (2010), "Carbon nanotube immobilized composite hollow fiber membranes for pervaporative removal of volatile organics from water." *The Journal of Physical Chemistry C* 114(39), 16351-16356.
7. Ornthida Sae-Khow, Somenath Mitra, (2010),"Simultaneous extraction and concentration in carbon nanotube immobilized hollow fiber membranes" *Analytical chemistry*, 82(13), 5561-5567.

Development of a new, effective and low-cost adsorption material to enhance Low Impact Development (LID) techniques for prevention of urban stormwater pollution in New Jersey

Basic Information

Title:	Development of a new, effective and low-cost adsorption material to enhance Low Impact Development (LID) techniques for prevention of urban stormwater pollution in New Jersey
Project Number:	2014NJ357B
Start Date:	3/1/2014
End Date:	2/29/2016
Funding Source:	104B
Congressional District:	NJ-008
Research Category:	Not Applicable
Focus Category:	Water Quality, Treatment, Methods
Descriptors:	None
Principal Investigators:	Hanieh Soleimanifar, Yang Deng

Publication

1. Soleimanifar, Hanieh, Y. Deng, D. Sarkar, 2014, Water Treatment Residual (WTR)-Coated Mulches for Mitigation of Toxic Metals and Nutrient in Polluted Urban Stormwater, New England Graduate Student Water Symposium, University of Massachusetts, Amherst, MA (Poster)

(1) **PI information**:

Graduate student: Hanieh Soleimanifar, PhD candidate in Environmental Management, Montclair State University; ML 252, 1 Normal Ave, Montclair, NJ 07043. Tel: 973-655-3456; FAX: 973-655-6810, Email: soleimanifh1@mail.montclair.edu

Thesis Advisor Dr. Yang Deng, Associate Professor, Department of Earth and Environmental studies, 1 Normal Ave, Montclair, NJ 07043. Tel: 973-655-6678; FAX: 973-655-6810; Email: dengy@mail.montclair.edu

(2) **Numbers of Students Supported**:

Undergraduates: 0
Masters' students: 0
Ph. D. students: 1
Postdoctoral associate: 0

(3) **Any Notable Achievements** (Awards, Recognition, etc.), or direct application of the research by Management Agencies, Nonprofits/NGOs, etc.
N/A

(4) **Project Summary**:

Problem and Research Objectives

Urban runoff, as a serious non-point source, is becoming a major pollution issue in urbanized areas such as New Jersey that is the most populous state (Duke et al., 1998). The most frequently found pollutants in urban stormwater include toxic metals (e.g. Cu, Zn and Pb), nutrients (N and P), and hydrocarbon (e.g. gasoline). Bioretention basin is a leading low-impact development (LID) technique that utilizes soil retention to mitigate stormwater pollutants, and allow for stormwater infiltration at a small scale in developed areas (Hsieh and Davis, 2005). A typical bioretention basin consists of sand and overlying vegetation and mulch. Although a bioretention basin can, to some degrees, reduce certain pollutants present in urban runoff, its application is restricted in the following three aspects. First, heavy metals are accumulated at the top soil so that frequent replacement of soil is required. Otherwise, certain metals in soil will finally exceed the EPA regulated levels (Weiss et al., 2008). Second, the reported nutrient P removal efficiencies of bioretention basins are highly unstable, and even the P release into infiltrated stormwater is observed (Dietz and Clausen, 2005; Dietz and Clausen, 2006; Wu et al., 1996). Third, hydrocarbon (e.g. petroleum) may significantly degrade the quality of soil in bioretention basins. Therefore, it is an urgent demand in New Jersey and many other states to develop appropriate technologies that can substantially enhance the performance of bioretention basins for urban stromwater management.

Water treatment residuals (WTR) are coagulation byproducts of traditional water treatment. Alum (Al) or iron (Fe) - WTRs have been reported to be produced over 2 million tons annually in USA (AWWARF, 1997). This waste is usually disposed of within landfills. However, this option is being challenged by limited landfill space and prohibitive disposal costs. Over the past decades, WTR has been demonstrated to remove toxic metals (e.g. Pb), metalloids (e.g. As), phosphorus, and certain organic wastes from water. However, direct application of WTR as filter media is not practically feasible, because WTR blocks are readily formed to prevent water

infiltration. This study will develop new mulch by coating recycled WTR on it. Benefits are pronged: 1) to reduce the pollutants entering soil in bioretention basins; and 2) to extend the lifetime of bioretention basins. Using different mulches for removal of common stormwater pollutants were attempted (Jang et al., 2005; Mahfoz, 2008). However, it is novel to reuse WTR (an industrial waste) as a new mulch coating is novel in urban stormwater management. And the research proposed here has not been supported by any other grants.

Specific objectives and hypotheses

The long term goal of this study is to develop effective, low-cost, and sustainable LID techniques to address stormwater pollution in an urbanized environment. The primary objective of this study is to evaluate the potential of WTR-coated mulch to strength the performance of bioretention basins in removal of typical urban runoff pollutants. The central hypothesis is that Al-WTR and/or Fe-WTR can effectively and irreversibly adsorb heavy metals, phosphorous and hydrocarbons in urban runoff. To test the hypothesis, the following specific objectives are pursued:

Objective I: to properly prepare and characterize different types of WTR-coated mulches;

Objective II: to determine the optimal modified mulch type and operating conditions;

Objective III: to evaluate leaching potential of undesirable chemicals from exhausted WTR-coated mulches under rainfall and landfilling conditions.

Methodology

Research methods, experimental design and expected results. Two coatings (i.e. Fe-WTR and Al-WTR) and two mulches (i.e. original wood mulch and scrap rubber mulch) were used to synthesize four different mulch types, including Fe-WTR-coated wood and tire mulches, and Al-WTR-coated wood and tire mulches. These materials were characterized with different analytical techniques. Thereafter, bench-scale batch tests were conducted with synthetic urban stormwater to obtain key kinetic data. Two types of stormwater pollutants were analyzed, including metals (Pb, Cu, and Zn) and phosphorous. Finally, column tests were carried out to test the performance of these WTR-coated mulches under a continuous flow condition. The optimal modified mulch type was selected in terms of the treatment performance. In addition, Synthetic Precipitation Leaching Procedure (SPLP) and Toxicity Characteristic Leaching Procedure (TCLP) tests examined whether certain chemicals of concern may leach out from the modified mulches under different scenarios.

Materials Fe-based and Al-based WTRs were provided from Passaic valley water commission and Bridgewater Water Treatment Plant respectively. The WTR was completely mixed, dried by air, and then sieved by 2-mm sieve (Deng et al., 2011). Wood mulch was purchased from HomeDepot, and original scrap rubber mulch was supplied from New Jersey RubbeRecycle Inc. The mulches were rinsed with deionized water a few times, and then air dried (Jang et al., 2005). Synthetic urban runoff was prepared with the composition as shown in the following table.

Chemical composition of synthetic polluted urban runoff

Parameter	Sources	Concentration(mg/L)
pH	$NaOH / HNO_3$	6.9
Cu	$Cu(NO_3)_2.2.5H_2O$	0.1
Zn	$Zn(NO_3)_2.6H_2O$	0.6
Pb	$Pb(NO_3)2$	0.1
P	Na_2HPO_4	3 (as P)
Motor oil	-	20
Total dissolved solids	$CaCl_2$	120
PIPES	$C_8H_{18}N_2O_6S_2$	10mM

Preparation of WTR-coating mulch

Wood and rubber mulches (1cm x 1cm) were selected, rinsed, and air dried. Mulch glue, an environmentally friendly binder, was used to completely attach the Fe-WTR and Al-WTR powders on the mulch surfaces. Raw wood and rubber mulches were used in the control group.

Experimental design

Characterization of WTR-coated mulch. Different analytical techniques were used to characterize the Fe-WTR-coated wood mulch, including: 1) electron microscopy (SEM) - Energy Dispersive Spectroscopy (EDS) (Hitachi S-3400N) – morphology and elemental composition of WTR coating. 2) BET analysis - specific surface area of the modified mulches; 3) zeta potential (ZP) analysis – ZPs of these mulches at different pH; and 4) CHNS analysis will be employed to measure total C, N and S contents in the WTR coatings.

Batch tests. Batch tests were carried out in flasks with 1L synthetic runoff on a rotary shaker. Reaction temperature was controlled at 25^{o}C. For each type of WTR-coated mulch, kinetics tests was first conducted to determine key kinetics data in removal of metals (Pb, Cu, and Zn) and phosphorous.

Column tests. Mini columns (3'' diameter and 15cm height) were loaded with 5 cm height of four different coated and raw mulches. The synthetic urban runoff was continuously pumped into the columns and filtrate was periodically collected for analysis. Tests proceeded until 50 bed volumes of solution passed through the column. Pumping for 9 hours with a 21 ml/min flowrate satisfied the 50 bed volume goal.

SPLP and TCLP tests. The spent WTR-coated mulches in column tests were collected for Synthetic Precipitation Leaching Procedure (SPLP) (EPA SW-846 Method 1312) and Toxicity Characteristic Leaching Procedure (TCLP) (EPA SW-846 Method 1311) tests, respectively. SPLP is designed to simulate material left in-situ exposed to rainfall and evaluate the leaching potential of the modified mulches caused by rainfall. TCLP is designed to evaluate mobility of hazardous wastes in simulated landfilling conditions.

Analytical method Heavy metals (i.e., Cu, Zn, and Pb) were quantified using an inductively coupled plasma-mass spectroscopy (ICP-MS) (Thermo, X Series II, XO 472). Phosphorous was measured with HACH tests kits using a UV/Vis spectrophotometer (HACH DR5000).

Principal Findings and Significance

Objective I: to properly prepare and characterize different types of WTR-coated mulches (to be continued)

1) Electron microscopy (SEM) and Energy Dispersive Spectroscopy (EDS) on Fe-WTR coated wood mulch showed that the Fe-WTR coating on the wood mulch was primarily a amorphous materials consisting of Fe, Al, Si, O and K.

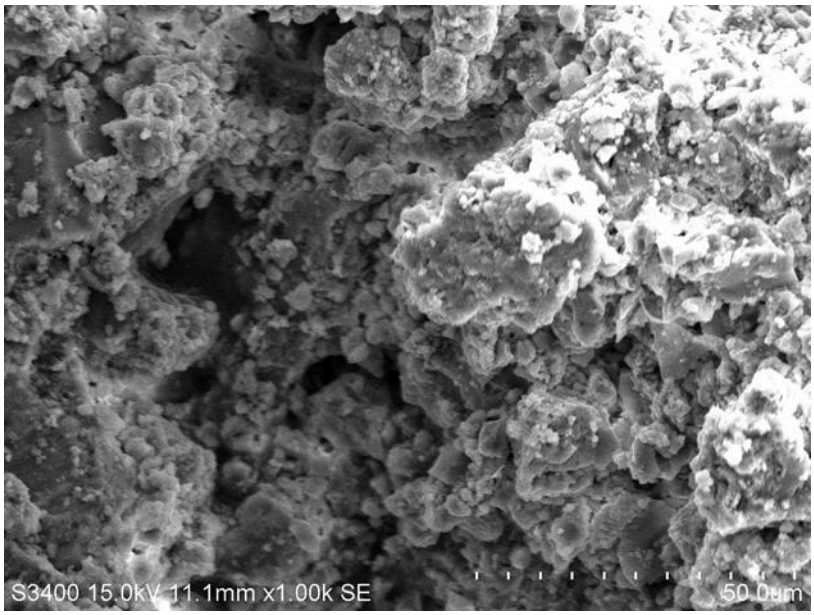

Fe-WTR coated mulch characterization (SEM image)

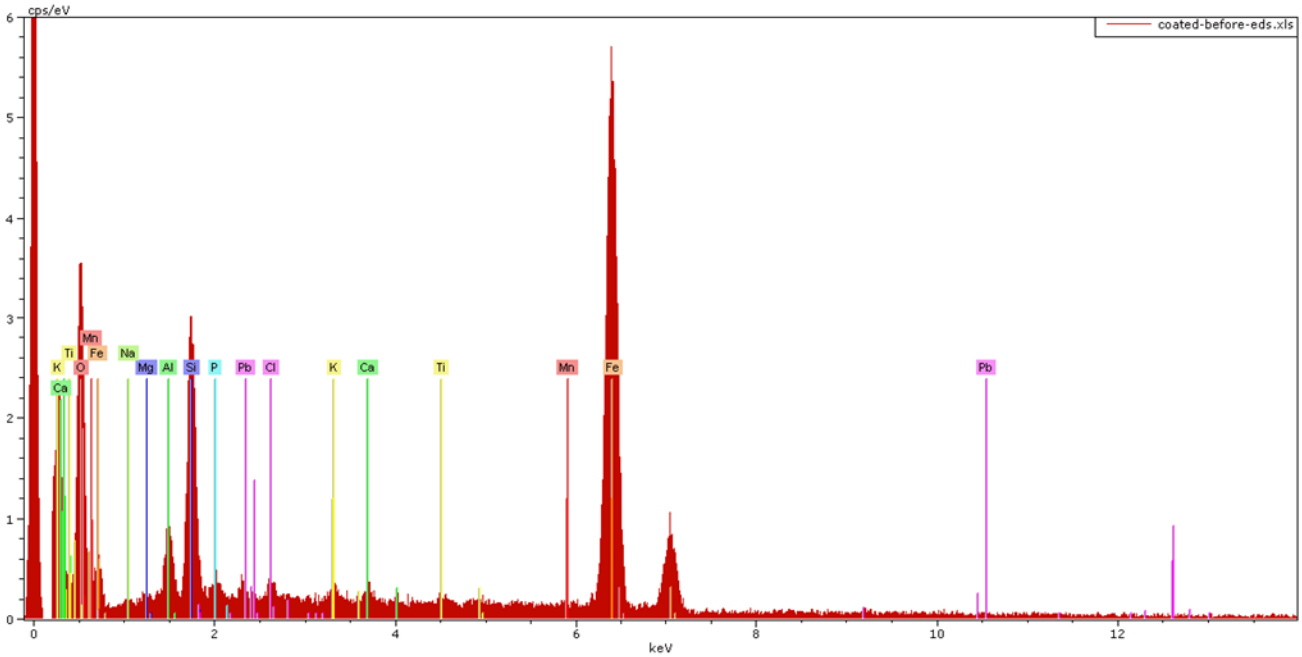

Fe-WTR coated mulch characterization (EDS data)

Objective II: to determine the optimal modified mulch type and operating conditions (100% completed)

Kinetic Tests

10 g/L Fe or Al-WTR were used in each test. To properly coat wood and rubber mulches, 1:3 and 1:6 WTR to mulch weight ratios were required, respectively.

Copper:

Eight different sorbents were tested. WTR only was better than WTR-coated mulch in terms of Cu removal because part of the active sites on WTRs were occupied by the mulch. Among 4 different coated mulches, Al-WTR coated wood mulch showed the highest and the most stable sorption capacity. Fe-WTR Rubber mulch removed copper immediately, but slightly released Cu with time. Of interest, Al-WTR coated tire rubber mulch released Cu.

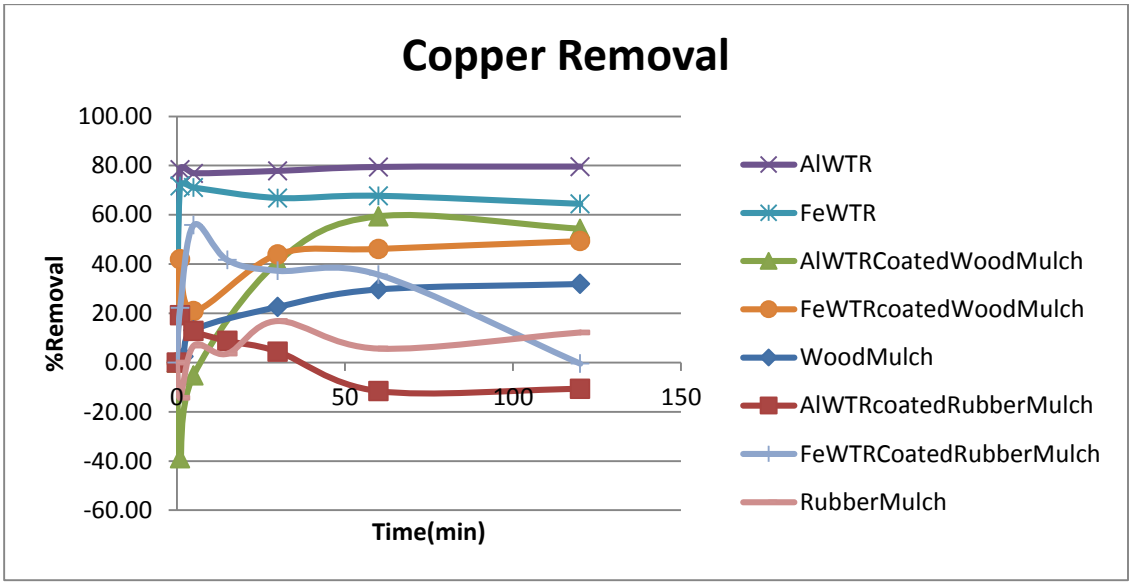

Zinc:

Similar to copper, zinc was also released from rubber. The removal process by Al or Fe-WTR coated rubber mulch was instant but the release of zinc occurred later. Fe-WTR coated wood mulch exhibited a better capacity for zinc.

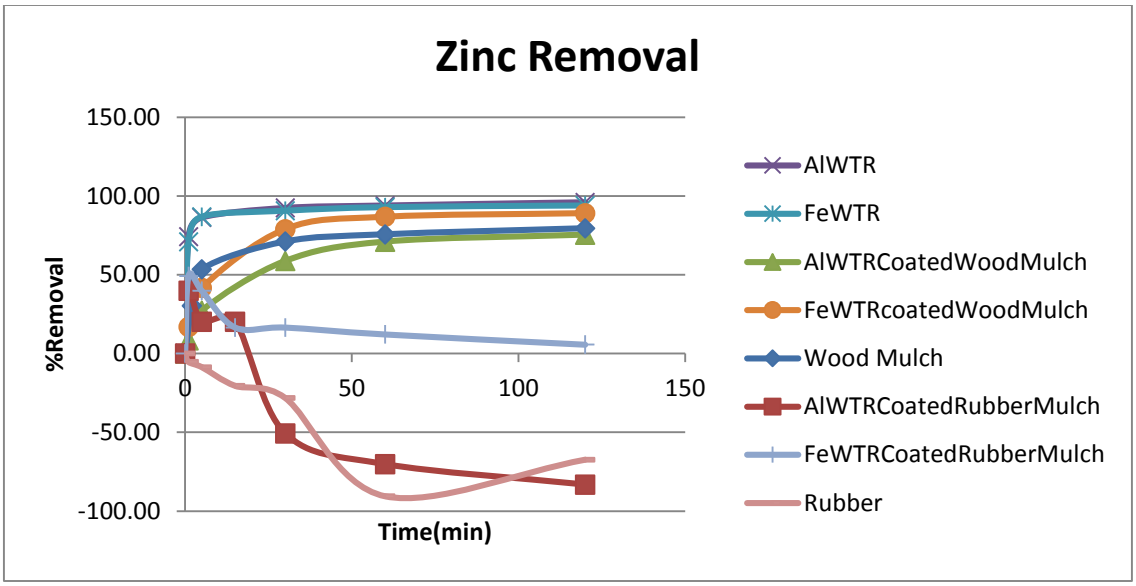

Lead:

Wood alone, Fe WTR coated wood mulch and Al WTR coated mulch appeared to release lead at the beginning but then the coated wood mulch was able to remove lead up to 70%. Fe-WTR coated Rubber mulch was able to remove lead almost by 100%.

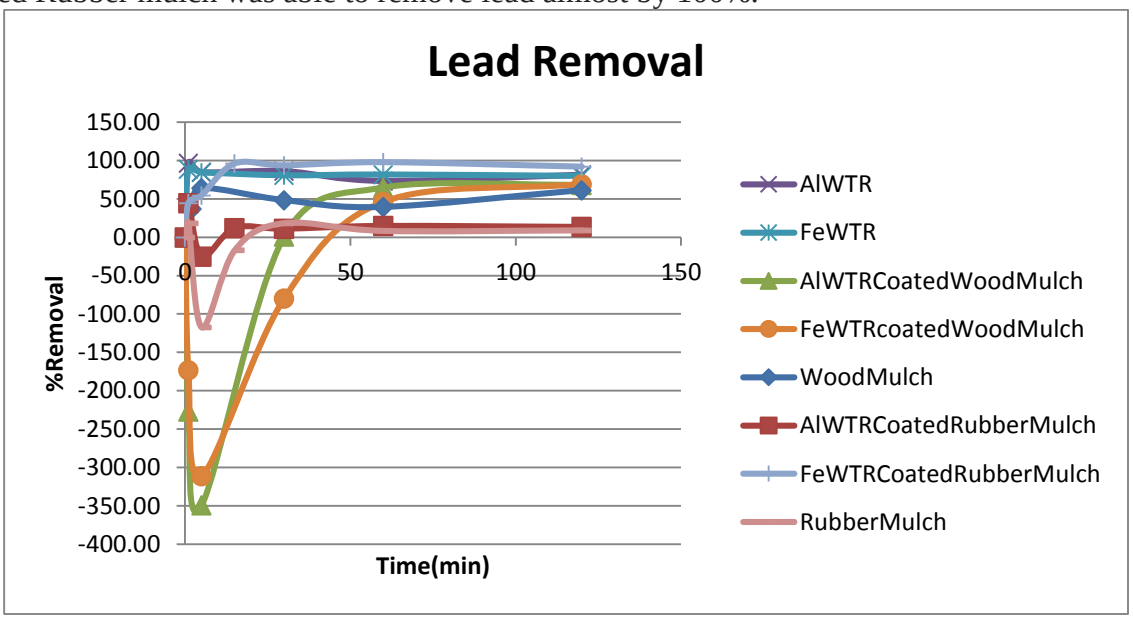

Phosphorous:

Wood and tire mulches only could not remove P. Even the former contributed P to the synthetic runoff. Al and Fe WTR coated rubber mulches both rapidly removed almost 98% of the phosphorous. Al-WTR coated wood mulch adsorption of P was relatively slow. Within 5 and 30 min., 65% and 90% of the phosphorous were reduced, respectively. Although the coated rubber mulches were effective for removal of Pb and P, they might release unwanted copper and zinc. Therefore, the following column tests were conducted to compare Al-WTR coated wood mulch and Fe-WTR coated wood mulch.

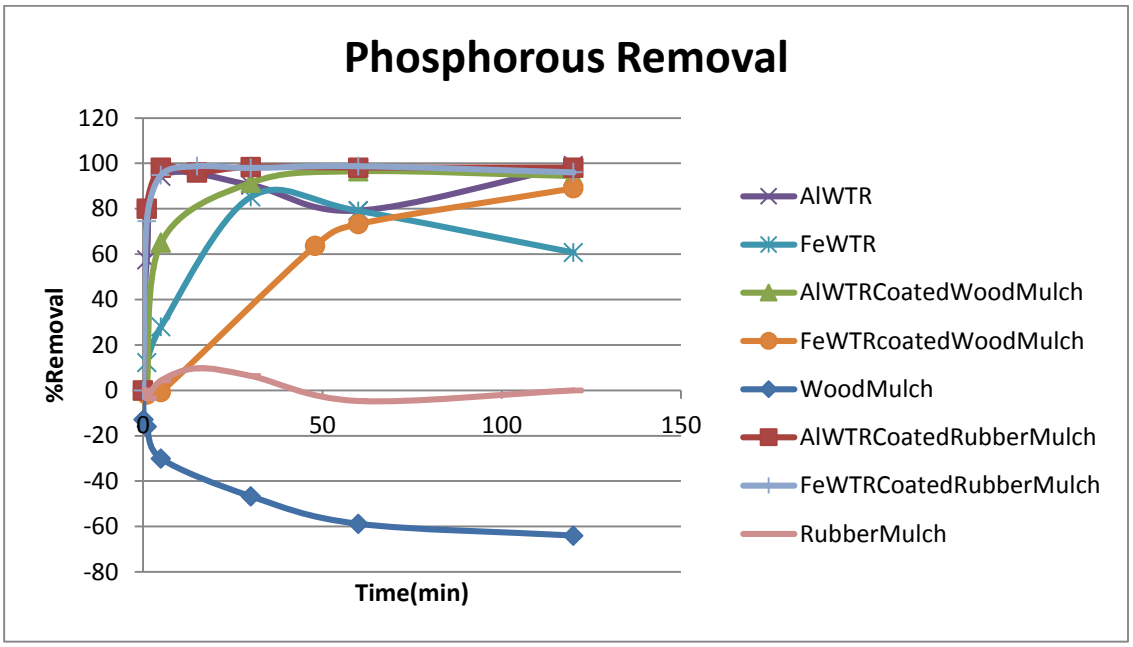

Kinetics Parameters:

Based on the data obtained, we determined key kinetics parameters including reaction orders and rate constants for four different sorbents.

Sorbent-Ion	0- order		1st order		2nd order	
	k	R^2	k	R^2	k	R^2
AlWTRCoatedWoodMulch-Cu	0.26	0.62	0.01	0.68	0.0003	0.70
AlWTRCoatedWoodMulch-Zn	4.52	0.72	0.01	0.82	0.00003	0.91
AlWTRCoatedWoodMulch-Pb	0.19	0.41	0.02	0.65	0.003	0.84
AlWTRCoatedWoodMulch-P	0.02	0.49	0.02	0.62	0.08	0.54
FeWTRCoatedWoodMulch-Cu	0.13	0.39	0.004	0.45	0.0001	0.50
FeWTRCoatedWoodMulch-Zn	5.35	0.63	0.02	0.78	0.00008	0.91
FeWTRCoatedWoodMulch-Pb	0.08	0.45	0.02	0.71	0.006	0.89
FeWTRCoatedWoodMulch-P	0.02	0.89	0.02	0.99	0.03	0.96
AlWTRCoatedRubberMulch-Cu	-0.002	0.59	-0.00004	0.56	-0.12	0.62
AlWTRCoatedRubberMulch-Zn	-0.008	0.66	-0.000007	0.56	-10.47	0.74
AlWTRCoatedRubberMulch-Pb	0.0015	0.01	0.0002	0.0008	-0.0001	0.0031
AlWTRCoatedRubberMulch-P	0.01	0.16	0.02	0.28	0.10	0.31
FeWTRCoatedRubberMulch-Cu	-0.11	0.15	-0.003	0.15	-0.00006	0.14
FeWTRCoatedRubberMulch-Zn	-1.72	0.22	-0.003	0.22	-0.000004	0.22
FeWTRCoatedRubberMulch-Pb	0.03	0.34	0.02	0.30	0.02	0.15
FeWTRCoatedRubberMulch-P	0.009	0.17	0.02	0.17	0.07	0.05

The removal of heavy metals by the coated wood mulch was better described by second-order model while the removal of phosphorous by the coated wood mulch showed mostly to be a first

order reaction. Examining three different kinetic order models in most cases did not give us a good model for the removal of heavy metals and phosphorous by the coated rubber mulch.

Column Tests:

Column tests including three sorbents (wood mulch alone, Al-WTR coated mulch and Fe-WTR coated Mulch) were performed. Results showed that Al-WTR coated mulch was the best candidate.

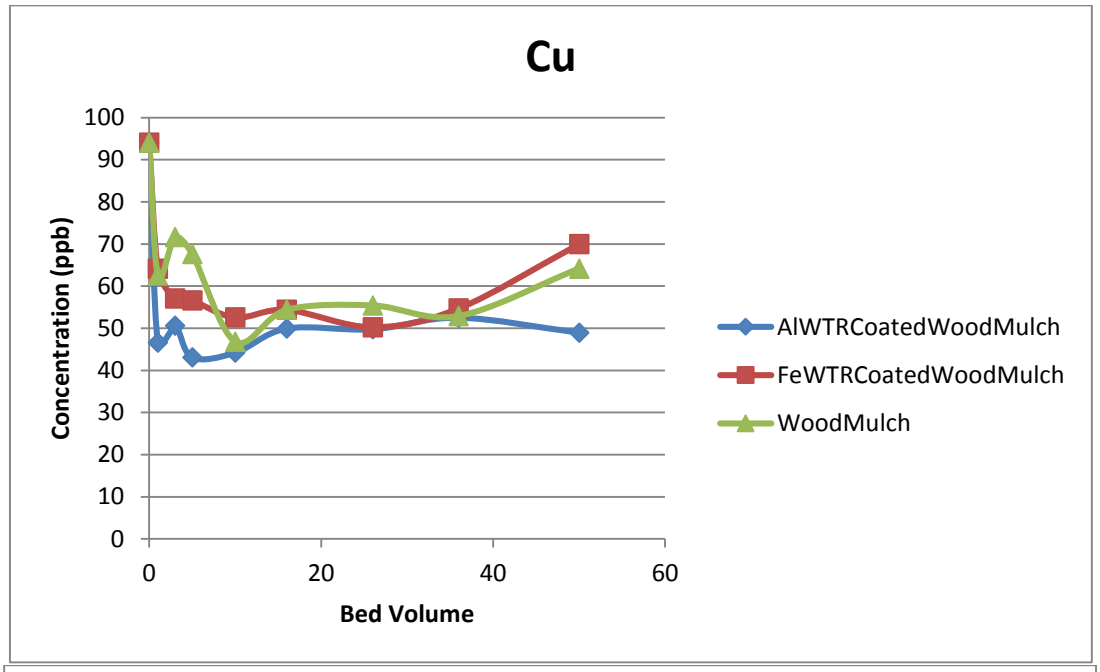

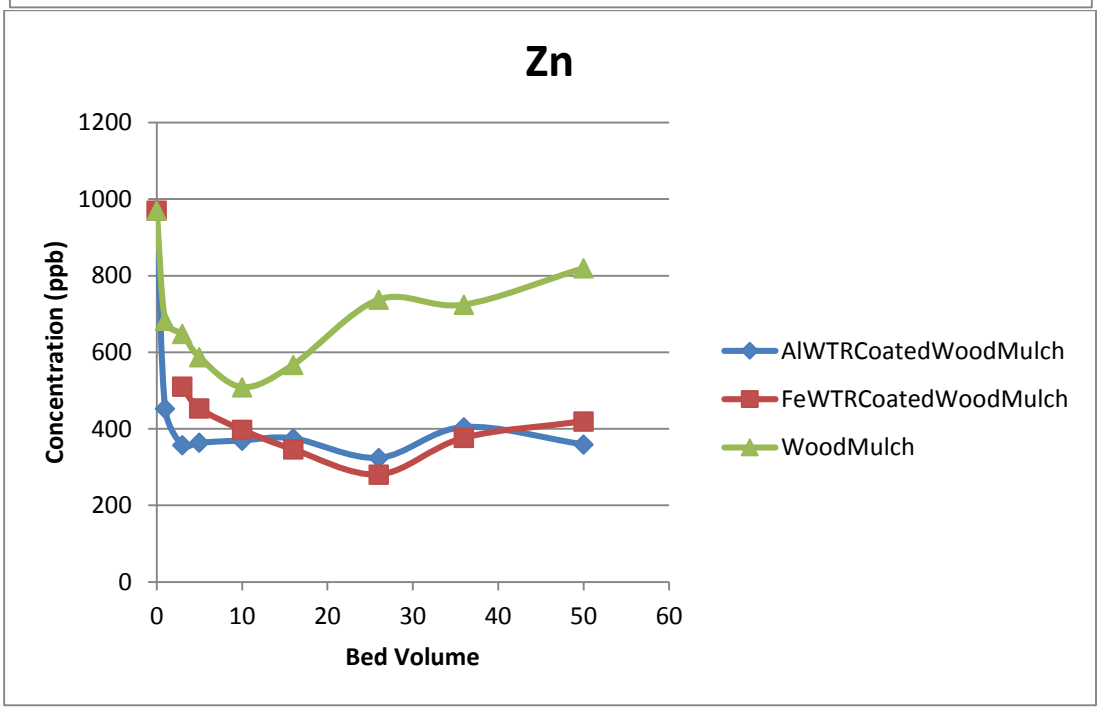

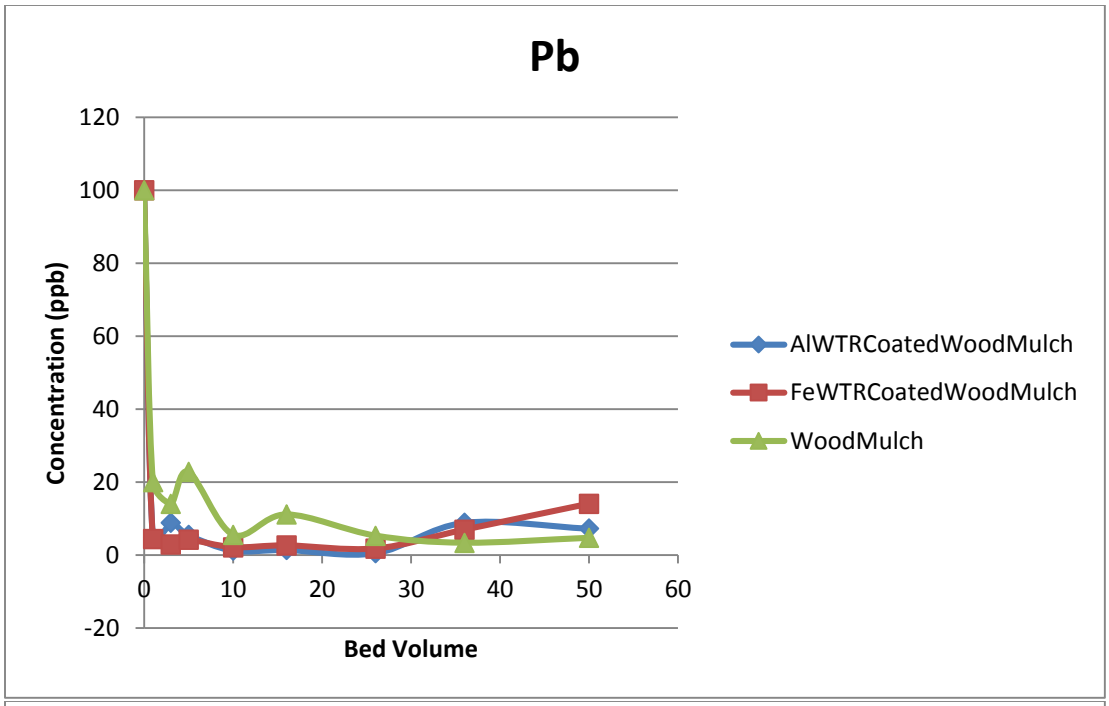

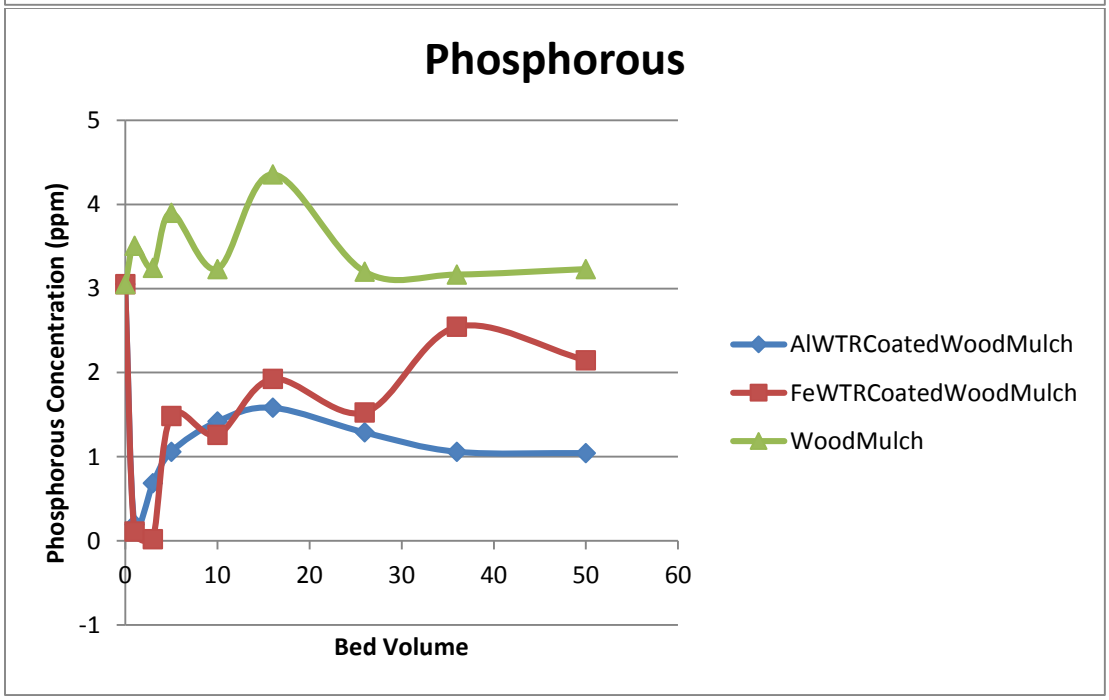

Objective III: to evaluate leaching potential of undesirable chemicals from exhausted WTR-coated mulches under rainfall and landfilling conditions (100% completed).

We examined Al and Fe WTR coated wood mulches before and after tests under landfill and rainfall situation and compared the amounts of released chemicals of concern with the standards. Data are shown below. Results suggest that the release of undesired chemicals under landfilling and rainfall conditions is not a concern.

	Concentration (ppb)							
	Cr	As	Se	Ag	Cd	Ba	Hg	Pb
TCLP-AlWTRcoatedWoodMulch-BeforeTest	47.29	2.977	-2.057	0.03	2.408	3603	4.287	7.513
TCLP-FeWTRcoatedWoodMulch-BeforeTest	30.15	2.537	0.552	0.055	2.052	2292	2.705	-0.024
TCLP-AlWTRcoatedWoodMulch-AfterTest	38.59	2.257	-1.86	0.065	3.025	8565	3.138	4.735
TCLP-FeWTRcoatedWoodMulch-AfterTest	5.356	0.948	-0.082	0.35	0.722	1223	2.404	1.545
SPLP-AlWTRcoatedWoodMulch-BeforeTest	29.33	1.972	-1.236	0.022	3.295	10230	2.015	2.043
SPLP-FeWTRcoatedWoodMulch-BeforeTest	14.16	1.97	1.402	0.118	2.711	2502	1.818	0.504
SPLP-AlWTRcoatedWoodMulch-AfterTest	3.918	0.867	-0.174	0.263	0.803	1766	1.861	0.593
SPLP-FeWTRcoatedWoodMulch-AfterTest	18.83	2.28	-0.307	0.05	3.184	4651	1.541	1.039
TCLP Limit	5000	5000	1000	5000	1000	100000	200	5000

(4) **Publications or Presentations**:
List any publications, presentations, published abstracts reporting the WRRI-supported work. Oral or poster presentations at conferences should be specified as such.

Poster Presentation: (Soleimanifar, Hanieh; Yang, Deng; Dibyendu, Sarkar) , 2014, Water Treatment Residual (WTR)-Coated Mulches for Mitigation of Toxic Metals and Nutrient in Polluted Urban Stormwater “in” New England Graduate Student Water Symposium, UMass Amherst.

Development of zirconium oxide biocomposite for drinking water defluoridation

Basic Information

Title:	Development of zirconium oxide biocomposite for drinking water defluoridation
Project Number:	2014NJ358B
Start Date:	3/1/2014
End Date:	2/28/2015
Funding Source:	104B
Congressional District:	NJ-010
Research Category:	Not Applicable
Focus Category:	Water Supply, Methods, Treatment
Descriptors:	None
Principal Investigators:	Megha Thakkar, Somenath Mitra

Publications

1. Thakkar, M., Z. Wu, L. Wei, S. Mitra, 2015, Water defluoridation using a nanostructured diatom-ZrO2 composite synthesized from algal biomass, Journal of Colloid and Interface Science 450: 239-245
2. Thakkar, M., May 2015, Removal of Fluoride using Nanostructured Diatom-ZrO2 composite, 100th NJWEA conference(Poster)
3. Thakkar, M., March 2015, Defluoridation using a Nanostructured Diatom-ZrO2 Composite Synthesized from Algal Biomass, 80th AWWA conference (Poster)
4. Thakkar, M., August 2015, Removal of Fluoride using a Nanostructured Diatom-ZrO2 Composite Synthesized from Algal Biomass, 250th ACS National Meeting, Boston, MA (Presentation)

Development of Zirconium Oxide Biocomposite for Drinking Water Defluoridation.

1. **Graduate Student Name: Megha Thakkar**

   Degree sought: Ph.D

   Institutional address: Department of Chemistry and Environmental Science

   New Jersey Institute of Technology, Newark, NJ 07102

   Telephone number: 973-596-5875

   Fax number: 973-596-3586

   Email address: mt69@njit.edu

2. **Thesis Advisor Name: Somenath Mitra**

   Institutional address: Department of Chemistry and Environmental Science

   New Jersey Institute of Technology, Newark, NJ 07102

   Telephone number: 973-596-5611

   Fax number: 973-596-3586

   Email address: somenath.mitra@njit.edu

Awards:

First place for poster presentation at AWWA Conference 2015

Second Pace for Poster presentation at NJWEA Conference 2015

Project Summary:

Abstract

Frustules or the rigid amorphous silica cell wall of unicellular, photosynthetic microalgae with unique porous architecture has been used to synthesize a composite by immobilizing ZrO_2 on its surface and in the pores. This was effective in water defluoridation. The average diameter of the composite was 80±2 nm and surface area was 140 m^2/g. The adsorption isotherms followed both Langmuir and Freundlich models, and the composite was regenerable. Adsorption kinetics followed second order model and the adsorption capacity was as high as 11.32 mg/g, while the Langmuir maximum adsorption capacity (q_m) reached 15.53 mg/g. The research findings highlight the potential of diatoms as hosts for nanomaterials for use in water treatment.

Priority issue

Fluoride is widely distributed in the geological environment and is generally released into groundwater by slow dissolution of fluoride containing rocks (Saxena and Ahmed 2001). Anthropogenic activities including ceramic/semiconductor manufacturing, electroplating, power generation and phosphate fertilizers also add to the high fluoride concentration in ground and surface water. Fluoride is unique because a dosage within 1.0 mg/L improves dental health while exposure to higher levels causes fluorosis that affects teeth and bones. Although fluoride is frequently added to municipal water supplies in some places, high fluoride content is a problem in many parts of the world with millions affected adversely (Ayoob and Gupta 2006). Conventional approaches to defluoridation include ion exchange and reverse osmosis (Joshi et al. 1992), use of manganese oxide and aluminium salts as precipitating agents (Teng et al. 2009), while alum, lime and activated alumina have been used as sorbents for fluoride (Ghorai and Pant 2005). As the awareness of the fluoride problem comes to the forefront, there arises a global need for the development of efficient defluoridation techniques.

Metal oxides have been known to bind to fluoride (Mohapatra et al. 2009). Zirconium has shown high adsorption capacity for fluoride and some of the strongest fluoride based coordination compounds are formed with zirconium (Ramamurthy et al. 2011).

Diatoms are unicellular, photosynthetic microalgae that are widely distributed in fresh and seawater. There are over eleven thousand known species whose size range from 2µm to 2 mm and they also have diverse morphology (Round et al. 1990). Frustules or the rigid amorphous silica cell wall of the diatoms have unique porous architecture (Hamm et al. 2003, Losic et al. 2006a) and their surface area can be as high as 200 m^2/g (Wang et al. 2013). It is possible that the diatoms can serve as hosts for immobilizing active sorbent particles on its surface. The surface of the diatom can have different functionalities such as -COOH, -NH_2, -OH and –SiOH, and different compounds can be immobilized on their surface by interactions with these functional groups (Gélabert et al. 2004, Gélabert et al. 2007). The objective of this research is to develop nanostructured sorbents by immobilizing ZrO_2 on diatoms to serve as active ingredient for fluoride removal. The

diatom-ZrO_2 composite developed here will serve as a platform technology that can be used in other water remediation applications.

Method

Synthesis of Diatom-ZrO_2 Composite

Diatom Phaeodactylum tricornutum was cultured and maintained in Aquil (Price et al. 1989) (artificial sea water) using a diurnal Chamber with 12 hour day/night cycles at 19°C±1°C. The diatom culture was flocculated with 0.8mM $ZrOCl_2.8H_2O$ (purchased from Sigma Aldrich) at pH 9. One molar NaOH was used to adjust the pH.

After flocculation, the culture was conditioned overnight with shaking (150 rpm, 2880 VWR orbital shaker). The resulting diatom-ZrO_2 mixture was separated by gravitational settling and membrane filtration (< 5 psi, 0.2 µm PTFE filter), and was washed with 500 mL Milli-Q water. The resulting slurry was transferred to 50-mL centrifuge tube and thermally treated at 70^{o}C in an oven for 10 h. Then, it was treated with 10 mL of concentrated H_2SO_4 and heated for 2 hrs at 200^{o}C, vacuum filtered using 0.2µm filter, washed with Milli-Q water to neutral pH and then dried at 200^{o}C in a vacuum oven. Five hundred milligram of the product was made using 40 L of Phaeodactylum tricornutum culture.

The diatom- ZrO_2 composite was characterized using transmission electron (HRTEM) equipped with Energy dispersive X-ray Spectrometer (EDX), scanning electron microscope (SEM, LEO 1530 VP), Thermogravimetric Analyzer (TGA using Pyris 1 from PerkinElmer Inc), BET surface area analyzer (Quantachrome Autosorb-1), FTIR (IRAffinity -1, Shimadzu) and dynamic laser scattering (ZetasizerNano by Malvern Instruments) for particle size and zeta potential measurements.

Defluoridation studies

The fluoride adsorption capacity of the diatom-ZrO_2 composite was investigated as follows. A fluoride ion stock solution at a concentration of 1000 mg/L was prepared and other standards were made by subsequent dilution. An Orion potentiometer (Model SA 720) with a omega fluoride ion selective electrode (FISE) in combination with a single-junction Ag ׀ AgCl ׀ Cl- reference electrode potentiometer was used to measure aqueous fluoride ion concentration. The fluoride solutions and the adsorbents were thoroughly mixed at a speed of 200rpm on a Remi shaker. The mixture was filtered through a 0.2µm membrane syringe filter. The filtrates of fluoride adsorbed were immediately analyzed by the Fluoride ion selective electrode.

The kinetics of adsorption was performed as follows. A 50 milliliter of 5 mg/L of fluoride solution was contacted with 0.01 g and 0.1 g of adsorbent in polycarbonate bottles and the samples were collected at 3, 10 and 15 min. followed by 1, 3, 5, 7 and 24 hrs. The adsorption capacity (q_e) and adsorption isotherms were obtained by varying the mass of adsorbent from 0.01 to 0.15 g with 50 mL of 5 mg/L fluoride containing water at pH 6 and the samples were collected at 0, 7 and 24 hours.

Results:

The diatom was contacted with $ZrOCl_2 8H_2O$ to take advantage of the biosilica structure in their native architecture. Under alkaline pH, the ZrO_2 precipitated on the diatom surface. The presence of ZrO_2 particles on diatom surface was studied at various steps in the process using SEM and TEM fitted with EDX. Fig. 1a shows SEM of the original diatom, 1b is diatom contacted with $ZrOCl_2 8H_2O$ and 1c is diatom- ZrO_2 composite. Similarly, Fig. 1d shows TEM image of the diatom, 1e diatom contacted with $ZrOCl_2 8H_2O$ and 2f diatom- ZrO_2 composite. SEM and TEM images showed that the original diatom was reduced to porous nano biosilica. Also, Figures 1c and 1f show that heat and acid treatment allowed precipitated Zr to form a composite with porous nano biosilica. EDX analysis using TEM confirmed presence of Si in the diatom, and Si and Zr from diatom-ZrO_2 composite. The TEM-EDX analysis showed comparatively higher Zr content than Si before and after acid treatment. The ratio of Si:Zr before acid treatment was 1:4.5 and after acid treatment was 1:4.0.

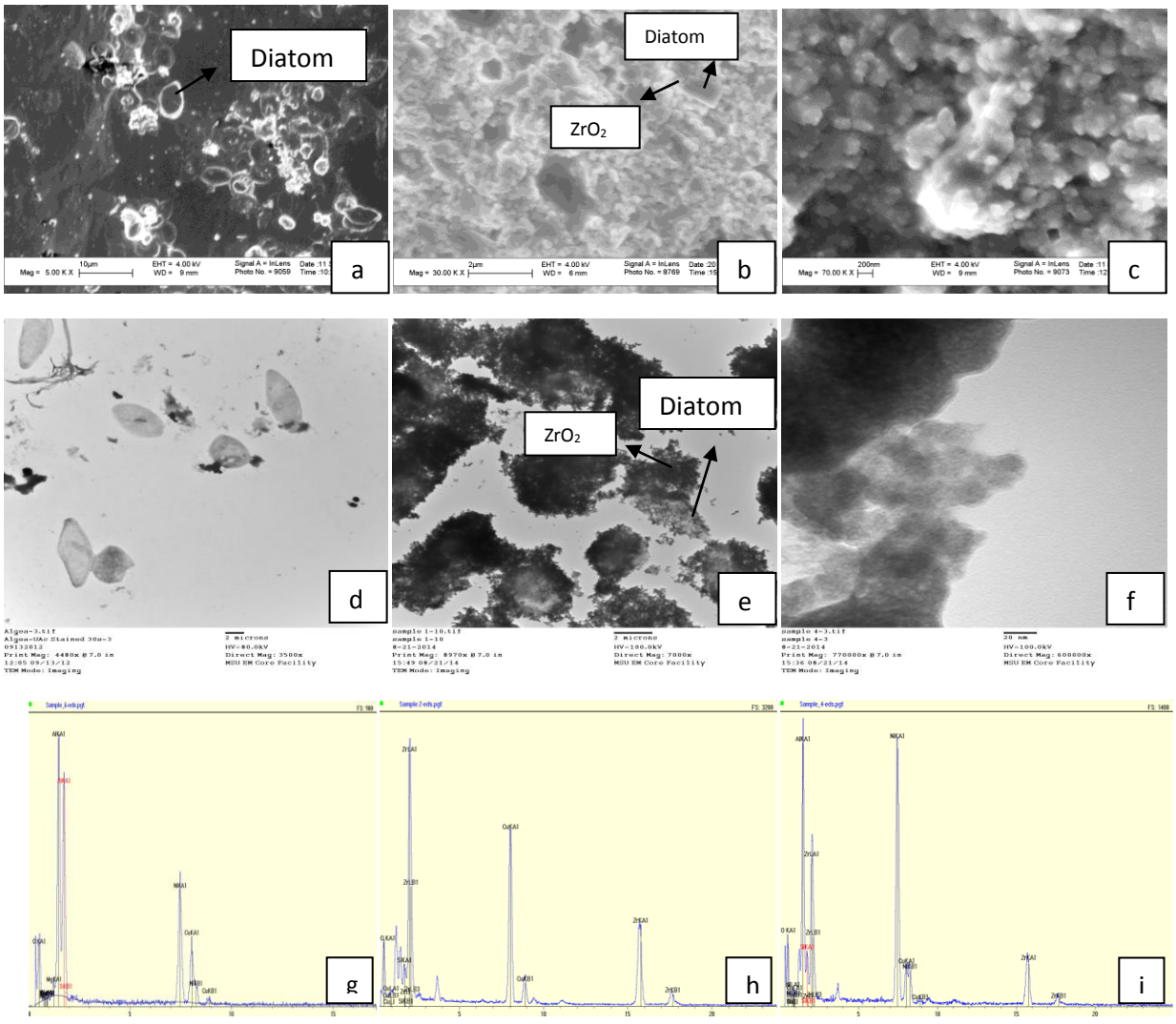

Figure 1: SEM of (a) diatom, (b) diatom with $ZrOCl_2.8H_2O$ and (c) diatom-ZrO_2 composite. TEM of (d) diatom, (e) diatom with $ZrOCl_2.8H_2O$ and (f) diatom-ZrO_2 composite. TEM EDX of (g) diatom, (h) diatom treated with $ZrOCl_2.8H_2O$ and (i) diatom- ZrO_2 composite

The specific surface area of diatom- ZrO_2 composite based on BET measurements was found to be 140 m^2/g and pore width was 9.7 Å. The particle size of diatom-ZrO_2 agglomerates in water were found to be 80 nm ± 2 nm (by DLS measurements) while zeta potential was –30. This indicated that the particles were quite stable in an aqueous suspension.

The FTIR spectrum (Fig. 2) was used to confirm the functional groups. The observed peak at 470 cm^{-1} was attributed to Zr-O vibration, which confirmed the ZrO_2 structure (Singh and Nakate 2014). The Zr-F stretch was between 375 and 475 cm^{-1}(Jere and Santhamma 1977). All the three spectra showed peaks at 1108 and between 3300 cm^{-1} to 3500 cm^{-1}. These were due to stretching of siloxane (Si-O-Si) and free silonal group (Si-OH) (Dalagan and Enriquez 2013).

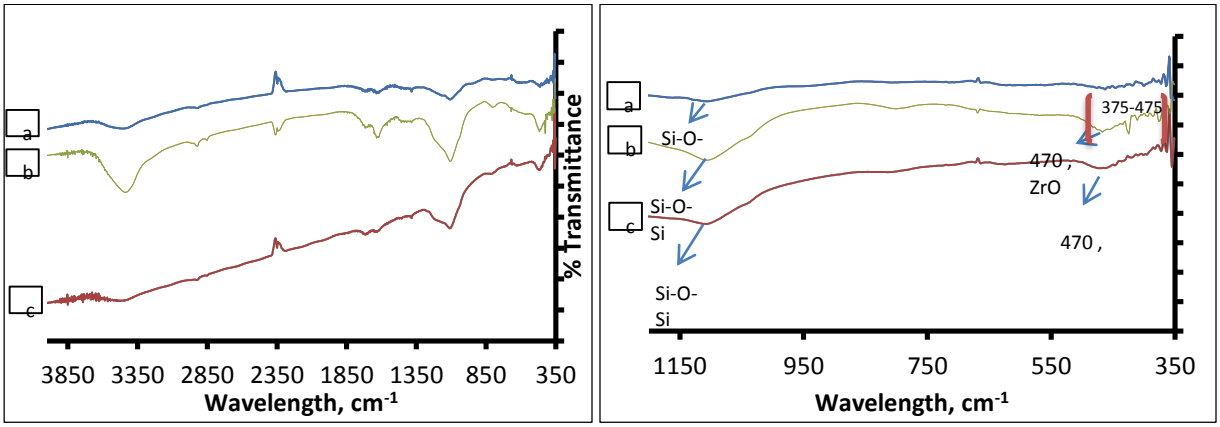

Figure 2: FTIR spectra of Diatom (a), diatom – ZrO_2 composite after fluoride adsorption (b), Diatom ZrO_2 composite before fluoride adsorption (c). Top shows can between 350-4000 cm^{-1} and below is the expanded view from 350 to 1200 cm^{-1}

TGA was used to test the thermal stability of the diatom-ZrO_2 composite (Fig. 3). The weight loss below 120 °C was attributed to the removal of physisorbed water while the loss between 120-300 °C was due to chemisorbed water (Guan et al. 2009). In the 300-400 °C range, the weight loss was from the oxidation and decomposition of mercaptopropyl or aminopropyl groups on diatom surface. The broad exothermic weight loss in the range of 400-600 °C was due to the decomposition of strongly tethered organosilanes and dehydration of silonol groups, and the weight reduction between 400–800 °C was due to the dehydroxylation of the silica surface. (Möller et al. 2007, Kao et al. 2008). TGA curve indicated that Diatom-ZrO_2 composite exhibited good thermal stability. It is worth noting that the observed weight loss (19%) below 300 °C was mainly ascribed to the evaporation of water. In the case of the diatom, only 23% of the mass remained as residue beyond 600 °C, and the residue was 38% in case of the diatom- ZrO_2 composite.

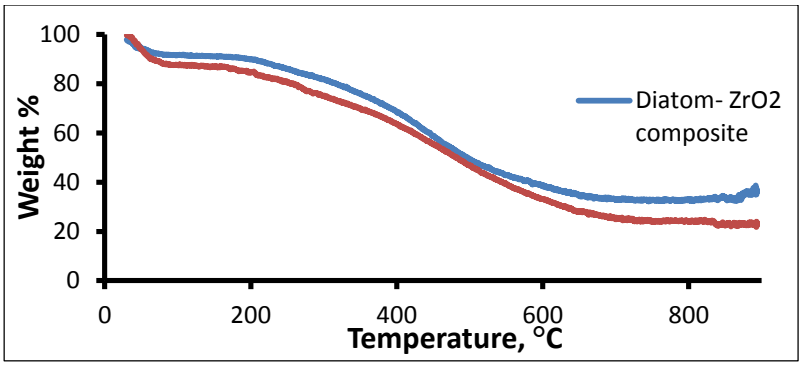

Figure 3: TGA of Diatom and Diatom-ZrO_2 composite

Fluoride removal using Diatom-ZrO_2 composite

It was observed that no fluoride was adsorbed on the pure diatom, but diatom- ZrO_2 composite was effective in removing fluoride from water. Fluoride uptake by diatom-ZrO_2 composite was studied as a function of time. Fluoride sorption increased exponentially as a function of contact time until equilibrium was reached. Fluoride uptake reached 79% of the equilibrium value within the first 15 minutes, indicating high rate of adsorption. The slow uptake after the initial period was attributed to diffusion controlled processes.

Amount of fluoride adsorbed was calculated using the following equation:

$$q_e = \frac{(C_0 - C_e)\,V}{m} \qquad (1)$$

where, C_o and C_e (mg/L) are the liquid-phase concentrations of fluoride at initial and equilibrium concentrations respectively. V is the volume of solution in (L) and m is the mass of the adsorbent used (g). Adsorbent dosage is an important parameter because this determines the capacity of an adsorbent. It was observed that at equilibrium, the percentage removal increased with the increase in the adsorbent concentration while the adsorption capacity qe decreased. It was seen that the initial adsorbent dose affects the adsorption capacity; qe dropped from 9.40 mg/g for 0.01 g of adsorbent to 1.58 mg/g for 0.15 g.

The kinetics of fluoride uptake was studied using Langereen (Lagergren 1898) as well as Ho and Mckay kinetic models (Ho and McKay 2000). The former models the rate of adsorption of pollutants based on pseudo first equation to describe the kinetics of liquid-solid phase adsorption (Yuh-Shan 2004).

The rate constant k_1 was calculated from a linear plot of log (q_e-q_t) verses t, where q_e and qt are the sorption capacity (mg/g) of the adsorbent at equilibrium and at time t (h^{-1}), and K_1 is the rate constant of pseudo first order. The second order equation from Ho and Mckay is based on the assumption that adsorption may be second order and the rate limiting step may be from chemical adsorption involving exchange of valence electrons (Bulut et al. 2008)

$$\log (q_e - q_t) = \log q_e - \frac{k_1}{2.303} t \qquad (2)$$

$$\frac{t}{q_t} = \frac{1}{k_2 q_e^{\,2}} + \frac{t}{q_e} \qquad (3)$$

The rate constant K_2 was calculated from a linear plot of t/qt verses t. Here k_2 is the pseudo-second order sorption rate constant (g/h/mg) and t is time (h^{-1}). The applicability of first and second order model was tested for adsorption of fluoride on diatom-ZrO_2. Table 1 presents the first and second order kinetics data, the best fit was selected based on the linear regression coefficient R^2. The models were fitted with the experimental data at different adsorbent dosage (0.01 and 0.1 g). Ho and Mac Kay second order equation was found to be a better fit (R^2 0.999) as compared with the first order equation.

Table 1: First order and second order kinetics. Initial fluoride concentration was 5 mg/L for 24 hours.

Model	**Concentration (g)**	**Experimental q_e (mg/g)**	**Calculated q_e (mg/g)**	**K**	**R^2**
First Order	0.010	9.40	7.15	0.0868	0.9296
Second Order			11.32	0.0177	0.9999
First Order	0.100	2.36	1.85	0.3454	0.8691
Second Order			2.36	0.0089	0.9999

Langmuir (Langmuir 1918) and Freundlich (Freundlich 1906) isotherms provided an insight into the surface coverage via physisorption or chemisorption. Langmuir Isotherm best describes the Chemisorption process. The adsorption involves the attachment of monolayer of molecules on the surface. The linear form of Langmuir adsorption isotherm, which involves a plot of $1/q_e$ vs. $1/C_e$, is represented as:

$$\frac{1}{q_e} = \frac{1}{q_m} + \frac{1}{bq_m C_e} \quad (4)$$

Here, q_m (mg/g) is the maximum sorption capacity of the sorbent; C_e (mg/L) is the equilibrium fluoride ion concentration and Langmuir constant b (L/mg) is indirectly related to the enthalpy of adsorption.

Freundlich adsorption was also tested. In its linearlized form, the Freundlich isotherm involves a plot of log q_e and log C_e :

$$\log q_e = \log k_f + n \log C_e \quad (5)$$

The values for log k_f and n were obtained as the intercept and slope respectively (Table 2). A measure of adsorption capacity and adsorption intensity was provided by the Freundlich constants k_f (mg g^{-1}) and $1/n$ respectively. Here, n was an indicator of the degree of nonlinearity between water concentration and sorption (n=1 denotes linear adsorption, n < 1 a chemisorption and if n > 1 implies physisorption (Poots et al. 1978).

Table 2: Model parameters of Langmuir and Freundlich isotherms for adsorption of fluoride.

Adsorbent	**Langmuir parameters**			**Freundlich parameters**		
	q_m (mg/g)	***b (L/mg)***	***R^2***	***k_f (mg/g)***	***n***	***R^2***
Diatom-ZrO_2	15.53	0.48	0.956	4.4	0.64	0.957

q_m - the maximum sorption capacity of the sorbent;

b - Langmuir constant;

k_f - Freundlich constant;

R^2 - correlation coefficient.

Conclusion

Diatom offers unique architecture with excellent mechanical strength. This paper highlights the potential of diatom as the host for immobilizing nanomaterials to form composite. Zirconium was successfully immobilized on diatom surface and a nanocomposite with high surface area was synthesized. This was achieved by precipitating ZrO_2 on the diatom and then oxidizing the organic mass. Maximum adsorption capacity of 15.0 mg/g adsorbent was calculated using the Langmuir adsorption isotherm.

References

Saxena, V. and Ahmed, S. (2001) Dissolution of fluoride in groundwater: a water-rock interaction study. Environmental Geology 40(9), 1084-1087.

Fluoride in Drinking-water: Background document for development of WHO Guidelines for Drinking-water Quality. World Health Organization 2004(2).

Ayoob, S. and Gupta, A.K. (2006) Fluoride in Drinking Water: A Review on the Status and Stress Effects. Critical Reviews in Environmental Science and Technology 36(6), 433-487.

Joshi, S.V., Mehta, S.H., Rao, A.P. and Rao, A.V. (1992) Estimation of sodium fluoride using HPLC in reverse osmosis experiments. Water Treatment 7(2), 207-210.

Teng, S.-X., Wang, S.-G., Gong, W.-X., Liu, X.-W. and Gao, B.-Y. (2009) Removal of fluoride by hydrous manganese oxide-coated alumina: Performance and mechanism. Journal of Hazardous Materials 168(2–3), 1004-1011.

Ghorai, S. and Pant, K.K. (2005) Equilibrium, kinetics and breakthrough studies for adsorption of fluoride on activated alumina. Separation and Purification Technology 42(3), 265-271.

Mohapatra, M., Anand, S., Mishra, B.K., Giles, D.E. and Singh, P. (2009) Review of fluoride removal from drinking water. Journal of Environmental Management 91(1), 67-77.

Pan, B., Xu, J., Wu, B., Li, Z. and Liu, X. (2013) Enhanced Removal of Fluoride by Polystyrene Anion Exchanger Supported Hydrous Zirconium Oxide Nanoparticles. Environmental Science & Technology 47(16), 9347-9354.

Ramamurthy, S.S., Chen, Y., Kalyan, M.K., Rao, G.N., Chelli, J. and Mitra, S. (2011) Carbon Nanotube-Zirconium Dioxide Hybrid for Defluoridation of Water. Journal of Nanoscience and Nanotechnology 11(4), 3552-3559.

Round, F.E., Crawford, R.M. and Mann, D.G. (1990) The diatoms: biology & morphology of the genera, Cambridge University Press.

Hamm, C.E., Merkel, R., Springer, O., Jurkojc, P., Maier, C., Prechtel, K. and Smetacek, V. (2003) Architecture and material properties of diatom shells provide effective mechanical protection. Nature 421(6925), 841-843.

Losic, D., Triani, G., Evans, P.J., Atanacio, A., Mitchell, J.G. and Voelcker, N.H. (2006a) Controlled pore structure modification of diatoms by atomic layer deposition of TiO 2. Journal of Materials Chemistry 16(41), 4029-4034.

Wang, Y., Cai, J., Jiang, Y., Jiang, X. and Zhang, D. (2013) Preparation of biosilica structures from frustules of diatoms and their applications: current state and perspectives. Applied Microbiology and Biotechnology 97(2), 453-460.

Losic, D., Rosengarten, G., Mitchell, J.G. and Voelcker, N.H. (2006b) Pore architecture of diatom frustules: potential nanostructured membranes for molecular and particle separations. Journal of Nanoscience and Nanotechnology 6(4), 982-989.

Gélabert, A., Pokrovsky, O.S., Schott, J., Boudou, A., Feurtet-Mazel, A., Mielczarski, J., Mielczarski, E., Mesmer-Dudons, N. and Spalla, O. (2004) Study of diatoms/aqueous solution interface. I. Acid-base equilibria and spectroscopic observation of freshwater and marine species. Geochimica et Cosmochimica Acta 68(20), 4039-4058.
Gélabert, A., Pokrovsky, O.S., Schott, J., Boudou, A. and Feurtet-Mazel, A. (2007) Cadmium and lead interaction with diatom surfaces: A combined thermodynamic and kinetic approach. Geochimica et Cosmochimica Acta 71(15), 3698-3716.
Price, N.M., Harrison, G.I., Hering, J.G., Hudson, R.J., Nirel, P.M., Palenik, B. and Morel, F.M. (1989) Preparation and chemistry of the artificial algal culture medium Aquil. Biological Oceanography 6(5-6), 443-461.
Singh, A. and Nakate, U.T. (2014) Microwave synthesis, characterization, and photoluminescence properties of nanocrystalline zirconia. The Scientific World Journal 2014.
Jere, G.V. and Santhamma, M.T. (1977) IR and laser raman studies on peroxo fluoro species of zirconium. Inorganica Chimica Acta 24(0), 57-61.
Dalagan, J.Q. and Enriquez, E.P. (2013) Interaction of Diatom Silica with Graphene. Phillippine Science Letters 6(1), 119-127.
Guan, M., Liu, W., Shao, Y., Huang, H. and Zhang, H. (2009) Preparation, characterization and adsorption properties studies of 3-(methacryloyloxy)propyltrimethoxysilane modified and polymerized sol–gel mesoporous SBA-15 silica molecular sieves. Microporous and Mesoporous Materials 123(1–3), 193-201.
Möller, K., Kobler, J. and Bein, T. (2007) Colloidal suspensions of nanometer-sized mesoporous silica. Advanced Functional Materials 17(4), 605-612.
Kao, H.-M., Shen, T.-Y., Wu, J.-D. and Lee, L.-P. (2008) Control of ordered structure and morphology of cubic mesoporous silica SBA-1 via direct synthesis of thiol-functionalization. Microporous and Mesoporous Materials 110(2), 461-471.
Lagergren, S. (1898) About the theory of so-called adsorption of soluble substances. Kungliga Svenska Vetenskapsakademiens Handlingar 24(4), 1-39.
Ho, Y.-S. and McKay, G. (2000) The kinetics of sorption of divalent metal ions onto sphagnum moss peat. Water Research 34(3), 735-742.
Yuh-Shan, H. (2004) Citation review of Lagergren kinetic rate equation on adsorption reactions. Scientometrics 59(1), 171-177.
Bulut, E., Özacar, M. and Şengil, İ.A. (2008) Adsorption of malachite green onto bentonite: Equilibrium and kinetic studies and process design. Microporous and Mesoporous Materials 115(3), 234-246.
Langmuir, I. (1918) THE ADSORPTION OF GASES ON PLANE SURFACES OF GLASS, MICA AND PLATINUM. Journal of the American Chemical Society 40(9), 1361-1403.
Freundlich, H. (1906) Over the adsorption in solution. J. Phys. Chem 57(385471), 1100-1107.
Hall, K.R., Eagleton, L.C., Acrivos, A. and Vermeulen, T. (1966) Pore- and Solid-Diffusion Kinetics in Fixed-Bed Adsorption under Constant-Pattern Conditions. Industrial & Engineering Chemistry Fundamentals 5(2), 212-223.
Malik, P. (2004) Dye removal from wastewater using activated carbon developed from sawdust: adsorption equilibrium and kinetics. Journal of Hazardous Materials 113(1), 81-88.
Poots, V., McKay, G. and Healy, J. (1978) Removal of basic dye from effluent using wood as an adsorbent. Journal (Water Pollution Control Federation), 926-935.

Publication:

Thakkar, M; Wu, Z; Wei, L; Mitra, S; Water defluoridation using a nanostructured diatom-ZrO_2 composite synthesized from algal biomass, Journal of Colloid and Interface Science 450 (2015) 239- 245.

Presentations:

Removal of Fluoride using Nanostructured Diatom-ZrO_2 composite, Poster presentation at 100th NJWEA conference, May 2015

Defluoridation using a Nanostructured Diatom-ZrO_2 Composite Synthesized from Algal Biomass, Poster presentation at 80th AWWA conference, March 2015

Removal of Fluoride using a Nanostructured Diatom-ZrO_2 Composite Synthesized from Algal Biomass, Oral presentation at 250th ACS National Meeting Boston, Massachusetts, August 16-20, 2015.

Information Transfer Program Introduction

None.

USGS Summer Intern Program

None.

Student Support					
Category	**Section 104 Base Grant**	**Section 104 NCGP Award**	**NIWR-USGS Internship**	**Supplemental Awards**	**Total**
Undergraduate	8	0	0	0	8
Masters	2	0	0	0	2
Ph.D.	7	0	0	0	7
Post-Doc.	0	0	0	0	0
Total	17	0	0	0	17

Notable Awards and Achievements

For 2014NJ351B: First Place Poster Presentation Award, New Jersey Water Environment Association conference held in Atlantic City, NJ, May 14, 2015, for Del Monaco, Nicole, C. Obropta, D. Swiderski-Soto, Impervious Cover Assessments: A New Tool for Promoting Climate Resiliency in New Jersey

For 2014NJ353B: January, 2015, Poster Prize, Symposium of Microbiology at Rutgers University, Dam, HT and MM Haggblom, Cultivating Traditions, Current Strength and Future Frontiers

For 2014NJ355B: 2015 Hutcheson Memorial Forest Summer Research Grant ($2,150), Rutgers School of Environmental and Biological Science; 2015 Woodstoich Travel Grant to attend Conference on Biological Stoichiometry in Canada ($400); 2014 NSF Junior Scientist Travel Grant to attend Theo Murphy Discussion Meeting in U.K. ($1,500); 2014 National Science Foundation Graduate Research Fellowship ($96,000 stipend and tuition over 3 years)

For 2014356B: First Place Graduate Poster Session at the 99th Annual New Jersey Water Environment Association Conference in Atlantic City, NJ in May 2014; First Place Poster Session at Xth Annual Graduate Research Day by Graduate Student Association at NJIT, Newark, NJ in October 2014

For 2014NJ358B: First Place for poster presentation at AWWA Conference 2015; Second Place for poster presentation at NJWEA Conference 2015